



Multistability and Transient Dynamics on Networked Systems

Der Fakultät für Mathematik & Naturwissenschaften
der Carl von Ossietzky Universität Oldenburg
zur Erlangung des Grades und Titels
Doktor der Naturwissenschaften (Dr. rer. nat.)
angenommene Dissertation

von

Kalel Luiz Rossi

geboren am 13.10.1997 in Curitiba, Parana, Brasilien

Gutachter: Prof. Dr. Ulrike Feudel

Gutachter: Prof. Dr. Klaus Lehnertz

Tag der Disputation:

Contents

List of Publications

This dissertation is based on the following publications:

Chapter 2.1.7: George Datseris, Kalel L. Rossi, and Alexandre Wagemakers. Framework for global stability analysis of dynamical systems. *Chaos* **33**, 073151 (2023).

Statement of authorship:

George Datseris: Conceptualization (lead); Investigation (equal); Formal analysis (equal); Software (equal); Visualization (lead); Writing – original draft (equal); Writing – review & editing (equal).

Kalel Luiz Rossi: Conceptualization (equal); Formal analysis (equal); Software (equal); Visualization (equal); Writing – original draft (equal); Writing – review & editing (equal).

Alexandre Wagemakers: Conceptualization (equal); Formal analysis (equal); Software (equal); Writing – original draft (equal); Writing – review & editing (equal).

Chapter 3: Kalel L. Rossi, Roberto C. Budzinski, Bruno R. R. Boaretto, Lyle E. Muller, and Ulrike Feudel. Small changes at single nodes can shift global network dynamics. *Physical Review Research* **5**, 013220 (2023).

Statement of authorship:

Kalel Luiz Rossi: Conceptualization (equal); Investigation (lead); Formal analysis (lead); Software (lead); Visualization (lead); Writing – original draft (lead); Writing – review & editing (lead).

Roberto C. Budzinski: Conceptualization (equal); Investigation (equal); Formal analysis (equal); Software (equal); Writing – original draft (equal); Writing – review & editing (equal).

Bruno R. R. Boaretto: Conceptualization (equal); Investigation (equal); Formal analysis (equal); Software (equal); Writing – original draft (equal); Writing – review & editing (equal).

Lyle E. Muller: Conceptualization (equal); Investigation (equal); Formal analysis (equal); Software (equal); Writing – original draft (equal); Writing – review & editing (equal).

Ulrike Feudel: Conceptualization (equal); Investigation (equal); Formal analysis (equal); Software (equal); Writing – original draft (equal); Writing – review & editing (equal); Supervision (lead).

Chapter 4: Kalel L. Rossi, Everton S. Medeiros, Peter Ashwin and Ulrike Feudel. Transients versus network interactions give rise to multistability through trapping mechanism.

Statement of authorship:

Kalel Luiz Rossi: Conceptualization (equal); Investigation (lead); Formal analysis (lead); Software (lead); Visualization (lead); Writing – original draft (lead); Writing – review & editing (lead).

Everton S. Medeiros: Conceptualization (equal); Investigation (equal); Formal analysis (equal); Writing – original draft (equal); Writing – review & editing (equal).

Peter Ashwin: Conceptualization (supporting); Investigation (equal); Formal analysis (equal); Writing – original draft (supporting); Writing – review & editing (equal).

Ulrike Feudel: Conceptualization (equal); Investigation (equal); Formal analysis (equal); Writing – original draft (equal); Writing – review & editing (equal); Supervision (lead).

Chapter 5: Kalel L. Rossi, Roberto C. Budzinski, Everton S. Medeiros, Bruno R. R. Boaretto, Lyle E. Muller, and Ulrike Feudel. Dynamical properties and mechanisms of metastability: a perspective in neuroscience.

Statement of authorship:

Kalel Luiz Rossi: Conceptualization (equal); Investigation (lead); Formal analysis (lead); Software (lead); Visualization (lead); Writing – original draft (lead); Writing – review & editing (lead).

Roberto C. Budzinski: Conceptualization (equal); Investigation (equal); Formal analysis (equal); Writing – original draft (equal); Writing – review & editing (equal).

Everton S. Medeiros: Conceptualization (equal); Investigation(equal); Formal analysis (equal); Writing – original draft (equal); Writing – review & editing (equal).

Bruno R. R. Boaretto: Conceptualization (equal); Investigation(equal); Formal analysis (equal); Writing – original draft (equal); Writing – review & editing (equal).

Lyle E. Muller: Conceptualization (equal); Investigation(equal); Formal analysis (equal); Writing – original draft (equal); Writing – review & editing (equal).

Ulrike Feudel: Conceptualization (equal); Investigation(equal); Formal analysis (equal); Writing – original draft (equal); Writing – review & editing (equal); Supervision (lead).

On top of these main thesis papers, I have also collaborated in other works, which resulted in two further publications, with me as a co-author. They are not included in this thesis.

- Bruno R. R. Boaretto, Roberto C. Budzinski, Kalel L. Rossi, Thiago L. Prado, Sergio R. Lopes and Cristina Masoller. Temporal Correlations in Time Series Using Permutation Entropy, Ordinal Probabilities and Machine Learning. *Entropy* **23**, 1025 (2021).
- Bruno R.R. Boaretto, Roberto C. Budzinski, Kalel L. Rossi, Cristina Masoller, Elbert E.N. Macau. Spatial permutation entropy distinguishes resting brain states. *Chaos, Solitons and Fractals* **171**, 113453 (2023).

Abstract

Field of complex systems, emergent phenomena. One such is multistability. Another is sync. Path towards the attractors is also important - transients. These are the objects of study in this thesis, which is subdivided into three main works. In the first, we study the robustness of solutions of phase oscillator networks. Malleability. 2 main factors: sts and multistabiltiy. Also study the emergence of multistability in coupled excitable neurons. We show a rich coexistence of oscilations arising from excitability, with only stable equilibrium. With two units XX, with more XX. We describe the different bifurcations giving rise to the attractors here and also provide a qualitative mechanism that describes all the attractors and also generalizes to more units. Then, switching the focus to transients, in particular long transients, metastability.

Many systems in nature and in theory display emergent behavior, in which relatively simple subunits interact together to create a complicated global behavior which is not present in any of the units alone. An important example of this is multistability, the coexistence of many stable solutions - attractors - to a dynamical system with fixed parameters.

Zusammenfassung

Chapter 1

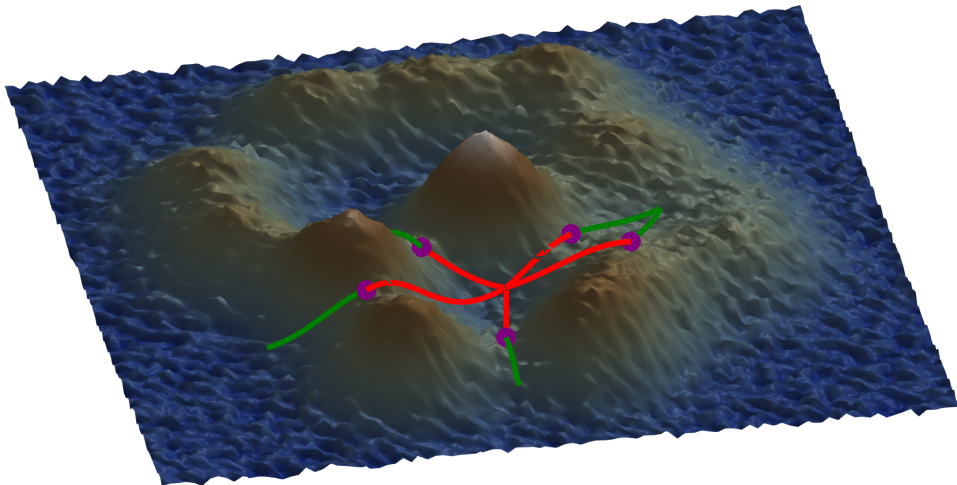
Introduction

Consider the unfortunate situation of falling down a mountain. Subject to the inexorable effect of gravity and friction, the hiker will roll downhill until they reach a certain valley, a spot at which they will finally terminate their unlucky dynamics. This final state is called an attractor, and the preceding rolling period is called a transient. Now, consider a landscape like the one in Fig. ??A. The mountain has several valleys, separated by peaks. An example of this separation is shown in Fig. ??B. Consider then the even more unfortunate situation of *two* people falling down a mountain. If they start very close together, on the same side of a peak, they will fall down to the same valley. If, however, they were separated by a peak when the fall started, then they will fall into distinct valleys. This is shown by the green and red trajectories in Figs. ??A-B. Again, each valley is an attractor. Which attractor the person falls into depends on their initial condition. If we consider this particular example to be a mechanical system with inertia, the initial condition corresponds to the person's initial position and velocity. In general, all initial conditions that lead to the same attractor form a set called the basin of attraction of that attractor. All the red trajectories in Fig. ??A belong to the same basin. Trajectories are typically separated by peaks in the landscape (green and red of Fig. ??B), so the peaks usually form the boundaries between basins of attraction.

The example of the hiking disaster serves as a good introduction to the notion of *multistability* - the simultaneous coexistence of different ending states, different attractors, in a dynamical system with constant parameters (notice that the mountain landscape does not change in time in the example!). This phenomenon is present in a wide variety of notable systems, with important real-world consequences [?, ?, ?]. In biology, multistability can explain how genetically identical cells can exist in multiple metabolically distinct stable states [?, ?]. Similarly, there has been evidence, and models, suggesting that multistability in the gut microbiome can explain microbiome shifts, which are changes in the composition of the microbiome in the gut [?]. On a technological side, power grids - networks of connected generators and consumers of electrical energy - need to operate on an attractor in which all units have their frequencies of oscillation synchronized in the 50-60Hz range [?]. Multistability in the grids can be dangerous, as perturbations can switch the system out of the operating state, potentially leading to blackouts. Studies on models try to look for conditions that make the desired state as stable as possible [?, ?]. Multistability can also be a powerful mechanism in brain dynamics. Some models for long-term memory consider that each memory corresponds to an attractor in the system [?, ?], and some models of large-scale brain dynamics exhibit multistability [?]. There are many more examples of multistability, such as in artificial neural networks [?], models for ice sheets [?], mechanical systems [?], and in tissue repair [?].

The examples in neural networks and power grids in particular highlight the ubiquitous presence of multistability in networked systems - systems formed by the interactions of smaller subunits, such as neurons or electric generators. Another phenomenon in networks that can coexist with multistability is *synchronization* [?, ?]. Often the interaction between units of a network can cause them to adjust their individual rhythms toward a collective motion, in which their activity becomes similar in some sense [?]. In this case,

A



B

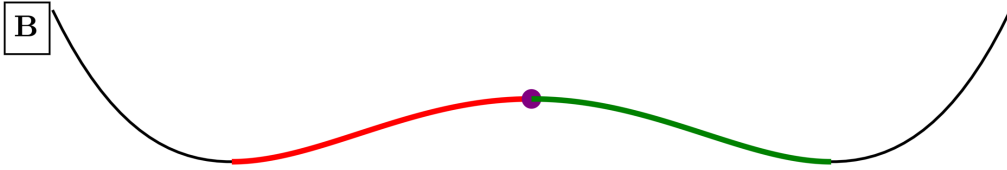


Figure 1.1: **Landscape with valleys and peaks constitutes an example of multistability for an unfortunate falling person.** Panels A and B respectively show a 3D and 2D example of a landscape, with red trajectories converging onto the same attracting region, and green trajectories, which start next to the red trajectories but on the other side of the peak, converge onto other attracting regions.

the network is said to be synchronized. There are many different types of synchronization, which can be defined based on what “similar” and “activity” are taken to mean. Three important properties that characterize the state of an oscillation at a certain time are the amplitude, phase, and angular frequency at that time. Roughly, the amplitude describes how high or how low the oscillation itself is; the phase describes the current position of the oscillation along its oscillation cycle; and the angular frequency describes how fast the phase itself is moving [?]. In many applications, the amplitudes of the oscillations turn out to not play a major role [?, ?]. For instance, if the coupling between the units is weak enough, the amplitudes of their oscillations are not particularly altered, but the phases are [?, ?]. When units adjust their individual frequencies to the same value, i.e. when they spontaneously lock into a common frequency, they become frequency synchronized (also called phase-locked) [?, ?]. One technically relevant example has been mentioned before for power grids, in which all the units must have their frequencies synchronized at the same value, such as 50 Hz [?]. In some cases, the phases

of the oscillations may also converge onto a common value. Then, the units are phase-locked and their phases converge to similar values. This is called *phase synchronization*. It has been proposed as an important mechanism for communication and exchange of information between brain circuits [?, ?, ?]. Interestingly, lack of phase synchrony can also play an important role, e.g. in the flight pattern of fruit flies [?].

The real-world relevance of such systems has stimulated a lot of research into their dynamics [?]. An approach taken by several works has been to study simple models that capture some essential properties of real world systems. A particularly important example, which has become paradigmatic in the synchronization literature, is that of Kuramoto oscillators (see Sec. ??). They constitute quite a beautiful example of how units with very simple dynamics can generate complex behavior when interacting together. Each unit in the model is described by a phase (angle) variable that by itself just varies linearly according to its own natural frequency. The interesting dynamics comes from the nonlinear coupling, done via the sin of the phase difference between coupled units, cf. Eq. ???. The model is simple enough to allow for analytic treatment but still complex enough to show relevant dynamics [?, ?]. In particular, it displays a continuous phase transition from desynchronization to frequency and phase synchronization as the strength of the inter-unit coupling is increased. Roughly, if the natural frequencies are spread too widely compared to the coupling between them, the units oscillate incoherently; if instead the coupling becomes large enough, the units start to oscillate with the same frequency - they become phase-locked. As the coupling increases, the phases also become more clustered together, although complete phase synchronization does not occur.

The Kuramoto model is also generic in the sense that it can be derived as an approximation of general limit cycle oscillators under weak coupling [?]. In this case, one considers units that oscillate on a periodic orbit. If the coupling between the units is weak enough, the amplitude of their oscillation is not significantly affected, only the phase along the limit cycle. Then, the interplay between the differences in frequency and the coupling determines the time evolution of the phases. The Kuramoto model is a somewhat more specific case of this phase reduction, in that one chooses a purely sinusoidal coupling [?]. Still, the combination of simplicity and complexity leading to a synchronization transition, and this argument of genericity, incited a lot of research and inspired new concepts [?, ?, ?].

This also inspired us to translate results we had from spiking neural networks [?]. In those networks we described a phenomenon we called *dynamical malleability*, the sensitivity of a whole network's dynamics to changes in parameters of single components, usually changes in parameters of single units. Similarly to the Kuramoto oscillator networks, the spiking neural networks we studied also present a transition to synchronization, in particular to phase synchronization, when the coupling strength is increased. They also present a transition to synchronization as the topology changes: as the connections in the system are changed from being restricted only to k -nearest neighbors to being randomly allocated, the neurons also start to synchronize their phases. Types of topologies are described in more detail in Sec. ???. In the neighborhood of both of these transitions, we showed that the network's dynamical malleability increases considerably. As we see in Chap. ??, this phenomenology generalizes for Kuramoto networks with heterogeneous frequencies. In fact, it occurs very strongly: changing the parameter of a single unit can drastically alter the behavior of the whole network in a very sensitive manner [?], which was until then not known.

In the literature for Kuramoto oscillators, the phenomenon of dynamical malleability has been studied from the point of view of statistical mechanics [?, ?]. Changing the parameters of a single unit leads to a different network, which is termed to be a different sample. In this case, one shows that the finite size of the networks leads only to an approximate phase transition, whose critical parameter varies depending on the sample. Therefore, in this case, one can show that *sample-to-sample (STS) fluctuations* increase near a phase transition. These studies did not, however, look closely at the dynamics of these finite networks. One work that looks at this more closely for all-to-all topologies was Ref. [?], where they propose that the kurtosis of the natural frequency distribution correlates with the critical coupling strength of the transition. Therefore, changing the frequency of the units changes the kurtosis and thus changes the critical coupling strength. However, they did not explore how this also interacted with more complex topologies. As we show in our work, their mechanism alone does not explain the malleability we describe: networks with shuffled natural frequencies have the same kurtosis but still can vary significantly. In our work, we therefore complement these studies by looking at the dynamics behind the malleable networks, and show that indeed the sample-to-sample fluctuations are a key effect leading to malleability. But we also show that another important effect comes from multistability, which is another behavior we analyzed.

We looked at *multistability* in the networks as a function of the coupling strength and topology, and showed the emergence of a large number of coexisting attractors at the transition to phase synchronization. This therefore means that the networks we studied are very sensitive to perturbations in the state variables (which can lead the system to switch to other attractors, due to multistability) and in the parameters (which can change the attractor considerably, due to malleability). This was another contribution from our work. Naturally, there have been studies on multistability in Kuramoto networks. In the case of heterogeneous frequencies, Tilles et al. studied multistability arising in nearest-neighbor rings [?]. In a related Kuramoto model, which has an inertial term, some studies have shown the coexistence of multiple attractors in random topologies [?], and in power grid topologies [?, ?]. Ref. [?] looks at how properties of power grid topologies relate to the dynamics of first-order Kuramoto models, but do not report multistability.

Multistability has been studied in detail for units with *homogeneous frequencies* (which are then identical) and which are coupled in k -nearest-neighbor topologies. In this case, the network can be written as a gradient system, meaning its only attractors are equilibria, which are single points in state space (cf., Secs. ??-??). This considerably simplifies their study. The networks can have multiple stable equilibria, each being characterized by neighboring units having a fixed and constant phase relationship. These equilibria are called twisted states [?], and their stability depends on the relationship between the number of nearest neighbors k and the size N of the network [?] - see Sec. ?? for more. For these networks there have been studies looking at the effect of the topology [?], showing a minimum coupling strength that guarantees complete synchronization globally. Another important contribution has looked at the basins of attraction for these networks: Zhang and Strogatz have shown that the basins behave like octopuses - the head of the octopus contains the attractor, an equilibrium. The head is relatively small compared to the tentacles: most of the volume of the basins is not concentrated around the equilibrium, but spread around in tentacle-like structures in state space [?].

In both the case of heterogeneous and of homogeneous frequencies, we are unaware of any systematic study on the emergence of multistability and effect of changing topology,

in particular for first-order Kuramoto models. Our work serves also as a step in this direction, but more research is needed.

In general, the mechanisms that give rise to multistability in networks are still not fully understood. In particular, during my PhD we started to study multistability in a network of bursting neurons coupled diffusively, looking to explain results from previous publications [?]. The neurons, which follow the Hindmarsh-Rose equations [?], have individually a stable periodic orbit as an attractor. By changing parameters of the neurons, one can make a certain region of this periodic orbit very slow, but without going through a bifurcation. Preliminary results showed that multistability only emerges in the coupled networks when the neurons have this slow region. To better understand this, we looked at a simpler conductance-based neuronal model [?] which also has regions of slow flow. We focused on the case when this model has excitable dynamics. The isolated neuron then has only one attractor, a stable equilibrium. And it also has two unstable equilibria, which force some trajectories to go on long excursions before converging to that attractor. These excursions are called excitations, and correspond to the neuron spiking. One of these unstable equilibria also slows down trajectories passing near it. By coupling two such neurons diffusively we show the emergence of different types of oscillating attractors, which can all coexist. We show the bifurcations giving rise to these attractors. Furthermore, we describe a qualitative mechanism for how they occur. The idea is that the diffusive coupling acts to repeatedly reinject the trajectories of each neuron into the region responsible for the excitations, thereby effectively *trapping the trajectories in the previously transient region* - see Chap. ?? for more. The slowness near one the equilibria plays an important role in this mechanism, which might help to explain the original problem we started on. For two units, it can happen that both are trapped in this excitability region, or just one is, generating in total three possible combinations. For more units, the number of possible combinations increases, and therefore so does the number of coexisting attractors. The emerging attractors are all oscillating, and can do so periodically, quasiperiodically, or chaotically - all despite the individual units having only equilibria! This mechanism is also a simple example of how coupling can interact with transients to generate attractors, an idea that has been studied in the literature under different circumstances. In particular, Medeiros et al. studied units which have a periodic attractor and a chaotic saddle, an unstable chaotic set, in their state space. They showed that diffusive coupling between them can counteract the divergence tendency near the chaotic saddle, effectively trapping the units in its neighborhood, and creating a chaotic attractor which coexists with the units' periodic attractor [?, ?]. However, the authors did not observe multiple attractors emerging from the trapping in the chaotic saddle. Therefore, the coupled excitable neurons, with their trapping mechanism, constitutes a simple yet powerful mechanism for generating a rich multistability in networks, which had not been described previously in the literature, to our knowledge.

This line of investigation on multistability also contributes to the study of how oscillations arise in non-oscillating units interacting via diffusive coupling. As discussed in Chap. ??, this line of work has a rich history, with an early work by Smale showing that Hopf bifurcations can give rise to oscillations [?] - see Sec. ?? for bifurcations. Later works showed the possibility of chaos, and also the emergence of multistability in repulsive coupling. Our contribution in this case has been to show a rich multistability, with the possible coexistence of periodic, quasiperiodic, and also chaotic solutions - with repulsive or attracting coupling.

These studies on multistability require efficient and reliable algorithms to identify the coexisting attractors of a system. To this end, I have contributed to creating Attractors.jl, an open-source package in the Julia programming language that collects such algorithms. In particular, George Datseris and Alexander Wagemakers had already introduced an algorithm to find attractors based on recurrences in state space [?], from an idea by Nusse and Yorke [?]. I then contributed to implementing and refining another algorithm, proposed in Refs. [?, ?], based on finding attractors by grouping trajectories with similar features. These algorithms are described more in Sec. ???. Together with Datseris and Wagemakers, we built a continuation framework that allows one to use either of these two methods across a parameter range. This idea is similar to linear continuation analysis, but generalizes to any type of attractor, including chaotic attractors. This led to a joint publication [?]. On top of the novelty of the continuation algorithm, and the improvements made to the state of the art algorithms for finding attractors, our contribution here was also to provide a package that is free and easy to use.

Going back now to the excitable neurons, the multistability seen there is remarkable: stable states arise from the interaction with transient behavior (the excitations). Often in the literature we are preoccupied with the final states of the system - usually justifiably so - but anyone who asks the falling hikers in our initial example will probably find out that transients should not be disregarded so easily. In particular for neuroscience, transient dynamics has been the object of a lot of recent work. For instance, transients can be harnessed to perform computations [?], particularly when they are long-lived [?]. Ref. [?] proposes that long-lived transients, particularly in the form of ghosts of saddle-node bifurcations, offer some distinct computational advantages, such as maintaining a dynamical memory of a signal. See Sec. ?? for more on ghosts. For instance, Ref. [?] studied a simple model for how cells respond to changing chemical signals and use them to move. Without any signal, the cell operates on a stable equilibrium. A signal causes a saddle-node bifurcation that leads it to another stable equilibrium. As the signal is removed, the inverse bifurcation happens, and the cell eventually converges back to the original equilibrium. But before returning, the cell stays for a while visiting the ghost of the second equilibrium. Biologically, this means that cell keeps the memory of the signal for a while [?, ?]. Indeed, long-lived transients are an ubiquitous phenomenon observed in neural activity [?, ?], and are often referred to as *metastable*. One interesting example comes from studies measuring how mice encode for tastants fed to them. The study measured the firing rate activity in the gustatory cortex of the mice as a response to different tastants [?]. They identified that the stimulus elicits a sequence of distinct long-lived but transient regimes. By regime here we mean an epoch of the time series with some unique properties - in their case, the configuration of the average firing rate across the ensemble of neurons. Each tastant evoked a specific sequence of such metastable regimes. The duration of these regimes varies across trials, but the sequence itself is consistent [?, ?].

Delving into the metastability literature, we found that a general conceptual framework in neuroscience was lacking. First, the very definition of metastability varied between works, leading to apparent inconsistencies, as explained in more details in Chap. ???. Second, the mechanisms proposed for metastability also varied. Some works propose ghost of saddle-node bifurcations [?] while others propose noise [?], with few works attempting to compare different proposals [?]. In our work, we drew from tools of dynamical systems theory to provide such a conceptual framework. We provide a simple definition of metastable regimes as long-lived transients, which encompasses the major-

ity of previous works not only in neuroscience, but also dynamical systems and even ecology. Previous inconsistencies between works can be neatly fit into distinct subtypes of metastability - for instance, when transitions between metastable regimes are spontaneously or externally driven. Then we use this definition to study general properties of metastability, making use of the concept of almost-invariant sets [?, ?]. We argue that metastable regimes in time correspond in state space to almost-invariant sets, regions in which trajectories tend to stay for long, but not infinitely long. We also propose several dynamical mechanisms that can generate metastable regimes. Importantly, we connect these dynamical mechanisms to previous literature in neuroscience, complementing the discussions there.

Taking all of this together, my PhD has been a journey into studying the long-term and the transient dynamics of networked systems - how multistability can emerge and how it affects their robustness - and how long transients (metastability) can arise. This thesis describes this journey and will hopefully reflect the excitement of doing all of this research. In Chap. ?? I introduce in greater depth the fundamental concepts needed for the studies performed in this thesis. These will then follow in Chaps. ??, ?? and ?? in the same order introduced here. Finally, in Chap. ?? I will take all of these results together and reflect on what we learned, what our contributions have been to the literature, and the open questions that lie ahead in the future.

Chapter 2

Methodology

2.1 Basics of dynamical systems theory

2.1.1 Dynamical systems and the uniqueness and existence of their solutions

In this thesis we study dynamical systems described by a state variable $x = (x_1, x_2, \dots, x_n)^T \in M$, where $M \subseteq \mathbb{R}^n$ is the state space, and T denotes the transpose operation. The state variable is a point in this n -dimensional state space. In a continuous-time dynamical system, the state evolves according to the equation:

$$\dot{x}(t) = f(x(t)) \quad (2.1)$$

where $f : M \rightarrow M$. Systems obeying Eq. ?? are deterministic: there is no randomness, no stochasticity, no noise. This means that, starting from one single state at time t , we can in principle describe the whole past and future evolution of the system. Furthermore, there is a lack of an explicit time dependence in f - i.e., $\partial f_i / \partial t = 0$ for $i = 1, \dots, n$. In this case, the dynamical system is said to be autonomous.

To obtain solutions to system ?? we need to provide one state, which we typically call an initial condition $x_0 = x(0) \in \mathbb{R}^n$. The combination of $\dot{x} = f(x)$ with $x(0) = x_0$ defines an initial value problem. A fundamental theorem makes our lives studying this problem much easier. This is the theorem of existence and uniqueness of solutions. For $x \in \mathbb{R}^n$ and $f : \mathbb{R}^n \rightarrow \mathbb{R}^n$, it requires that f is continuous and that all of its partial derivatives $\frac{\partial f_i}{\partial x_j}$, for $i, j = 1 \dots n$ are continuous in some open connected set $D \subset \mathbb{R}^n$. This basically means that it requires our function f to be sufficiently smooth. Then, for initial conditions $x_0 \in D$, the initial value problem has a solution $x(t)$ on some time interval $(-\tau, \tau)$ about $t = 0$, and the solution is unique! [?]

In state space, each solution describes a trajectory, a path, that goes through its initial condition x_0 . The uniqueness of solutions implies that, within this time interval $(-\tau, \tau)$, different trajectories do not intersect in state space. This is a crucial property underlying all systems we study.

A useful notation for the evolution of a continuous dynamical system is through the evolution operator $\Phi^t(x)$, which, informally defined, evolves the point x forward t time units. That is, $\Phi^t(x(0)) = x(t)$.

2.1.2 The fate of linear dynamical systems

Although trajectories do not cross, they can share the same fate, meaning they can converge to the region in state space. We can introduce this notion with a very simple mathematical example of a linear system. It has the form

$$\dot{x}(t) = Ax(t) \quad (2.2)$$

where A is a constant $(n \times n)$ matrix.

If the eigenvalues $\lambda_i \in \mathbb{C}$ of A are all unique, its eigenvectors $v_i \in \mathbb{R}^n$ are linearly independent. Then, the general solution to this system can be written as Ref. [?]:

$$x(t) = \sum_{i=1}^n C_i e^{\lambda_i t} v_i. \quad (2.3)$$

Then, each initial condition determines the constant coefficients $C_i \in \mathbb{R}$. From Eq. ?? we can already notice that the origin of the system, $o = (0, \dots, 0)^T$, is a solution. In fact, it is an equilibrium: $\dot{x} = f(o) = 0$. A trajectory on the origin does not change over time.

As we see from Eq. ??, the behavior of trajectories depends on the eigenvalues λ_i of the matrix A . We can classify the equilibrium at the origin based on these eigenvalues, as shown in Fig. ???. If the real parts of all the eigenvalues are negative, then all trajectories in state space converge to the origin as $t \rightarrow \infty$. In this case, the origin is said to be a stable equilibrium (Figs. ??A-B). If at least one eigenvalue is negative, the trajectories diverge from the origin, which is then an unstable equilibrium (Figs. ??C-E). Stability here refers to the behavior of trajectories near the equilibrium. If it is stable, nearby trajectories converge to the equilibrium - or, equivalently, small perturbations that take a trajectory away from the equilibrium will eventually go back to the equilibrium. If it is unstable, then nearby trajectories diverge from it.

Stable equilibria are the only attracting solution, or attractor, of linear systems. In this case, although different trajectories cannot not intersect, they all converge to the origin as $t \rightarrow \infty$. In summary, the ultimate fate of linear systems is kind of boring: either trajectories end up at the origin or they diverge off to infinity. But the journey, the path that trajectories take before before the end, the *transient dynamics*, is more interesting. As shown in Fig. ??, this is dictated by the constellation of eigenvalues λ_i . For more details, the reader can refer to standard books on linear/nonlinear dynamics, such as Ref. [?].

2.1.3 The fate of nonlinear dynamical systems I: attractors

As just seen, stable equilibria are the only possible attractors in linear systems. Going beyond Eq.??, nonlinear systems can have more interesting and complicated long-term dynamics (Fig. ??). Stable equilibria are still possible, as shown in Figs. ??A-B. The system here is a conductance-based neuronal model following equations [?]

$$\begin{aligned} \dot{x} &= (I - g_L(x_i - E_L) - g_{Na}m_\infty(x_i)(x_i - E_{Na}) - g_Ky_i(x_i - E_K))/C, \\ \dot{y} &= (n_\infty(x) - y_i)/\tau, \end{aligned} \quad (2.4)$$

with all parameters and functions defined in detail in Chapter ???. The input current I is chosen to be $I = 2.0$ so the system has excitable dynamics. Its state space is composed of a stable equilibrium, the only attractor, and two unstable equilibria, which create excitable dynamics. Excitability is a type of transient different than seen for linear systems. Some trajectories are forced to go on long excursions (excitations) before converging to the stable equilibrium. We study more about this again in Chapter ??.

Besides equilibria, nonlinear systems can also have periodic solutions. These orbits vary in time with a certain period T (Fig. ??C) and correspond to closed curves in state space (Fig. ??). In several cases these periodic solutions are isolated, in the sense that there are no other periodic orbits in some neighborhood around them. In that case, they

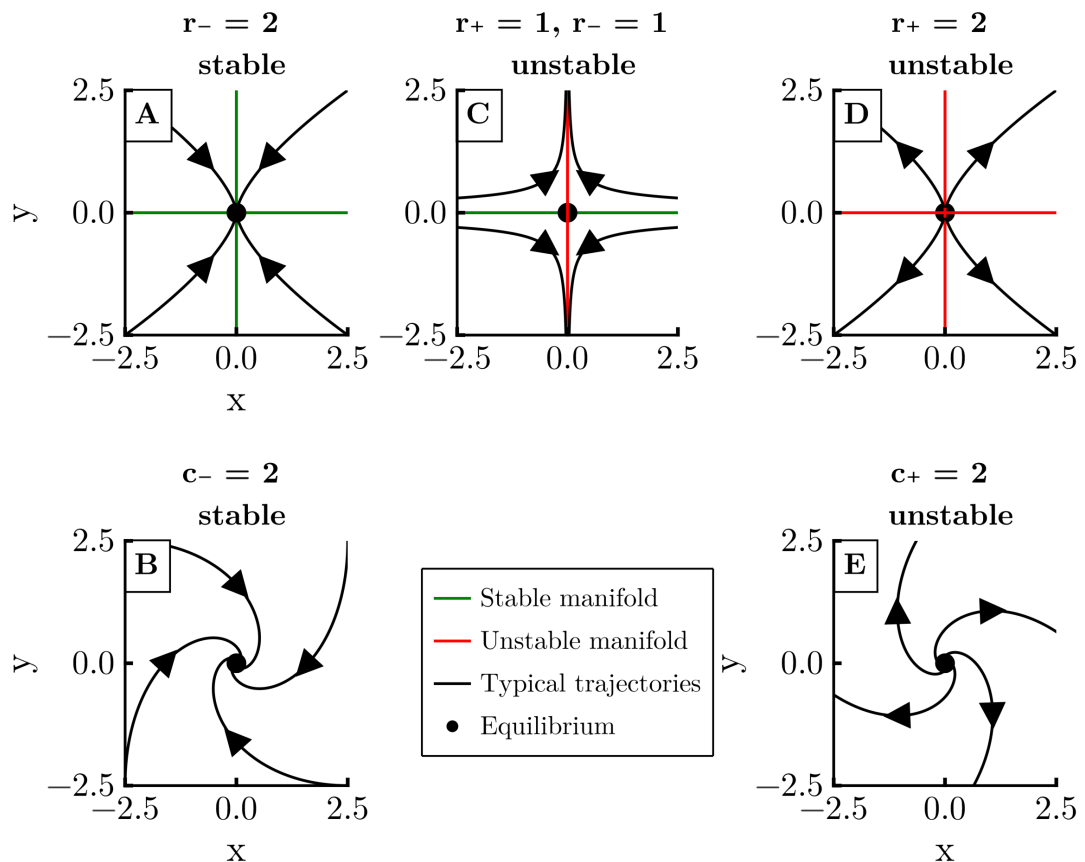


Figure 2.1: **Hyperbolic equilibria in 2D linear systems.** The title specifies the number of eigenvalues that are purely real negative r_- or positive r_+ , or that are complex with real part negative c_- or positive c_+ . The first row shows equilibria whose eigenvalues are purely real, while the second one shows equilibria with complex eigenvalues. In the first column, the equilibria are stable - they are the two possible attractors in linear systems. In the second column, we have a saddle-point for purely real eigenvalues. In the third column, the equilibria are completely unstable, known as repellers.

are called limit cycles. The system used in this example is still the neuronal model of Eq.??, but with a different parameter $I = 6$, which leads to the system now having a stable limit cycle. We see in this figure again an example of a long transient, with the trajectory initially going on a long excursion before converging to the limit cycle.

Not all curves in state space are closed, however. One can have quasiperiodic dynamics, in which trajectories never repeat exactly, although they might almost repeat. This is seen in Figs. ??E-F. Simulating the trajectory for longer times would fill up the figure more and more. Further, note the varying amplitude of the time series. The system in this example is the forced Van der Pol oscillator,

$$\dot{x} = v \quad (2.5)$$

$$\dot{v} = \mu(1 - x^2)v - \alpha x + g \cos(\omega_f t),, \quad (2.6)$$

with parameters $\mu = 0.1$, $\alpha = 1.0$, $g = 0.5$, $\omega_f = \sqrt{3}$ taken from Ref.[?].

Finally, one can also have chaotic attractors (Figs. ??G-H). These solutions have a wild behavior that nearby trajectories tend to diverge at an exponential rate []. Despite this local divergence, however, the solutions remain bounded in space. In other words, systems with chaotic attractors are very sensitive to the initial conditions - small changes in initial conditions lead to trajectories that can look very different. The system used to generate is shown as the Lorenz system, with equations

$$\dot{x} = \sigma(y - x) \quad (2.7)$$

$$\dot{y} = x(\rho - z) - y \quad (2.8)$$

$$\dot{z} = x * y - \beta * z, \quad (2.9)$$

and $\sigma = 10$, $\rho = 28$, $\beta = 8/3$. This chaotic attractor in particular has a shape that resembles a butterfly, with trajectories spending some time on one wing before switching to the other wing [?].

Given now these examples, let us now define the terms we have used a bit more properly.

2.1.4 Formalizing attractors and basins

We have just presented examples of attractors, sets of points in state space to which trajectories eventually converge, and their basins of attraction, the regions containing those converging trajectories. Since in this thesis we will deal a lot with these concepts, we provide now an attempt at formalizing. The idea is to have the concepts clear in mind for later. In practice, we will only use the informal definition we just gave. In particular, the definition of attractor can vary considerably in the literature. Without attempting to claim any superiority, we attempt here to provide a definition that suits our studies.

First, we define an omega limit set $\omega(x)$ of a point $x_0 \in M$ as [?]:

$$\omega(x_0) = \{x : \forall T \forall \epsilon > 0 \text{ there exists } t > T \text{ such that } |f(x_0, t) - x| < \epsilon\}. \quad (2.10)$$

Consider a point $x \in \omega(x_0)$ in the ω limit set of x_0 . Then, by definition, a trajectory that passes through x_0 comes arbitrarily close to x infinitely often as t increases.

From this, we can define the *basin of attraction* of a set A as $\mathcal{B}(A) = \{x \in M : \omega(x) \subset A\}$. This only looks at the long-term behavior of trajectories; the transient

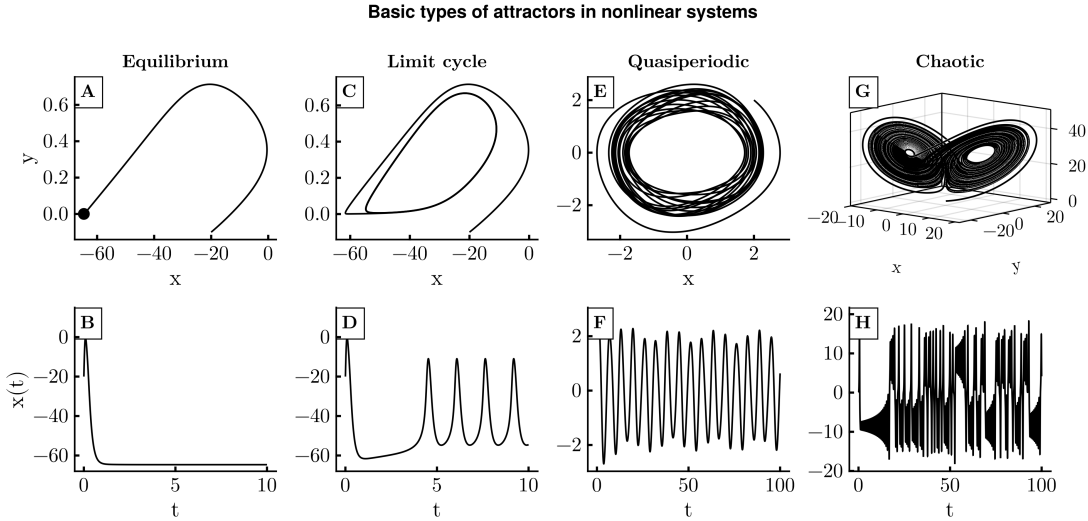


Figure 2.2: **Basic types of attractors in nonlinear dynamical systems.** Each column shows respectively the state space and a time-series of a typical trajectory converging to a type of attractor. The first column corresponds to the neuronal model of Eq.?? with $I = 2.0$, which has excitable dynamics, converging to a stable equilibrium. The second column shows again the neuronal system of Eq.?? but with $I = 6.0$, when the attractor is now a stable limit cycle. The third column shows the system defined in Eqs.??, with a quasiperiodic attractor Finally, column four has an example of a chaotic trajectory on the Lorenz system (Eq. ??).

dynamics could be anything, including the case that trajectories go very far from A , as long as they go back to it and stay there eventually.

Now to define an attractor, we first define a weaker (or, on the more optimistic side, a more general) version, called the *Milnor attractor*. It is a useful concept when dealing with metastability. A set A is a Milnor attractor if:

1. Its basin of attraction $\mathcal{B}(A)$ has strictly positive measure (i.e., if $m(\mathcal{B}(A)) > 0$), where $m(S)$ denotes a measure equivalent to the Lebesgue measure of set S [?]. This condition says that there is some probability that a randomly chosen point will be attracted to A [?].
2. For any closed proper subset $A' \subset A$, the set difference $\mathcal{B}(A) \setminus \mathcal{B}(A')$ also has strictly positive measure. This ensures that every part of A plays an essential role - one cannot decompose A into an attracting part and another part that does not attract [?, ?]. A closed set here means that it contains all its limit points. And proper means its non-empty.

Furthermore, the Milnor attractor does not have to attract all the points in its neighborhood, and there can also be orbits that transiently go very far from the attractor, even if initially close, before eventually getting close to it. Further, it can in principle be composed into the union of two smaller Milnor attractors. To avoid these cases, we call a set A an *attractor* if

1. A is a Milnor attractor.

2. A contains an orbit that is dense in A . Basically, this means that there is an orbit in A that passes arbitrarily close to every point in A . This condition ensures that the attractor is not the union of two smaller attracting sets [?].
3. There are arbitrarily small neighborhoods U of A such that $\forall x \in U$ one has $\Phi^t(x) \subset U \forall t > 0$ and such that $\forall y \in U$ one has $\omega(y) \subset \omega(x)$. That is, there are arbitrarily small neighborhoods around the attractor in which points inside stay inside and converge to A . This criterion is given in Ref. [?].

2.1.5 Invariant manifolds: structures that organize state space

In Sec. ?? we only considered the case when all the eigenvalues of the matrix A in the linear system $\dot{x} = Ax$ were positive. If one eigenvalue λ_k is positive, then trajectories will diverge to infinity following the corresponding eigenvector v_k . When some eigenvalues are positive, and some are negative, the origin is a saddle-point. If all eigenvalues are positive, it is called a repeller. Figure ?? shows examples of equilibria in 2D linear systems. Note that typical trajectories approach the saddle-point along the y -axis and then diverge along the x -axis. That is, for $t \rightarrow -\infty$, trajectories converge to the y -axis and for $t \rightarrow \infty$ they converge to the x -axis. The y -axis is called the stable manifold $\mathbb{W}^s(o)$ of the origin o and the x -axis is the unstable manifold $\mathbb{W}^u(o)$ of the origin. We can define these manifolds

$$\mathbb{W}^s(o) = \{x \in M : \Phi^t(x) \rightarrow o \text{ as } t \rightarrow \infty\}, \quad \mathbb{W}^u(o) = \{x \in M : \Phi^t(x) \rightarrow o \text{ as } t \rightarrow -\infty\}. \quad (2.11)$$

Let us separate the eigenvectors v_i into two parts: the ones with negative eigenvalues $v_1^-, \dots, v_{n_s}^-$ and the ones with positive eigenvalues $v_1^+, \dots, v_{n_u}^+$. Then we can define the stable and unstable subspaces, respectively, as

$$\mathbb{E}^s = \text{span}(v_1^-, \dots, v_{n_s}^-) \quad \mathbb{E}^u = \text{span}(v_1^+, \dots, v_{n_u}^+) \quad (2.12)$$

For a linear system, the stable manifold of the origin coincides with the stable space \mathbb{E}^s and the unstable manifold coincides with the unstable space. In general, as in the example of the saddle-point, these manifolds act to organize the behavior of trajectories in state space.

These concepts can be extended for nonlinear systems. To do this, the first step is to think about the linearization of the nonlinear system. Suppose our nonlinear system of interest has an equilibrium $x^* \in M$. It turns out that the behavior sufficiently close to this equilibrium is linear, despite the system globally being nonlinear [?, ?]! To see this, we first move the origin of our system to x^* by defining a new variable $y(t) = x(t) - x^*$. Then,

$$\dot{y} = \dot{x} = f(y + x^*) \equiv g(y) \quad (2.13)$$

where we define a convenience function $g(y)$. Expanding $g(y)$ around $y = 0$ (i.e., around the equilibrium $x(t) = x^*$) gives us

$$\dot{y} = g(0) + J_g(0)y + \mathcal{O}(y^2), \quad (2.14)$$

where $J_g(y) = \frac{\partial g_i(y)}{\partial y_j}$ is the Jacobian of g . It is related to the Jacobian of f by $J_g(y) = J_f(x)$, so $J_g(y=0) = J_f(x=x^*)$. Since $g(0) = f(x^*) = 0$, then if we are

sufficiently close to the origin we can also ignore the terms $\mathcal{O}(y^2)$ and therefore we get

$$\dot{y} = J_g(0)y. \quad (2.15)$$

That is, the behavior of the nonlinear system sufficiently close to the equilibrium is linear, with the constant matrix function being the Jacobian evaluated at the equilibrium!

But the good news don't stop here! There is the Hartman-Grobman theorem, which basically shows that the state space near a hyperbolic equilibrium to the state space of the linearization. An equilibrium is hyperbolic if the eigenvalues of the Jacobian evaluated on it are all nonzero, i.e., if $\lambda_i \neq 0 \forall i = 1, \dots, n$. *Topologically equivalent* means that the linearized state space and the local state space near the equilibrium are distorted versions of each other. They can be bended and warped, but not ripped. In particular, closed orbits have to remain closed, and connections between saddle points have to remain [?]. Mathematically, topologically equivalent means there is a *homeomorphism* (continuous deformation with continuous inverse) from one state space into the other; trajectories can be mapped from one to the other, and the direction of time is the same [?].

Stating the theorem more formally, suppose a hyperbolic equilibrium $x^* \in M$ such that $f(x^*) = 0$ and such that all its eigenvalues are nonzero. Then, there is a neighborhood N of x^* and a homeomorphism $h : N \rightarrow M$ such that [?]

- $h(x^*) = 0$
- the flow $\dot{x} = f(x)$ in N is topologically conjugate to the flow of the linearization $\dot{y} = Ay$ by the continuous map $y = h(x)$. Topologically conjugate basically meaning a change of coordinates in a topological sense.

This guarantees that the stability of the equilibrium is the same in both cases, so we can use the linearization to gain important insights about the stability of equilibria in the nonlinear system!

What about the stable and unstable manifolds? In analogy to the linear case, we can define local stable and unstable sets near a neighborhood U of an equilibrium x^* for the nonlinear system [?]:

$$\mathbb{W}_{\text{loc}}^s(x^*) = \{x \in M : \Phi^t(x) \rightarrow o \text{ as } t \rightarrow +\infty \text{ and } \Phi^t(x) \in U \forall t \geq 0\}, \quad (2.16)$$

$$\mathbb{W}_{\text{loc}}^u(x^*) = \{x \in M : \Phi^t(x) \rightarrow o \text{ as } t \rightarrow -\infty \text{ and } \Phi^t(x) \in U \forall t \leq 0\}. \quad (2.17)$$

Herein comes the stable manifold theorem. It states that, for a hyperbolic equilibrium x^* :

- The local stable set $\mathbb{W}_{\text{loc}}^s(x^*)$ is a smooth manifold whose tangent space has the same dimension n_s as the stable space \mathbb{E}^s of the linearization of f at x^* . $\mathbb{W}_{\text{loc}}^s(x^*)$ is also tangent to \mathbb{E}^s at x^* .
- The local unstable set $\mathbb{W}_{\text{loc}}^u(x^*)$ is a smooth manifold whose tangent space has the same dimension n_u as the unstable space \mathbb{E}^u of the linearization of f at x^* . $\mathbb{W}_{\text{loc}}^u(x^*)$ is also tangent to \mathbb{E}^u at x^* .

The homeomorphism guaranteed by the Hartman-Grobman theorem maps $\mathbb{W}_{\text{loc}}^s(x^*)$ into \mathbb{E}^s and $\mathbb{W}_{\text{loc}}^u(x^*)$ into \mathbb{E}^u one-to-one, as shown in Fig. XX. Further, the stable manifold theorem guarantees that \mathbb{E}^s and \mathbb{E}^u actually approximate the local manifolds

$\mathbb{W}_{\text{loc}}^s(x^*)$ and $\mathbb{W}_{\text{loc}}^u(x^*)$, respectively [?]. As a consequence, we get the behavior illustrated in Fig. ??

The manifolds we just looked at are defined for a local neighborhood U around the equilibrium. We can extend them towards the whole of state space by defining global manifolds as:

$$\mathbb{W}^s(x^*) = \bigcup_{t \leq 0} \Phi^t(\mathbb{W}_{\text{loc}}^s(x^*)) \quad (2.18)$$

$$\mathbb{W}^u(x^*) = \bigcup_{t \geq 0} \Phi^t(\mathbb{W}_{\text{loc}}^u(x^*)) \quad (2.19)$$

That is, the global stable manifold is obtained by integrating the local stable manifold backwards, looking at where the trajectories on it came from. For the unstable manifold, we integrate the local unstable manifold forwards, to see where it goes to.

An important fact about the local and global manifolds that follows from their definitions is that they are invariant: trajectories starting on these manifolds stay on them forever [?]. Furthermore, the uniqueness of solutions prohibits certain crossings of manifolds: stable manifolds of two distinct equilibria cannot cross, unstable manifolds of two distinct equilibria also cannot, and the same manifold cannot cross itself - otherwise, where the crossing points would have to obey two distinct paths! Meanwhile, stable and unstable manifolds, either of the same equilibrium or of two different equilibria can cross.

As mentioned before, these manifolds usually play a big role in organizing state space. As we will see in Chapter ??, they can organize the transient dynamics of systems. There, we study a dynamical system wherein certain trajectories are forced to go on long excursions before converging to the stable equilibrium, the only attractor in state space (see Figs. ??A-B). As explained there, this long excursion is generated by the arrangement of the invariant manifolds of the saddle-point that exists in state space. The invariant manifolds can also organize the long-term behavior of systems: the next section briefly shows how stable manifolds of unstable equilibria can act as the boundary separating two basins of attraction.

2.1.6 The fate of nonlinear dynamical systems II: multistability and basins of attraction

In Sec. ?? we saw that the ultimate fate of nonlinear systems, their attractors, can be much more complicated than that of linear ones. Not only are the attractors themselves complicated, but they can also coexist in state space. If there are two coexisting attractors, this means that the state space will be separated into three regions: the basin of attraction of attractor one, the basin of attractor two, and the boundary between them. Usually, the basin boundary is formed by stable manifolds of saddle-type objects: saddle-points, saddle-limit-cycles, and even chaotic saddles! [?]. Figure ?? illustrates this for a relatively simple system with two stable equilibria, where the basin boundary is the stable manifold of the saddle-point in the middle. This system is known as the Duffing oscillator:

$$\dot{x} = v \quad (2.20)$$

$$\dot{v} = -(-kx + cv + lx^3)/m, \quad (2.21)$$

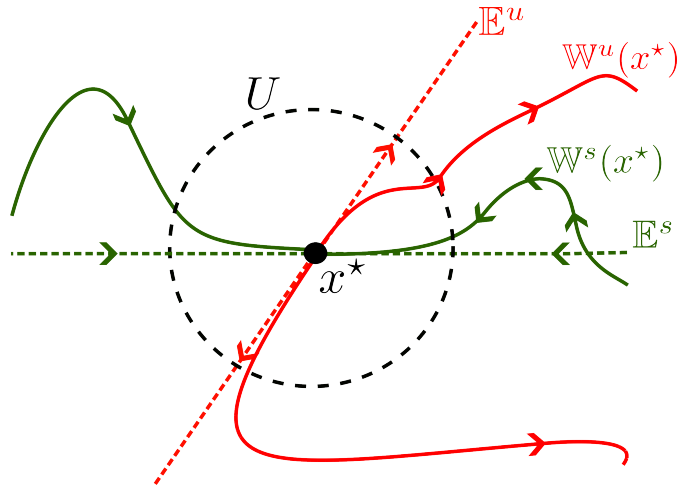


Figure 2.3: **Invariant manifolds of saddle point x^* .** The local stable $W_{\text{loc}}^s(x^*)$ and unstable $W_{\text{loc}}^u(x^*)$ manifolds of the saddle point x^* respectively can be associated with the stable E^s and unstable E^u subspaces and become tangent to them near the saddle. This follows from the Hartman-Grobman and the stable manifold theorems. The global stable $W^s(x^*)$ and unstable $W^u(x^*)$ manifolds extend the definition of the local manifolds beyond the neighborhood U . Figure is inspired by Fig. 6.2.4 from Ref. [?].

with $k = 1$, $c = 0.5$, $l = 1$, $m = 1$. This system represents a ball of mass m rolling downhill at position x and velocity v on a quartic potential landscape of the form $U(x) = -lx^4/4 - kx^2/2$ with a friction term $-cv$. Following the definition of global manifolds in Eq.??, these global manifolds are essentially obtained by integrating trajectories starting on the local manifolds of the saddle-point.

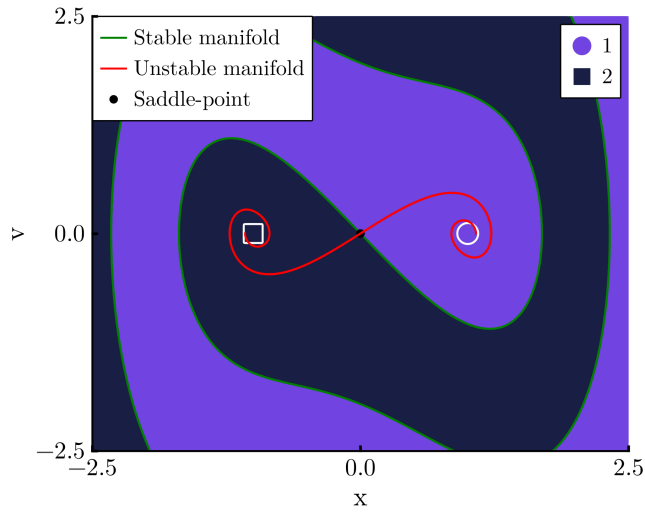


Figure 2.4: **Bistability in Duffing model.** Two stable equilibria (white square and circle) are shown with their respective basins of attraction in two shades of purple. The global stable and unstable manifolds of the saddle-point (black point) in the middle are also shown as green and red lines respectively. The global stable manifold of the saddle coincides with the boundary between the basins.

In this thesis we study two examples of multistability occurring in networked systems. In Chapter ?? we study networks of Kuramoto units, and see there the coexistence of multiple attractors depending on how strongly the units are interacting. We also see how this multistability impacts the sensitivity of the system to small changes in parameters of the units. Later, in Chapter ?? we study how multistability arises when two excitable neurons are coupled together diffusively. Both studies require that we find the attractors in the systems. This is what we deal with in the next section.

2.1.7 How to find attractors

Finding all the attractors of a given dynamical system is not necessarily a trivial task. For equilibria, one can find all the roots of the system function, i.e., $f(x^*) = 0$ and then check their stability through the eigenvalues of the Jacobian evaluated on them. However, problem becomes more complicated for other types of attractors. To start off, simply proving that a set is an attractor, following the criteria given in Sec. ??, is usually not possible. Instead, in practice we use the looser definition of an attractor simply as the long-term dynamics of trajectories. Numerically, this means a brute-force approach of simulating several trajectories in state space for long integration times and seeing where they converge.

This comes with two problems. First, it does not rule out the possibility that a certain set is just a very long transient. To remedy this, we usually integrate trajectories on the set for very long and check if there is any escape. Second, some attractors might have very small basins of attraction, such that randomly chosen initial conditions are unlikely to end on them, so it is unlikely that we find those attractors. So far, however, this brute force approach is the best we have for general systems []. Within this approach, there are two main methods in the literature for finding attractors. They differ in how they check convergence to attractors.

The first approach was proposed in Ref. [?] and implemented with improvements in Ref. [?]. The idea is that a typical trajectory, initialized in a certain box in state space, will evolve, visiting other boxes, until it converges to the attractor. It will then stay on the attractor, repeatedly visiting the same state space boxes. Using this idea, the algorithm discretizes the state space into boxes, integrates trajectories, and looks for recurrences. Then, basically, when boxes are visited repeatedly a certain prescribed amount of times, then it considers that these boxes constitute the attractor. It is also smart in that it keeps track of the state of each box. So it knows that the boxes visited by the trajectory before converging to the attractor - the transient section of the trajectory - belongs to the basin of attraction of that attractor. This algorithm works really well for periodic, quasiperiodic, and chaotic attractors in low-dimensional systems. For chaotic attractors in high-dimensional systems it does not work well, because the time that trajectories take to recur on a chaotic attractor becomes too long to simulate numerically.

An alternative approach does not rely on discretizing state space, and is designed to work well for high-dimensional systems. In this case, one spreads a number \mathcal{N} of initial conditions in state space and integrates them to obtain \mathcal{N} trajectories. Each trajectory $x(t)$ is then converted to a vector of features $\mathcal{F} \in \mathbb{R}^n$ of n numbers that all collectively describe the trajectory. This is done by the featurizing function $\phi : M \times \mathbb{R} \rightarrow \mathbb{R}^n$, such that $\mathcal{F} = \phi(x(t), t)$. Each attractor should correspond to a unique \mathcal{F} . Then, the \mathcal{N} vectors of features are grouped together via any of several possible grouping or clustering

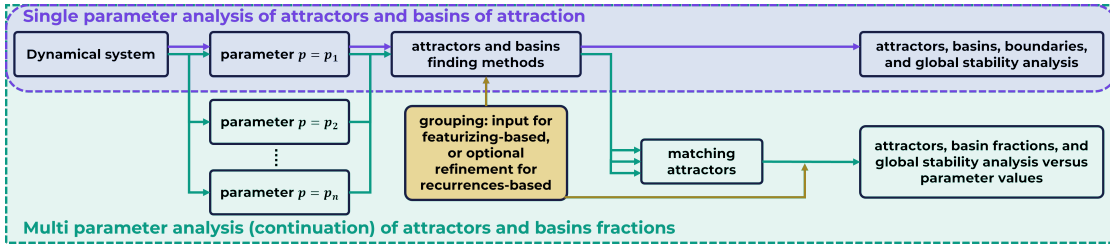


Figure 2.5: **Schematic illustration of the continuation method used to find and match attractors across a parameter range.** The first row illustrates the single-parameter attractor finding algorithms. The second row illustrates how they can be combined across parameters to perform a continuation analysis. Figure taken from Ref. [?].

algorithms, and each grouping corresponds to one attractor. This approach can work very well, but it relies on pre-existing knowledge about the system to find a suitable featurizer function ϕ . To be confident about the results, one also has to verify that the total integration time is long enough, and that the transients of all trajectories were removed. This relies on experimentation. This method has been proposed in Ref. [?] and soon thereafter also in Ref. [?]. Together with colleagues, I implemented efficient and open-source code for this method with improvements in the `Attractors.jl` package Ref. [?].

Both methods can be applied across a parameter range and used in a continuation fashion, as illustrated in Fig. ??A. For the first parameter, the attractors of the system are found using any of the two methods just described. Then, points on these attractors are used as additional initial conditions for the next parameter value. The originally prescribed initial conditions, together with the original ones, are then used to find attractors in the subsequent parameter value. This process of seeding initial conditions from the previously found attractors is repeated for the whole parameter range. Then, one has all the attractors for each parameter value, and the remaining problem is to link attractors from one parameter to the next. This matching of attractors is done by computing the distance between attractors at one parameter to attractors at the previous parameter, and matching the attractors by the shortest distance. The distance metric can be chosen by the user, including Euclidean distance between the centroids of the attractors, or a Hausdorff distance, or distance between the features of the attractors. I have also collaborated in the implementation of this method in efficient and open-source code, described in the publication in Ref. [?].

2.2 Basics of bifurcations

What happens to the attractors - and, in general, to the state space structures - of a dynamical system when we vary its parameters? In terms of the qualitative properties, there are two possibilities: either they stay similar or they change drastically. We can be a bit more rigorous. Two systems are qualitatively similar if they are topologically equivalent. The notion of topological equivalence was already mentioned in Sec. ???. As a reminder, two systems are topologically equivalent if the state space of one can be obtained by a continuous transformation of the other [?]. Mathematically, this means

that they are topologically equivalent if there is a homeomorphism $h : M \rightarrow M$ mapping orbits of the first system onto orbits of the second, preserving the direction of time.

As the parameters of a system are varied, we obtain different dynamical systems that are usually topologically equivalent. The attractors, for instance, may move, but they retain their stability. At some point, however, there may be a drastic change, and the new system may no longer be equivalent. The attractor may have disappeared, or lost its stability. Or a new attractor may have emerged. These drastic qualitative changes in the behavior of a dynamical system are called bifurcations. A bit more rigorously, a bifurcation is a change in the topological type of a system as its parameters pass through a critical (bifurcation) value [?]. There are many different types of bifurcations, and one can literally write a whole book about this [?]. For this thesis we focus briefly on just a few bifurcations that will be relevant for later. For simplicity, we focus also on the simplest version of these bifurcations.

2.2.1 Saddle-node bifurcation of equilibria

In a saddle-node bifurcation of equilibria we see the emergence, or destruction, of a stable (node) and an unstable (saddle) equilibrium. Starting from the side of the bifurcation in which the equilibria exist and approaching the bifurcation parameter, we see the equilibria approaching each other, coalescing at the critical parameter, and annihilating each other thereafter. The simplest form of this bifurcation occurs in one dimension in the system

$$\dot{x} = f(x) = \alpha + x^2, \quad (2.22)$$

with the critical value of the bifurcation being $\alpha = 0$. As shown in Figs. ??, for $\alpha < 0$ we see that the parabola $f(x)$ has two roots, so the system has two equilibria, in positions $x^* = \pm\sqrt{-\alpha}$. From the figure directly we can already see that the equilibrium on the left is stable and the equilibrium on right is unstable. We can confirm this with a linearization analysis - the Jacobian here is simply $df/dx = 2x$, so the eigenvalue of the left and right equilibrium are $-2\sqrt{-\alpha}$ and $+2\sqrt{-\alpha}$. As α increases towards 0 the parabola moves up, the equilibria approach each other, their eigenvalues approach zero, and at $\alpha = 0$ they all coalesce into one single equilibrium. At this point, the eigenvalue of the system is zero: this equilibrium is non-hyperbolic! For $\alpha > 0$ there are no more equilibria. Equation ?? is called the normal form of the saddle-node bifurcation, because any generic system obeying some conditions will be topologically equivalent to it locally, near the equilibrium. For a system $\dot{x} = f(x, p)$, with $x \in \mathbb{R}$ and $p \in \mathbb{R}$, $\partial f(0, 0)/\partial x = 0$, an equilibrium $x = 0$ at the critical parameter $\alpha = 0$, the conditions are [?]:

$$\frac{\partial^2 f(0, 0)}{\partial x^2} \neq 0 \quad (2.23)$$

$$\frac{\partial f(0, 0)}{\partial \alpha} \neq 0. \quad (2.24)$$

They guarantee that the system $\dot{x} = f(x, p)$ can be transformed into Eq. ?? or into $\dot{x} = \alpha - x^2$, which just inverts the direction of α .

After the two equilibria are destroyed, the system does not have an Just after the bifurcation, the region previously occupied by the two equilibria is still quite slow. Note how \dot{x} is very close to zero near $x = 0$ in Fig.?.?. This region of slow flow is called the ghost of the saddle-node [?]. In a way, it retains properties of the two equilibria

- particular, trajectories still flow towards the ghost from the side previously occupied by the stable equilibrium, remain in its neighborhood for a while, but then eventually depart through the side previously occupied by the unstable equilibrium [?]. The ghost is not an invariant set, but is an example of a metastable regime, which we study in greater depth in Chapter ??.

Saddle-node bifurcations can also occur analogously for periodic orbits [?] - a stable limit cycle then collides with an unstable limit cycle, and leave behind a ghost of a limit cycle!

2.2.2 Hopf bifurcation

Keeping with the spirit of describing the simplest cases, let us now imagine a system written in polar coordinates (ρ, θ) :

$$\dot{\rho} = f_\rho = \rho(\alpha - \rho^2) \quad (2.25)$$

$$\dot{\phi} = f_\phi = 1. \quad (2.26)$$

Because the two equations are decoupled, we can analyse the ρ equation separately first. First, note that its Jacobian $\partial f_\rho / \partial \rho = \alpha - 3\rho^2$. For all values of α , f_ρ has an equilibrium at $\rho = 0$ - with eigenvalue $\lambda = \alpha$. This is linearly stable for $\alpha < 0$ and linearly unstable for $\alpha > 0$. At $\alpha = 0$ it is non-hyperbolic! What happens then? The first equation has another root for $\alpha > 0$ at $\rho = \sqrt{\alpha}$ - so the eigenvalue is $\lambda = -2\alpha$. This equilibrium is unstable for $\alpha < 0$ and stable for $\alpha > 0$. Notice the change of stability of the equilibria: when one is unstable, the other is stable, and vice versa. Considered for f_ρ alone, this is an example of a Pitchfork bifurcation [?]. Considering the full system, with the rotation induced by $\dot{\phi} = 1$, the equilibrium at the origin remains an equilibrium, but the equilibrium at $\sqrt{\alpha}$ becomes a limit cycle with amplitude $\sqrt{\alpha}$. Putting everything together, we have the behavior in Fig. ??G-H. A stable limit cycle becomes unstable at $\alpha = 0$ and from it a stable limit cycle emerges. This is called a supercritical Hopf bifurcation [?]. If we write this system in Cartesian coordinates and compute the eigenvalues of the Jacobian at the origin, we see they are $\lambda_{1,2} = \alpha \pm i$. This gives us another general property of this bifurcation: at the critical point, the eigenvalues at the origin cross the imaginary axis.

Now consider the system

$$\dot{\rho} = f_\rho = \rho(\alpha + \rho^2) \quad (2.27)$$

$$\dot{\phi} = f_\phi = 1. \quad (2.28)$$

Now the Jacobian is $\partial f_\rho / \partial \rho = \alpha + 3\rho^2$. There is still an equilibrium at the origin, in which the eigenvalue is still α - its stability is the same as before. However, the other equilibrium, now $\sqrt{-\alpha}$ has the associated eigenvalue as -2α . It therefore exists for $\alpha < 0$ when it is unstable. This thus corresponds to an unstable limit cycle, which coexists with a stable equilibrium for $\alpha < 0$. For $\alpha > 0$, the limit cycle disappears and the system is left with only an unstable equilibrium. This is called a subcritical Hopf bifurcation [?]. The eigenvalues of the Cartesian Jacobian at the origin behave in the same way as for the supercritical Hopf.

2.2.3 Homoclinic bifurcation

Both the saddle-node and the Hopf bifurcations happen in the neighborhood of equilibria - for this reason, they are called local bifurcations. Now we move to a bifurcation in

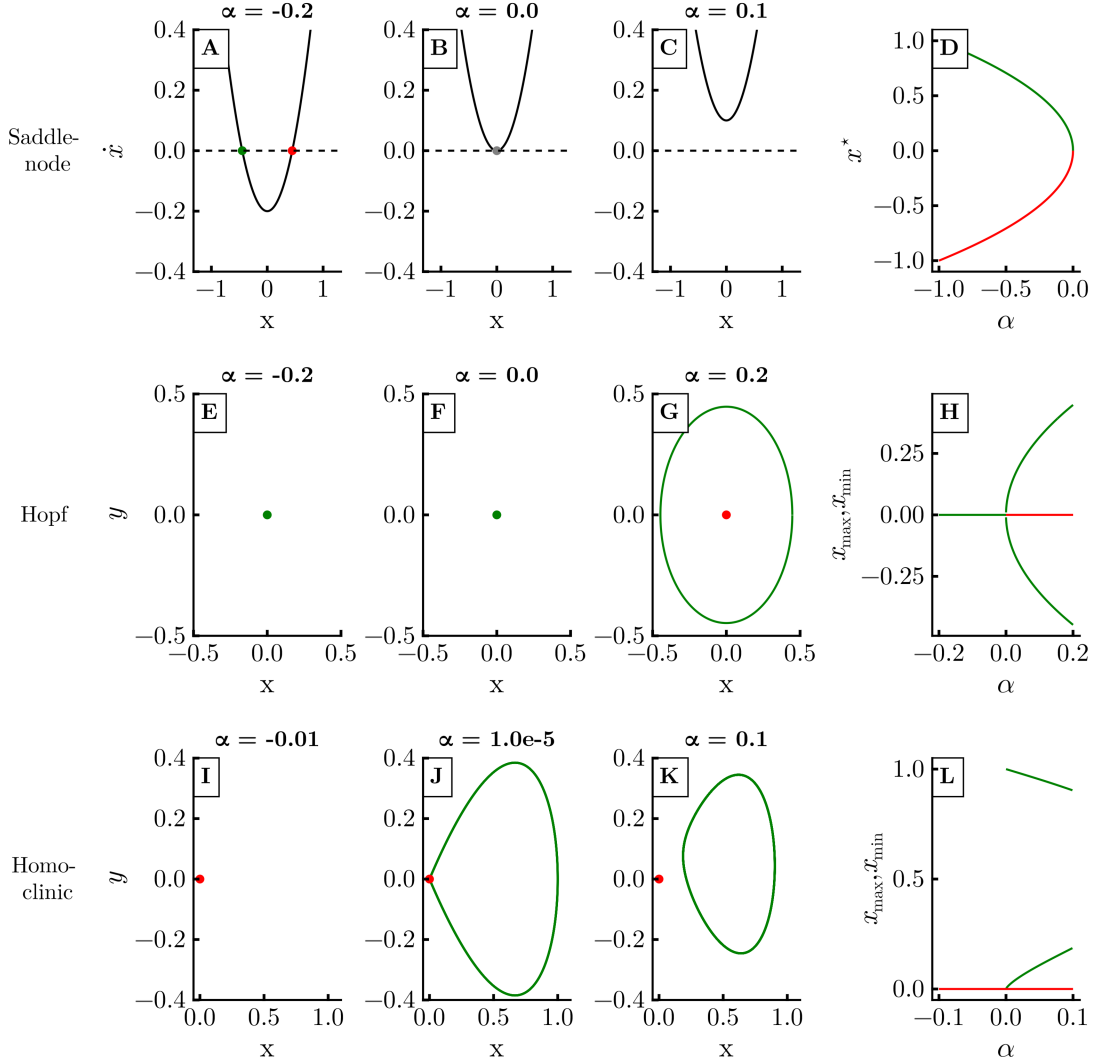


Figure 2.6: Some important bifurcations. The saddle-node bifurcation is shown for the normal form $\dot{x} = x^2 + \alpha$ in panels A-D. A stable and an unstable equilibria, represented respectively by green and red circles (panel A), come together as the bifurcation parameter α is changed. Eventually they coalesce (panel B) and are subsequently destroyed (panel C). The position of these equilibria as a function of α is shown in panel D. The supercritical Hopf bifurcation is shown for Eq. ?? in panels E-H. Before and at the bifurcation there is a stable equilibrium in state space (panels E and F respectively), which becomes unstable when a stable limit cycle emerges (panel G). Panel H shows this behavior as a function of α , taking the maximum and minimum values of x to represent the limit cycle. The homoclinic bifurcation to a saddle point is shown in panels I-L. Before the bifurcation there is a saddle point (panel I). At the bifurcation, an orbit homoclinic to this saddle point appears (represented approximately in panel J). After the bifurcation, a stable limit cycle emerges (panel K). This is also summarized in panel L.

which this is no longer the case - the state space beyond only the equilibrium is affected, and it is thus called a global bifurcation [?]. The formal description of this bifurcation is consequently more involved, and goes beyond the scope of this thesis. For here it is enough to describe the bifurcation more qualitatively.

In the homoclinic bifurcation we study here, occurring on the plane, we have the emergence of a limit cycle. Before the bifurcation, there is only a saddle point. At the bifurcation, the unstable manifold of the saddle becomes tangential to its own stable manifold - this constitutes a homoclinic orbit. After the bifurcation, the homoclinic orbit becomes a limit cycle whose stability depends on the eigenvalues of the saddle. Defining the saddle quantity $\sigma = \lambda_1 + \lambda_2$, it can be shown [?] that the limit cycle is stable for $\sigma < 0$ and unstable if $\sigma > 0$.

Varying the bifurcation parameter α close to the homoclinic orbit, the limit cycle approaches more and more the saddle point, and touches it at $\alpha = \alpha_c$. The region of the limit cycle close to the saddle-point has a very slow dynamics, such that the period of the limit cycle diverges to infinity as the critical point is approached. In higher dimensional systems, different types of homoclinic bifurcations are possible, with potentially much more complicated dynamics. The homoclinic bifurcations we deal with in this thesis are always related to simple saddle points, and so are analogous to the planar case shown now.

An example of a planar system with this bifurcation is due to Sandstede [?]

$$\dot{x} = -x + 2y + x^2 \quad (2.29)$$

$$\dot{y} = (2 - \alpha)x - y - 3x^2 + (3/2)xy. \quad (2.30)$$

The origin is a saddle which, at $\alpha = 0$, has eigenvalues $\lambda_1 = 1$ and $\lambda_2 = -3$ - its saddle quantity is therefore $\sigma = 2 < 0$, so the limit cycle that emerges here is stable [?].

2.3 Basics of network theory

An incredibly powerful abstraction about real-world systems can be achieved through the concept of networks, here used as synonyms for graphs, which are composed of nodes that are connected by edges. Networks can represent friendships - with people being the nodes and their friendships being the edges -, brain circuits - neurons are nodes, synapses are edges [?] -, ecological systems - for instance, ecological regions are nodes, and migrations between them are edges [?]. In this thesis we make use of this abstraction and consider that the nodes are dynamical systems $\dot{x}_i = f(x_i)$, $x_i \in \mathbb{R}^n$ on their own, with certain interactions between them. Together, the whole networked system is a dynamical system of the form:

$$\dot{x}_i = f(x_i) + \sum_{j=1}^N A_{ij}g(x_j, x_i), \quad i = 1, \dots, N \quad (2.31)$$

with N units, whose interactions are described by the function g . The adjacency matrix A_{ij} describes the strength of interactions between the units. Typically it is a binary matrix, such that $A_{ij} = 1$ if unit i receives a connection from unit j and $A_{ij} = 0$ otherwise. It can also be weighted, in which case the entry $A_{ij} \in \mathbb{R}$ represents the strength of interactions. Usually for binary matrices, we rewrite Eq. ?? as

$$\dot{x}_i = f(x_i) + \sum_{j \in \Omega_i} g(x_j, x_i), \quad i = 1, \dots, N \quad (2.32)$$

where $\Omega_i = \{j \in [1, N] : A_{ij} = 1\}$ is called the neighborhood of unit i . The number of elements in Ω_i , i.e., the number of connections of unit i , is called the unit's degree.

The adjacency matrix A describes the topology of the network, meaning the architecture of the connections. There are many different types of topologies, which describe well different types of systems. One type of topology is the regular, also called k -nearest-neighbors topology. As the name suggests, one can think of all nodes arranged on a ring, with each node connected to the k nearest nodes on each side. Another type of topology is the random topology, in which connections are chosen at random between the nodes. One consider the regular and random topologies as two extremes, and interpolate between them in what is called the Watts-Strogatz algorithm [?]. In this case, one starts with a k -nearest neighbor ring of nodes. Then, choose connections with a probability p . For each chosen connection (i, j) , keep the source node i , randomly choose a new node j' in the network, and switch (i, j) to (i, j') . This effectively switches short-range connections (between nearest nodes) to long range connections (between nodes that are potentially far away). For this rewiring probability p at $p = 0$ one has the regular topology; for $p = 1$ one has the random topology.

Informally speaking, a regular network is considerably clustered, with its short-range structures. And the average distance (in terms of numbers of edges) in the network is considerably high. In a random network, clustering is very small, but the average distance is small. One can formalize these concepts and show how this transition occurs as p is changed [?]. Here, we mention that, when p is relatively small, only a few short-range connections are rewired as long-range. This does not change the clustering characteristics much, but considerably lowers the average distance between nodes - those few long-range connections act as efficient shortcuts between nodes. Networks in this regime are usually called small-world networks [?].

In Chap. ?? we also study distance-dependent networks. The adjacency matrix is then defined as

$$A_{ij} = \frac{1}{\eta(\alpha)(d_{ij})^\alpha}, \quad (2.33)$$

with $d_{ij} = \min(|i - j|, N - |i - j|)$ is the edge distance along the ring, and $\eta(\alpha) = \sum_{j=1}^{N'} \frac{2}{j^\alpha}$ is a normalization term. All units are thus connected, but the weight of the connections decays with the distance following the α parameter. This parameter can also be called the locality parameter, since $\alpha = 0$ leads to an all-to-all equally connected network and $\alpha \rightarrow \infty$ leads to a first-nearest-neighbor topology ($k = 1$). In between we get distance-dependent weights.

2.4 Basics of Kuramoto oscillators

2.4.1 Derivation of the model and transition to synchronization

The Kuramoto model, written in general as

$$\dot{\theta}_i = \omega_i + \epsilon \sum_{j=1}^N A_{ij} \sin(\theta_j - \theta_i) \quad (2.34)$$

serves as a paradigm for studies on synchronization phenomena [?]. Its usefulness comes it being simple enough to be mathematically tractable, sufficiently generic, and

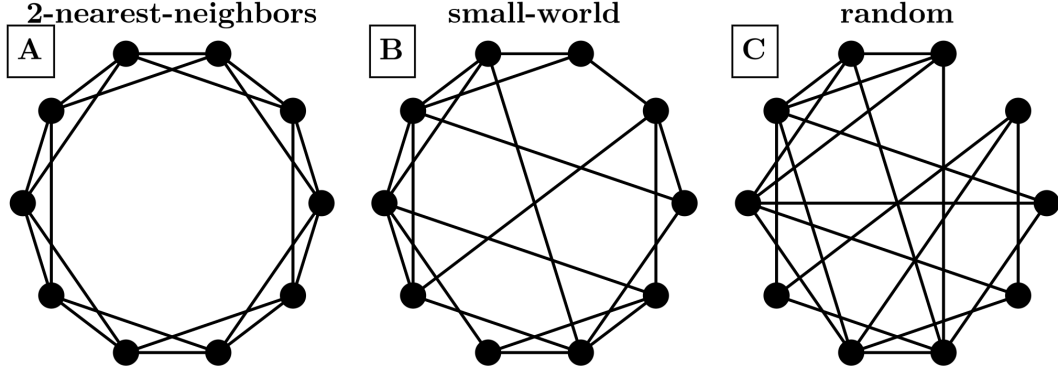


Figure 2.7: Illustration of networks generated by the Watts-Strogatz procedure. First, a k -nearest neighbor topology is created (Panel A). Then, some connections are randomly rewired, keeping the source node but changing the target node. With a few rewirings, this creates small-world networks (Panel B). With many rewirings, the network becomes randomly connected (Panel C).

also complex enough to display interesting dynamics. To reach it, Kuramoto started from generic oscillators near supercritical Hopf bifurcations. Each unit i follows

$$\dot{Q}_i = (i\omega + \alpha)Q_i - \beta|Q_i|^2Q_i, \quad (2.35)$$

where ω is the natural frequency of the oscillator, $\alpha > 0$ and $\beta > 0$ are parameters and $Q \in \mathbb{C}$. This is the normal form of the Hopf bifurcation we saw in Sec. ?? but written in complex numbers. Kuramoto chose a simple and natural way to couple these oscillators: via a common coupling term, that is proportional to the value Q_i of each oscillator:

$$\dot{Q}_i = (i\omega + \alpha)Q_i - \beta|Q_i|^2Q_i + \frac{K}{N} \sum_{j=1}^N Q_j \quad (2.36)$$

which corresponds to an all-to-all topology, with K being the coupling strength. Here the natural frequencies are assumed to be drawn from a certain distribution $g(\omega)$, usually unimodal.

One can then rewrite (??) in polar coordinates by using $Q_i = e^{i\theta_i}\rho_i$. Substituting it one gets the equations

$$\dot{\rho}_i = (\alpha - \beta\rho_i^2) + \frac{K}{N} \sum_{j=1}^N \rho_j \cos(\theta_j - \theta_i) \quad (2.37)$$

$$\dot{\theta}_i = \omega_i + \frac{K}{N} \sum_{j=1}^N \frac{\rho_j}{\rho_i} \sin(\theta_j - \theta_i) \quad (2.38)$$

Kuramoto studied these equations in the limit of $\alpha \rightarrow \infty$ and $\beta \rightarrow \infty$ with α/β constant. Then, one gets that the radial variables ρ_i approach a stable fixed point in

arbitrarily fast. The radial variable is therefore just a constant and one just needs to consider the phase variables:

$$\theta_i = \omega_i + \frac{K}{N} \sum_{j=1}^N \sin(\theta_j - \theta_i). \quad (2.39)$$

A very useful way to quantify the spread of the phases θ_i is through the complex order parameter:

$$Z = re^{i\psi} = \frac{1}{N} \sum_{j=1}^N e^{i\theta_j}, \quad (2.40)$$

which corresponds to the centroid of the phases and therefore characterizes well the collective behavior of the system. The radius r measures the phase synchronization of the system: r is close to 0 if the phases are uniformly spread or clustered in anti-phase clusters and r is close to 1 if the phases are aligned together. Here we should clarify that phase synchronization denotes the alignment of phases of oscillations - complete phase synchronization corresponds to $r = 1$, meaning that the phases are the same (up to a 2π offsets). On the other hand, frequency synchronization denotes the alignment of the frequencies of oscillations - complete frequency synchronization corresponds to $\dot{\theta}_i = \Omega$, $\forall i = 1, \dots, N$. Networks that are frequency synchronized are also said to be phase-locked - the phase differences are constant. But it does not imply phase synchronization, as the phase differences may be non-zero. Figures ??A-B exemplify the behavior of r for weak and strong phase synchronization.

The angle ψ corresponds to the average phase of the units. Using this order parameter, the Kuramoto model can be rewritten as

$$\dot{\theta}_i = \omega_i + Kr \sin(\phi - \theta_i), \quad i = 1, \dots, N. \quad (2.41)$$

This form highlights the mean-field character of the model [?]. The oscillators now interact through the mean-field quantities r and ψ . The phase θ_i is pulled towards the mean phase ψ . And the effective coupling strength becomes Kr , so it is modulated by the degree of phase synchronization r . This creates a positive feedback loop, wherein as the system phase synchronizes more, the coupling becomes stronger and so the system tends to phase synchronize even more. This is a very clear mechanism for spontaneous synchronization [?].

These equations always have a solution for $\theta_i = 0$, $\forall i$. What about others? Kuramoto considered these equations in the infinite size limit $N \rightarrow \infty$. By seeking steady-state solutions, with r constant noted that oscillators will distribute into two groups: (i) with $|\omega_i| < Kr$ which phase-lock together and (ii) with $|\omega_i| > Kr$ which keep rotating with nonuniform velocity $\dot{\theta}_i$. He then showed that a branch continuously bifurcates from $r = 0$ at $K = K_c$, a critical coupling strength, given by:

$$K_c = \frac{2}{\pi g(0)} \quad (2.42)$$

Near $K = K_c$, this branch has a square-root behavior: $r \propto \sqrt{K - K_c}$. In particular for ω_i following a Lorentzian distribution, one can show that [?, ?]

$$r = \sqrt{1 - \frac{K_c}{K}}, \quad (2.43)$$

as illustrated in Fig. ??C. One can verify this behavior numerically: Fig. ??D illustrates the results of simulations for a network of $N = 1000$ oscillators under a Gaussian distribution with zero mean and unitary standard deviation. The y -axis denotes the time-averaged behavior of $r(t)$, which oscillates in time.

Many open questions remain from the treatment just shown, such as the stability of these branches. There have been many extensions made to this model [?, ?]. In the context of multistability, some basic results come from studying an even simpler configuration, where the units are identical and coupled in a k -nearest-neighbor ring.

2.4.2 Multistability in homogeneous case: twisted states

In the case of homogeneous oscillators with $\omega_i = \omega$ coupled in a k -nearest-neighbor topology, the equations become

$$\dot{\theta}_i = \omega + \epsilon \sum_{j=i-k}^{j=i+k} \sin(\theta_j - \theta_i). \quad (2.44)$$

One can switch to a corotating frame with angular velocity ω to get rid of the ω term and appropriately rescale time to get rid of ϵ and simplify down to

$$\dot{\theta}_i = \sum_{j=i-k}^{j=i+k} \sin(\theta_j - \theta_i). \quad (2.45)$$

Note therefore that changing the coupling strength in this system only rescales time, and does not change the state space significantly! This can be written as a gradient system $\dot{\theta} = -\nabla U(\theta)$, where $U(\theta)$ is a scalar differentiable function of $\theta \in \mathbb{R}^n$ [?, ?]. As a consequence, the only attractors in this system are equilibria [?]. Therefore to find all the attractors in the system one can first find the equilibria and then determine their linear stability. By doing this this, one finds that the equilibria obey the relation:

$$\theta_i = \omega t + \frac{2\pi q}{N} i + C \quad (2.46)$$

where $C \in \mathbb{R}$ is a constant and $q \in \mathbb{Z}$ is the twisting number. If one looks at the phase difference between two adjancent units one sees that it is constant across the ring: $\theta_{i+1} - \theta_i = \frac{2\pi q}{N}$. In particular, the completely synchronized is included here in the $q = 0$ case. Some important stability results are:

- For small values of k many twisted states can be stable. As k is increased, these twisted states start to lose stability, with higher q values starting earlier. Eventually, the completely synchronized state ($q = 0$) becomes globally stable at $k > k_c \approx 0.34N$ [?].
- If we fix k and look at estimates of the size of the basins of all stable twisted states we find that they can be parametrized by a Gaussian curve [?, ?] (Fig. ??E).
- Estimates of the size of the basin of attraction for $q = 0$ increase monotonically with k (Fig. ??F): the completely synchronized state starts to dominate the state space for denser networks [?].

- The shape of the basins is still a topic under research, but they appear to form octopus-like structures. The twisted state itself (a point) is on the head of the octopus, which a small volume around it. The majority of the volume of the basin is concentrated on the tentacles, which are structures that spread around in state space [?].

Studies have also been made for other topologies. Some important results have accumulated to show that networks with homogeneous frequencies are guaranteed to globally synchronize if the nodes are sufficiently well connected (if the networks are sufficiently dense). Taking the least connected node, with degree k_{\min} , and comparing it with the maximum possible degree of the network, $N - 1$, one can define the network's connectivity μ as the ratio $\mu = k_{\min}/(N - 1)$. Then, in networks with $\mu > \mu_c$, the only attractor is the fully synchronized state. Estimates have that $\mu \in [0.6818, 0.7889]$ [?, ?].

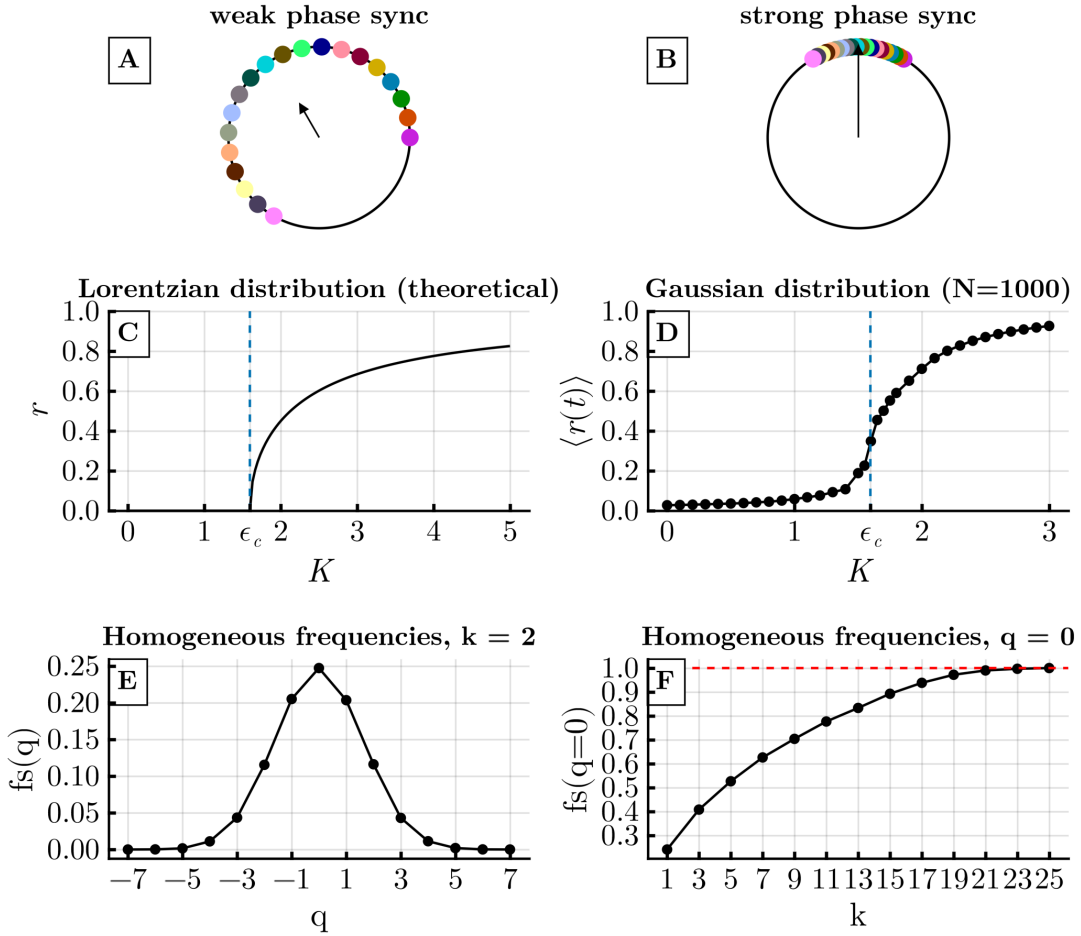


Figure 2.8: **Basics of Kuramoto oscillators.** Panels A and B respectively illustrate the concept of weak and strong phase synchronization (PS), captured by the complex order parameter Z (Eq. ??). The radius r denotes the degree of PS and the angle ψ denotes the centroid of the phases - respectively, they correspond to the magnitude and direction of the arrow in the figure. Panel C illustrates the behavior of the order parameter r as a function of coupling strength K (see Eq. ??) for a Lorentzian distribution of the frequencies (Eq. ??). The blue line denotes the critical coupling strength for the transition to synchronization. Panel D illustrates a similar behavior obtained from numerical simulations in a network of size $N = 1000$ under a Gaussian distribution of the natural frequencies. Only one attractor is ever observed in the simulations. Going now to homogeneous frequencies, panel E illustrates the fraction fs of randomly chosen initial conditions that converge to each q twisted state, in a network with $k = 2$ nearest neighbors. Panel F looks at this fraction for the completely synchronized state ($q = 0$) only, under different values of k . Panels E and F replicate results from [?].

Chapter 3

Transients versus network interactions give rise to multistability through trapping mechanism

Abstract

In networked systems, the interplay between the dynamics of individual subsystems and their network interactions has been found to generate multistability in various contexts. Despite its ubiquity, the specific mechanisms and ingredients that give rise to multistability from such interplay remain poorly understood. In this chapter ¹, for a network of coupled excitable units, we show that this interplay generating multistability occurs through a *competition* between the units' transient dynamics and their coupling. Specifically, the diffusive coupling between the units manages to *reinject* them in the excitability region of their individual state space and effectively trap them there. We show that this trapping mechanism leads to the *coexistence* of multiple types of oscillations: periodic, quasiperiodic, and even chaotic, although the units separately do not oscillate. Interestingly, we show that the attractors emerge through different types of bifurcations - in particular, the periodic attractors emerge through either saddle-node or limit cycles bifurcations or homoclinic bifurcations - but in all cases the reinjection mechanism is present.

3.1 Introduction

The long-term behavior of dynamical systems is determined by their attractors, which are stable states that attract certain sets of initial conditions. Dynamical systems can possess several attractors coexisting for the same parameters, such that different initial conditions can lead to different long-term behaviors - a phenomenon called *multistability* [?, ?]. In power grids, this can mean the difference between the proper functioning of the grid and a blackout [?]; in ecological systems, it can mean the difference between extinction of a certain species and their survival [?]. In neuronal circuits, multistability has been shown to be important for computations [?], and may, for instance, implement memory storage if the attractors correspond to different memories [?, ?].

Many systems display multistability, particularly networked systems, in which individual units are coupled together according to some type of interaction [?]. An important type of interaction in networked system is diffusion. One example is found in interacting ecological patches, in which each patch has its own dynamics but also interacts with

¹This chapter is a modified form of a manuscript under review: Kalel L. Rossi, Everton S. Medeiros, Peter Ashwin and Ulrike Feudel. Transients versus network interactions give rise to multistability through trapping mechanism

other patches by migration, or diffusion, of species [?]. Another example is found in neuronal networks, in which neurons interact with each other through the transport of ions across their cell membrane [?, ?]. In these two examples, the interaction between units can be modeled by a linear diffusion term dependent on the difference $x_j - x_i$ between the state variables x_i and x_j of units i and j [?, ?, ?, ?, ?, ?, ?, ?]. Understanding the emergence of multistability in networked systems with this kind of interaction therefore finds applications in many fields, and is still an area of active research.

For networked systems with diffusive coupling, multistability is known for cases in which the units oscillate individually. The emergence of different types of attractors has been shown [?], often with these attractors coexisting [?, ?, ?, ?, ?, ?, ?, ?, ?, ?]. For instance, Ref. [?] studied two coupled repressilators, 7-dimensional units that have stable oscillations when uncoupled, and find the emergence of different types of attractors. Some attractors have two units oscillating with a large amplitude and some have one unit at a large amplitude and another with a very small amplitude, called inhomogeneous limit cycles. When more units are coupled in a big network with $N = 100$ units, the authors showed in Ref. [?] that a large number of such attractors can coexist. In coupled mechanical oscillators, two coupled rotors have also been shown to exhibit large multistability (more than 3000 attractors) [?].

Less is known about multistability when the units individually do not oscillate, although it is known that oscillations can still arise due to the coupling. This originates from work by Smale in 1976 based on an idea by Turing in 1952 [?]. Smale proposed the emergence of oscillations from non-oscillating units which have only one equilibrium that is stable and globally attracting in a region of their state space. It was shown that the oscillations come from a Hopf bifurcation, in which the equilibrium becomes unstable and a stable oscillation emerges [?, ?]. Chaotic oscillations can also emerge from diffusive coupling applied to units with a single stable equilibrium in a region of state space. An example was given in Ref. [?] for two coupled Chua circuits. Recently, researchers provided rigorous conditions for the emergence of chaos due to diffusive coupling [?]. However, these works generally do not look at multistability. Furthermore, they deal with a single equilibrium in a region of state space, and have not yet looked at a scenario in which more invariant sets, such as unstable equilibria, may also play a role.

The presence of unstable equilibria can alter the transient dynamics of non-oscillating systems. In some classes of models, which we study here, the unstable equilibria lead to a type of excitability [?]. In this case, the unstable equilibria force part of the trajectories to go through a long excursion in state space, called an *excitation*, before reaching the stable equilibrium. These excitations are common in neuronal models, where they correspond to a neuronal spike [?]. Reference [?] has described multistability emerging in two excitable FitzHugh-Nagumo neurons that were coupled repulsively, but over a relatively small parameter range. For attractive coupling, the authors did not observe multistability.

In this work, we present two findings. First, we show that an attractive diffusive coupling can indeed create new attractors in coupled excitable systems. In fact, a wide variety of them: periodic, quasiperiodic and even chaotic oscillations arise by coupling excitable units, with $N = 2$ units already being sufficient for periodic and quasiperiodic attractors. For larger networks of $N = 10$ units, we show that these attractors, periodic, quasiperiodic and chaotic attractors can *coexist* in the same system, for a range of coupling strengths, in line with results of strong multistability in networks with many units [?, ?, ?].

The second finding contributes to an understanding of one mechanism through which these attractors emerge. We study their geometry, looking at the interaction between the units' local dynamics, which creates the excitability, and the diffusive coupling term, which pulls the units toward each other. We show that the competition between these two terms manages to trap the units in a particular region of their state space where excitability occurs. Based on this mechanism, the previously transient excitable dynamics is now repeatedly activated, generating permanent oscillations. This occurs for all the attractors observed, which emerge under different bifurcation scenarios. It also extends to networks with more than two interacting units, suggesting a powerful mechanism for the coexistence of a multitude of attractors in networked systems.

A similar idea of attractors emerging when units are trapped in transient regions of state space has been previously reported in the literature [?, ?, ?, ?, ?]. The mechanisms underlying this trapping were different, and multistability had not been reported. In Refs. [?, ?, ?] the authors study units with chaotic saddles (unstable chaotic sets) in their uncoupled state space. They show that the diffusive coupling manages to trap the units in that region, generating a seemingly stable chaotic motion. Meanwhile, authors in Ref. [?] have shown the emergence of solutions in the vicinity of canard transitions. Because the local dynamics we study here is relatively simple, and yet can create rich multistable dynamics, our study serves as a simple yet powerful example of the more widespread phenomenon of multistability through trapping.

The chapter is organized as follows. We describe the model and algorithms in Sec. ???. Then, Sec. ?? introduces the rich multistability seen in a network of $N = 10$ units, from which we reduce to $N = 2$ units to better understand the mechanism giving rise to this multistability. In Sec. ?? we then discuss these findings in relation to each other and to preexisting literature.

3.2 Methods

3.2.1 Model

In this work we study networks formed by coupling two-dimensional units with state variables x and y whose evolution we write as:

$$\dot{x}_i = f_1(x_i, y_i) + \epsilon_1 g_i(\mathbf{x}) \quad (3.1)$$

$$\dot{y}_i = f_2(x_i, y_i) + \epsilon_2 g_i(\mathbf{y}) \quad (3.2)$$

with $\mathbf{x} = (x_1, \dots, x_N) \in \mathbb{R}^N$ and $\mathbf{y} = (y_1, \dots, y_N) \in \mathbb{R}^N$ are the state variables of the system. We refer to $\mathbf{f}_i = \mathbf{f}(x_i, y_i) = (f_1(x_i, y_i), f_2(x_i, y_i))$ as the local dynamics of unit i and to $\mathbf{g}_i = (g_i(\mathbf{x}), g_i(\mathbf{y}))$ as the coupling term of unit i , which allows it to receive influence from other units. The parameters ϵ_1 and ϵ_2 control the strength of the interactions, with $\epsilon_1 = \epsilon_2 = \epsilon$ unless stated otherwise. The interaction is specified by a diffusive coupling of the form:

$$g_i(\mathbf{z}) = \sum_{j \in \Omega_i} (z_j - z_i), \quad (3.3)$$

where \mathbf{z} is either \mathbf{x} or \mathbf{y} , and Ω_i is the set containing the indices j of units connected to unit i , also called the neighborhood of i .

For the local dynamics, we choose a simple two-dimensional model for a spiking neuron following the Hodgkin-Huxley formalism, as written by Ref. [?]. The dynamics of this model is described by the following functions:

$$\begin{aligned} f_1(x_i, y_i) &= (I - g_L(x_i - E_L) \\ &\quad - g_{Na}m_\infty(x_i)(x_i - E_{Na}) \\ &\quad - g_Ky_i(x_i - E_K))/C, \end{aligned} \tag{3.4}$$

$$f_2(x_i, y_i) = (n_\infty(x) - y_i)/\tau, \tag{3.5}$$

where the neuron membrane potential and conductance variable are represented by x and y , respectively. The activation functions $m_\infty(x_i)$ and $n_\infty(x_i)$ are given by:

$$m_\infty(x_i) = \frac{1}{1 + \exp((x_{1/2,m} - x_i)/k_m)}, \tag{3.6}$$

$$n_\infty(x_i) = \frac{1}{1 + \exp((x_{1/2,n} - x_i)/k_n)}. \tag{3.7}$$

The parameters used are $\tau = 0.16$ ms, $C = 1$ μ F/cm 2 , $E_L = -80$ mV, $g_L = 8$ mS/cm 2 , $E_{Na} = 60$ mV, $g_{Na} = 20$ mS/cm 2 , $E_K = -90$ mV, $g_K = 10$ mS/cm 2 , $x_{1/2,m} = -20$ mV, $k_m = 15$, $x_{1/2,n} = -25$ mV, $k_n = 5$ and $I = 2.0$ μ A/cm 2 . The dynamics of this system is very similar to that of the Morris-Lecar model [?, ?]. A slight increase in the membrane voltage x leads to a quick increase in the Sodium current, which is negative ($(x - E_{Na}) < 0$) and acts to increase the voltage even further in a positive feedback that rapidly increases x , initiating the excitation (spike). At sufficiently high voltage, the Potassium current increases, being activated by the conductance variable y . This current is positive ($(x - E_K) > 0$) and becomes sufficiently large that it overcomes the Sodium current and decreases the voltage back to baseline, terminating the excitation and returning to the stable equilibrium. For a more in-depth explanation of the model and a complete explanation of the parameters, we refer the reader to Ref. [?]. For simplicity, from now on we refer to the parameters without their corresponding units.

For fixed $I = 2.0$, the neuronal dynamics of the uncoupled units ($\epsilon_1 = \epsilon_2 = 0$) is excitable. The state space of the unit, shown in Fig. ??, is composed of a stable node (green circle), a saddle-point $\mathbf{x}_s^{\text{unc}}$ (red circle close to the node), and an unstable focus (red circle). The stable manifold $\mathbb{W}^s(\mathbf{x}_s^{\text{unc}})$ and the unstable manifold $\mathbb{W}^u(\mathbf{x}_s^{\text{unc}})$ of the saddle are depicted in green and red lines, respectively. Additionally, the x -nullcline, defined as $\dot{x} = 0$, and the y -nullcline, defined as $\dot{y} = 0$, are shown in gray and white, respectively. As indicated by the vector field, the stable manifold $\mathbb{W}^s(\mathbf{x}_s^{\text{unc}})$ roughly separates the state space into two regions: one that directly converges to the stable equilibrium, and another wherein trajectories go through long excursions before converging to the equilibrium. The long excursions are called excitations, and the region is called the *excitability region*.

In the main text of the manuscript, we focus on the phenomenology underlying the excitable case prescribed by $I = 2.0$. In the Supplemental Material, we show that increasing I leads to a homoclinic bifurcation, creating a stable limit cycle, followed by a saddle-node bifurcation that destroys the node and saddle of the units. We then discuss the effects of these bifurcations on the results presented in the chapter.

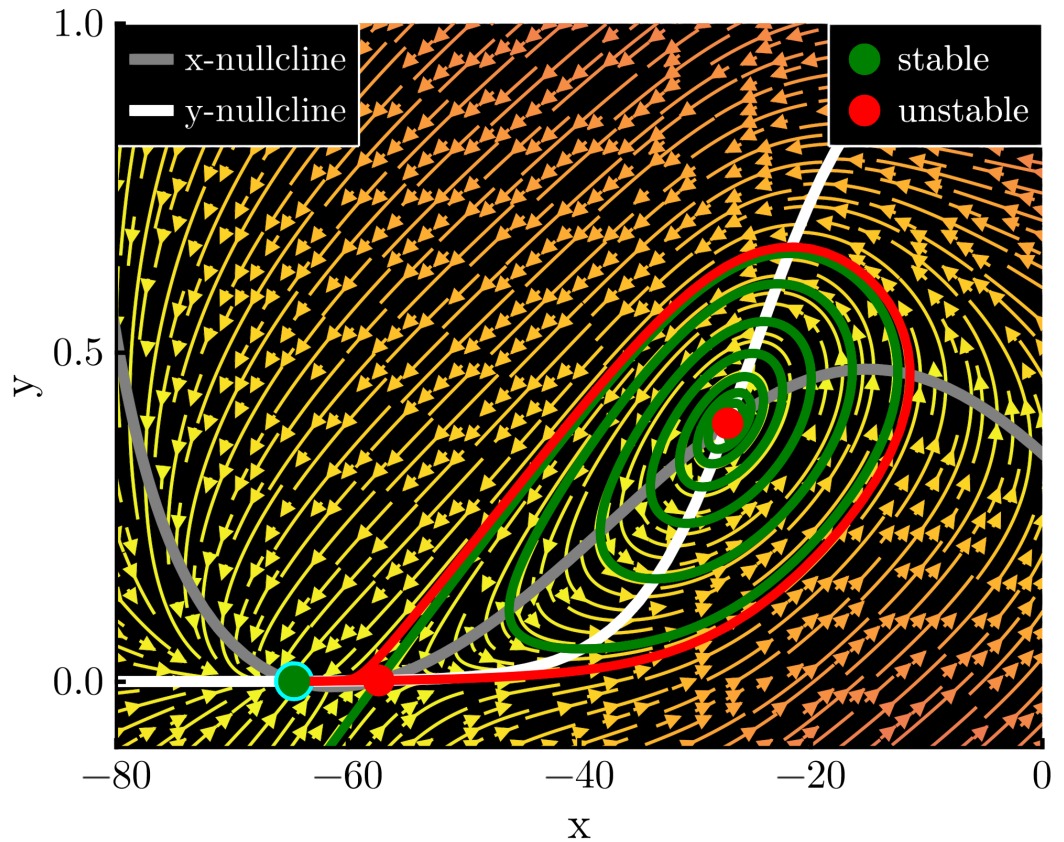


Figure 3.1: Phase portrait of the excitable uncoupled units. The green dot represents the stable node of the system, the red dots represent the unstable focus and the saddle point, with its stable and unstable manifold branches in the green and red lines. The phase portrait is represented by the arrows, indicating the directions of the flow. As the flow indicates, there is a wide region in which trajectories must go around the stable manifold to reach the node. They correspond to a neuronal spike, since this is a sharp increase and then decrease in the membrane potential. This region is called the excitability region. Attractors emerging from the coupling live in this region of long transients.

3.2.2 Numerical algorithms

To find the attractors in our networked systems, we followed the method developed in Refs. [?, ?, ?], which distinguishes between attractors based on user-defined features that uniquely characterize the attractors. To achieve this, it first integrates randomly chosen initial conditions in a specified region of the state space. The corresponding trajectories are then labeled based on their features, such as the mean value of their amplitude. These features must be chosen so that trajectories on different attractors exhibit distinct feature values. Subsequently, the features are separated using a grouping algorithm, which may involve clustering or simply distinguishing features that are more distant than a predefined threshold. This method works well for both low- and high-dimensional systems. We performed extensive numerical studies to ensure no attractors were missed, but this cannot be guaranteed. An attractor with a sufficiently small basin may, by chance, not be found. To reduce the risk of missing attractors, we used 5000 initial conditions for the $N = 10$ results and 1000 for $N = 2$. Test runs with more initial conditions did not find any further attractors. Each trajectory was integrated for a very long time, with a total transient time of 7000 and total integration time of 40000. The features used were the average pairwise Euclidean distance between the states of the units, their frequencies, amplitudes, and average position in state space. For equilibria, only the average position is considered, as the frequencies and amplitudes are zero. The algorithms, with a complete documentation, are implemented in the Julia [?] package Attractors.jl [?, ?]. We also verified the accuracy of results shown through continuation analysis using the XPPAUT 8.0 software [?], finding the bifurcations giving rise to the attractors.

Integration was done with the package DifferentialEquations.jl [?], with the aid of packages DynamicalSystems.jl [?] and DrWatson.jl [?]. Plots were made with Makie.jl [?]. The Tsitouras 5/4 Runge-Kutta method was used for the integrations, with absolute and relative tolerances of 10^{-9} . The code for the analysis is publicly available in a GitHub repository [?].

3.3 Results

3.3.1 Rich multistability of oscillations with 10 units

The diffusive coupling between the excitable units can generate rich oscillatory dynamics, in which equilibria coexist with periodic, quasiperiodic, and even chaotic oscillations. As we see later, these oscillations arise from the interplay between the diffusive coupling and the local flow field of the units. An example of these attractors is shown in Fig. ??A-I, in a network of $N = 10$ excitable units randomly connected with each other, following the topology shown in Fig. ??J. In this figure, we project the network state space into subspaces $x_i - y_i$ corresponding to each unit i , and overlay them all on top of each other. In addition, the coupling strength is chosen as $\epsilon_1 = \epsilon_2 = \epsilon = 0.15$.

The first type of attractor is shown in Fig. ??A. It corresponds to all units on the stable equilibrium, which is already present in the uncoupled units. This is the simplest solution, which must exist because, when the units are completely synchronized, the coupling term becomes zero and they follow their uncoupled dynamics, converging to the equilibrium.

The second type of attractor corresponds to one unit oscillating periodically with a large amplitude while the $N - 1$ other units oscillate with a very small amplitude at a

position between the stable equilibrium and the saddle of the uncoupled dynamics. The dynamics in this type of attractor resembles the so-called solitary states, since one unit behaves differently from the rest of the network. Such symmetry-broken solutions have been observed in regular [?, ?, ?, ?], adaptive [?], and complex networks [?]. For the chosen parameters, we have identified four stable solitary states, shown in Figs. ??B-E. The unit displaying a high-amplitude oscillation is said to be solitary. Interestingly, the amplitude of its oscillation is inversely proportional to the number of neighbors it has. With more neighbors, the coupling terms $\mathbf{g}_i(\mathbf{x})$ and $\mathbf{g}_i(\mathbf{y})$ of the solitary unit i increase, and the amplitude of its oscillation decreases. The reason for this will become clearer in Section ??, where we study in depth the case $N = 2$. Bifurcation analysis (not shown) reveals that these periodic attractors emerge in homoclinic bifurcations and disappear in saddle-node of limit cycle bifurcations (SNLC).

The third type of attractor corresponds again to periodic oscillations, but with two high-amplitude units, shown in Figs. ??F-G. In Fig. ??F, the units exhibiting high-amplitude oscillations are 2 and 9. Note that unit 2 has one more neighbor than unit 9, and its amplitude is smaller. In Fig. ??G, the units are 4 and 5. They have the same number of neighbors, so their amplitudes are identical. This type of attractor is thus a two-unit cluster periodic state. Bifurcation analysis reveals that these attractors emerge and disappear through SNLC bifurcations.

A fourth type of attractor also involves two units (1 and 10) oscillating with large amplitude, but now quasi-periodically, as shown in Fig. ??H. Similarly to the previous cases, the amplitude of their oscillations is proportional to the number of neighbors they have. As shown in the topology in Fig. ??J, the oscillating units (1 and 10) are connected, so they also pull each other in directions perpendicular to their oscillations as they oscillate. Intuitively speaking, we can imagine that this interaction enlarges the width of the torus. Indeed, if one introduces a coupling parameter directly between units 1 and 10, i.e., setting $g_i(\mathbf{z}) = \sum_{\Omega_i} \epsilon_{i,j}(z_j - z_i)$, and specifically increasing $\epsilon_{1,10} = \epsilon_{10,1}$ from 0 to ϵ , the width of the torus in the $x_i - y_i$ projection increases. Thus, when oscillating together with different amplitudes, the coupling between the units causes their quasi-periodic curves to become broader. We see the emergence of tori in greater depth when we study the $N = 2$ case in Section ??.

Finally, the fifth type of attractor involves all units oscillating together chaotically. All neuronal units are thus spiking chaotically in this attractor in a desynchronized fashion. The chaotic behavior, along with the periodic and quasiperiodic examples from earlier, has been verified by calculating the Lyapunov exponents of these attractors.

The results conveyed in Fig. ?? occur for an intermediate range of coupling strength values, at and around $\epsilon = 0.15$. Bigger coupling strengths tend to generate fewer attractors, and ultimately for strong coupling only the stable equilibrium exists. For weaker coupling, even more attractors can appear. In fact, for a range roughly between $\epsilon = 0.05$ and $\epsilon = 0.1$, more than 50 attractors can be found. These correspond to the various combinations of units having a very small amplitude oscillation, and units having a large amplitude oscillation.

Furthermore, in the network we analyzed so far the units are coupled in both x and y directions (i.e., $\epsilon_1 = \epsilon_2 = \epsilon$). If only the x -direction is coupled ($\epsilon_1 = \epsilon$, $\epsilon_2 = 0$), there still is multistability, but with fewer attractors. The x -coupling tends to stabilize attractors with more units oscillating at a higher amplitude, such that one can have 5 units oscillating periodically at a large amplitude and 5 with small amplitude, for instance.

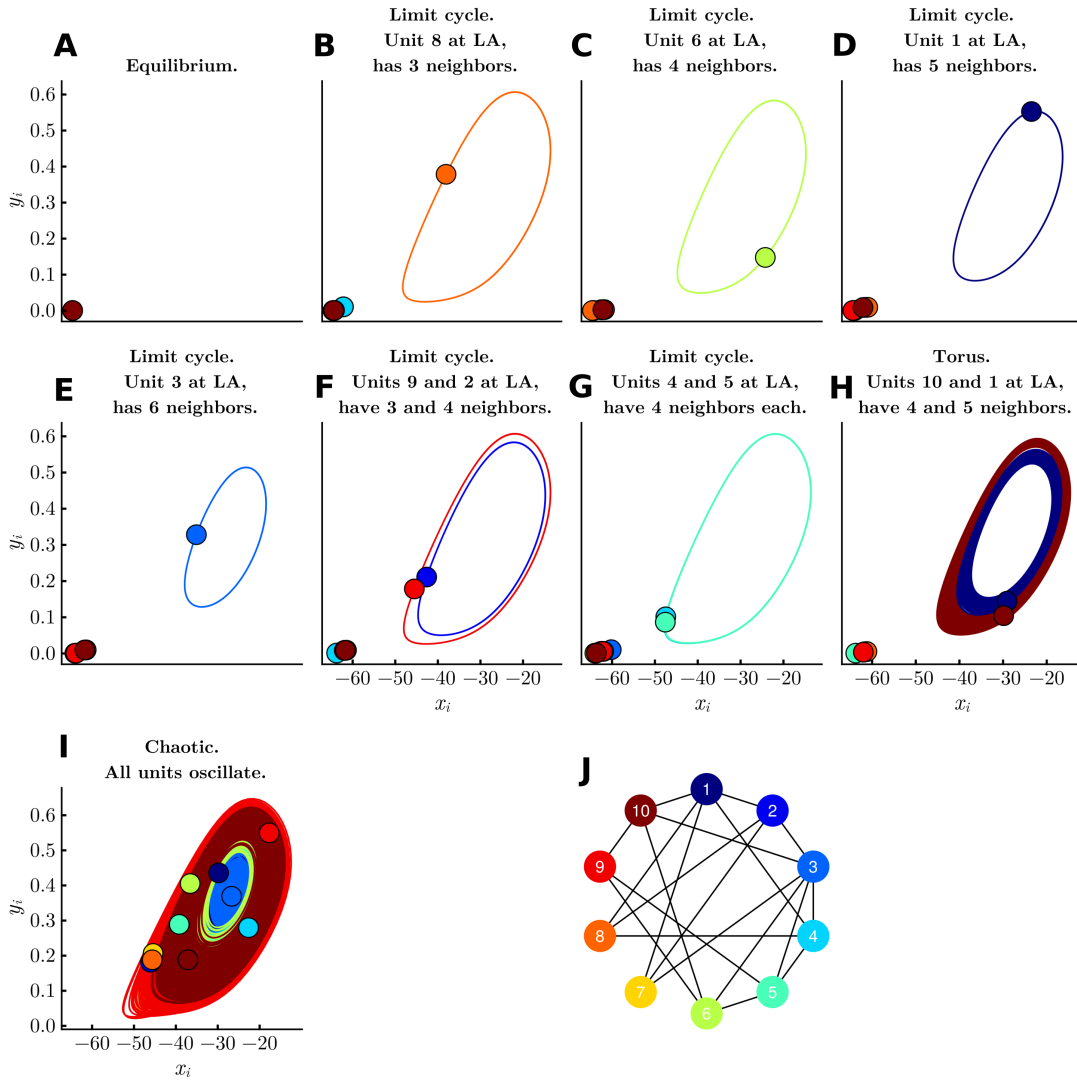


Figure 3.2: Rich multistability arising from diffusive coupling. Panels I-H show the stable equilibrium, periodic, quasi-periodic and chaotic attractors that coexist in the same network with $N = 10$ randomly coupled units (shown in Panel J) with $\epsilon = 0.15$. Each panel shows a trajectory on one of the attractors, projected onto the $x_i - y_i$ subspaces of each unit, all overlaid on top of each other. Circles correspond to the positions of the units at some arbitrarily chosen time point. The units are colored from blue to red according to their index, as shown in the topology of panel J, such that unit 1 is a deep blue and unit 10 is a deep red.

To summarize, the addition of a simple linear interaction through the attractive diffusive coupling creates a plethora of oscillations from non-oscillating units in an excitable regime. The coupling is clearly able to counteract the units' tendency to converge onto the stable equilibrium. Our goal in the following sections is to elucidate this mechanism in more detail. To achieve this, we simplify our system and reduce the problem to $N = 2$ interacting units.

3.3.2 Emergence of attractors in a two-unit network

To illustrate the effect of the diffusive coupling on the excitable neurons, we show the attractors of the system for different coupling strengths for $N = 2$ coupled units. Similarly to Fig. ??, each panel in Fig. ?? shows the variables $x_i - y_i$, now for $i = 1, 2$. An important difference now is that the colors refer to the attractors. The units are distinguished by markers: circles for unit 1 and diamonds for unit 2. These markers correspond to the positions of the units at some arbitrarily chosen time point.

To begin this analysis, we recall that each uncoupled unit has three equilibria. Consequently, a system of two coupled units, under sufficiently weak coupling, has $3^2 = 9$ equilibria, corresponding to all combinations of the individual equilibria. Naturally, the symmetric combinations node-node, saddle-saddle, and focus-focus correspond to the two units being together in the same equilibrium. Since the coupling term becomes zero when the units are completely synchronized, these symmetric equilibria occupy the same positions as their uncoupled counterparts when projected into the units' subspace $x_i - y_i$. The other equilibria are asymmetric and have non-zero coupling terms, which shift their positions as a function of the coupling strength ϵ . However, for simplicity, we still label the equilibria as combinations of the uncoupled equilibria, e.g. node-saddle denoting an equilibrium with 3 negative eigenvalues and 1 positive eigenvalue.

For $\epsilon = 0.05$, the node-node is the only attractor in the system (Fig. ??A). In this solution, both units are in a steady state (SS), so we label the attractor as SS-SS (also called homogeneous steady state HSS [?]).

Next, at $\epsilon \approx 0.065$, a stable oscillation emerges, in which both units oscillate with a large amplitude (Fig. ??B). Therefore, we label this attractor LA-LA. It initially forms near the saddle point $\mathbf{x}_s^{\text{unc}}$, located near the lower left corner. This proximity to the saddle point causes trajectories in that region to slow down significantly. As the coupling increases, the limit cycle moves farther away from the saddle point, resulting in a decreasing amplitude. This progression can be observed by comparing the attractors in subsequent panels.

At $\epsilon \approx 0.117485$ a pair of asymmetric attractors emerges, in which one unit has a large amplitude oscillation (LA) and the other unit has a small amplitude oscillation (SA), and vice-versa (Fig. ??C). Because the units are identical, the system has a permutation symmetry, so both attractors, LA-SA (large amplitude in unit 1 and small amplitude in unit 2), and SA-LA (reciprocal case) are simply permuted versions of each other. Consequently, these attractors overlap each other in Figs. ??C-D. They can be distinguished by the position of the units, indicated by the markers. Please note that the small amplitude oscillation has such a small amplitude that it is barely visible in the figures. In the literature, the LA-SA attractors have also been called inhomogeneous limit cycles [?, ?] (IHLC).

At this coupling strength $\epsilon \approx 0.117485$, the system has four coexisting attractors, three of them being oscillations, even though the uncoupled dynamics only has equilibria! Eventually, for stronger coupling the pair LA-SA and SA-LA disappears around $\epsilon \approx 0.22$, and the system becomes bistable again. The result is shown in Fig. ??E. At $\epsilon \approx 0.27$, the periodic LA-LA attractor is replaced by a quasi-periodic LA-LA attractor, which again has both units oscillating with a large amplitude. In the quasi-periodic attractor, the units have different frequencies, and are desynchronized in both frequency and phase (cf. Fig. ??F). Eventually it disappears and only the stable equilibrium remains for sufficiently strong coupling.

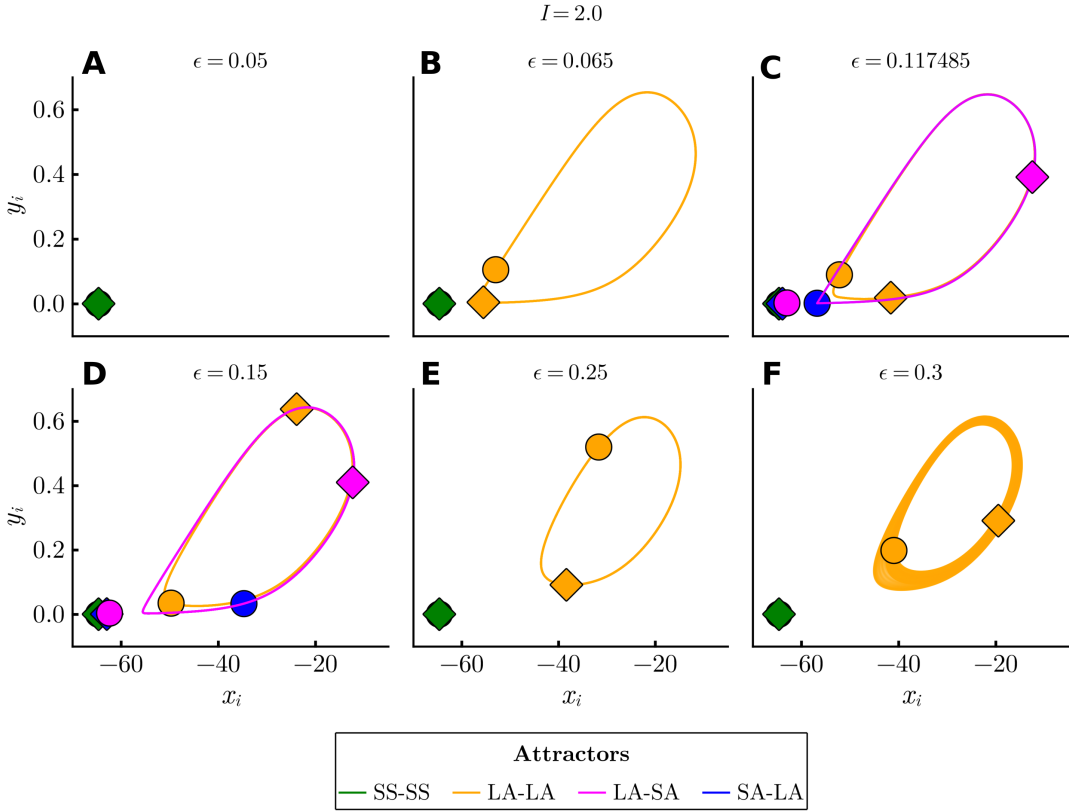


Figure 3.3: Attractors created by the diffusive coupling for $N = 2$. Each panel is a projection onto 2D space of $x_i - y_i$ for different coupling strengths. The markers denote the positions of the units for an arbitrarily chosen time point, with unit 1 shown as a circle and unit 2 as a diamond. The stable equilibrium is the only attractor existing for weak coupling strengths, as shown for $\epsilon = 0.05$. Another attractor emerges at $\epsilon \sim 0.065$ corresponding to two units oscillating with large amplitude - it is thus labelled as LA-LA. A pair of asymmetric attractors emerges at $\epsilon \sim 0.117485$ corresponding to one unit oscillating with large amplitude and the other oscillating with small amplitude; they are labeled respectively as LA-SA and SA-LA. The pair eventually disappears and the system becomes bistable again at $\epsilon = 0.25$. At $\epsilon = 0.3$, the LA-LA attractor is quasi-periodic. For stronger coupling ϵ , only the stable equilibrium is left.

3.3.3 Bifurcations giving rise to the attractors

To understand the emergence and disappearance of the attractors in the $N = 2$ case, we start by studying their associated bifurcations. We perform a continuation analysis using the XPPAUT 8.0 software [?]. This analysis is shown in Fig. ??, where the period T of oscillation is estimated as a function of the coupling strength ϵ . In this figure, the green and red colors indicate stable and unstable solutions, respectively. First, in Fig. ??A, we present the continuation analysis for the LA-LA attractor, where both units oscillate with a large amplitude. We observe that this attractor arises from a saddle-node bifurcation of limit cycles (SNLC) at $\epsilon \approx 0.06432$. Subsequently, the stable limit cycle undergoes a Neimark-Sacker (torus) bifurcation (TR) at $\epsilon \approx 0.2701$, becoming unstable and being

replaced by a stable torus. Next, this unstable limit cycle disappears in a supercritical Hopf bifurcation (HB) at $\epsilon \approx 0.4088$. Meanwhile, the saddle limit cycle that emerges at the SNLC bifurcation disappears in a homoclinic bifurcation (HOM) involving a saddle-saddle equilibrium at $\epsilon \approx 0.07285$. While it exists, the saddle limit cycle forms the basin boundary between the stable equilibrium and the stable limit cycle. When it disappears in the homoclinic bifurcation, it is immediately replaced by a pair of asymmetric saddle limit cycles that also emerges in a homoclinic bifurcation to the same equilibrium at the same parameter value, as shown in Fig. ??B. These saddle limit cycles then compose the basin boundary between the attractors. They correspond to the unstable version of the LA-SA and SA-LA attractors, which are later born also in a homoclinic bifurcation at $\epsilon \approx 0.1175$, but involving a saddle-node equilibrium. Eventually, both the stable and the unstable limit cycles collide and disappear in a SNLC bifurcation at $\epsilon \approx 0.2179$. The files used to perform the analysis are freely available at [?].

3.3.4 Emergence of oscillations through reinjection mechanism

To gain insights into how the coupling between the units supports the emergence of oscillations in a system whose uncoupled units exhibit only steady states, we now examine the geometry of the emerging attractors. As we see in Eqs. ??, the dynamics of unit i can be decomposed into two terms: the local dynamics, governed by $\mathbf{f}_i(x_i, y_i)$, and the coupling, governed by $\epsilon \mathbf{g}_i(\mathbf{x})$. The local dynamics $\mathbf{f}_i(x_i, y_i)$ generates a vector field dictating the trajectories of the uncoupled units. As described in Sec. ??, \mathbf{f}_i creates an excitability region, on which trajectories go through long excursions in state space before converging to the stable equilibrium. They follow the stable manifold $\mathbb{W}^s(\mathbf{x}_s^{\text{unc}})$ of the saddle point $\mathbf{x}_s^{\text{unc}}$ in the uncoupled system on their way to the equilibrium. The coupling dynamics $\mathbf{g}_i(\mathbf{x}) = (x_j - x_i, y_j - y_i)$ generates a vector field that points from unit i to unit j , with an amplitude proportional to their distance. For $\epsilon > 0$, the coupling $\epsilon \mathbf{g}_i$ is attractive, as it pulls unit i towards unit j . In the following examples, we see how interaction between these two terms leads to the emergence of the stable oscillations.

Figure ??A1 illustrates this scenario for the LA-LA attractor at $\epsilon = 0.065$, already introduced in Fig. ??B. In Fig. ??A1, the structures in the complete 4D space are projected onto the $x_i - y_i$ subspace of each unit. For reference, we overlay on top of this plot the structures of the uncoupled unit, as seen already in Fig. ???. The stable equilibrium is represented as a green cross, while the saddle point $\mathbf{x}_s^{\text{unc}}$ and the focus are shown as red crosses. The stable manifold $\mathbb{W}^s(\mathbf{x}_s^{\text{unc}})$ of the saddle is a green line, while its unstable manifold $\mathbb{W}^u(\mathbf{x}_s^{\text{unc}})$ is a red line. A trajectory converging to the LA-LA attractor is shown as a solid black line. Starting from an initial condition near the focus, at the center of the figure, the trajectory spirals outwards. This spiralling can be understood as the coupling being weak enough that the local dynamics \mathbf{f}_i dominates the trajectory here, such that it roughly follows $\mathbb{W}^s(\mathbf{x}_s^{\text{unc}})$.

Looking at an amplification of the region near $\mathbf{x}_s^{\text{unc}}$ in Fig. ??A2, we see that the trajectory follows $\mathbb{W}^s(\mathbf{x}_s^{\text{unc}})$ almost until the saddle $\mathbf{x}_s^{\text{unc}}$ (red cross). Then, we see the crucial effect of the coupling. Without it, the trajectory would have followed along the left branch of $\mathbb{W}^u(\mathbf{x}_s^{\text{unc}})$ and converged to the stable equilibrium. This is shown in the black dashed line, which shows a trajectory of the uncoupled system starting at the same initial condition (in (x_1, y_1)) as the black solid line. However, the coupled trajectory does not do that. Instead, it goes rightward, influenced by the coupling $\epsilon \mathbf{g}_i$. This effect can be seen by the rightward pointing arrows attached to the circles. The arrows correspond

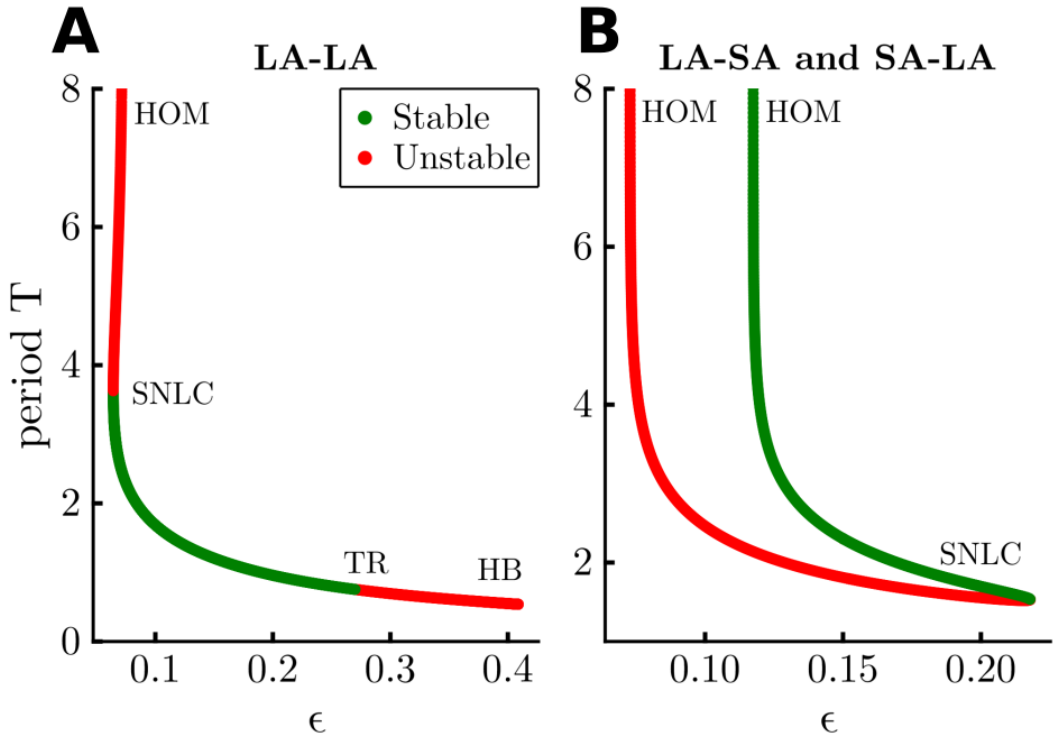


Figure 3.4: Continuation analysis for oscillations in two-unit case. Each panel shows a continuation of the limit cycles, plotting their period T as a function of the coupling strength ϵ for fixed $I = 2.0$. The left panel shows the analysis for the LA-LA attractor, which emerges in a saddle-node bifurcation of limit cycles (SNLC) together with a saddle limit cycle (red curve) at $\epsilon \approx 0.06432$. The unstable LC goes through a homoclinic bifurcation (HOM) where it collides with a saddle-saddle equilibrium at $\epsilon \approx 0.07285$ and disappears. The LA-LA attractor (in green) remains stable until it loses stability due to a Neimark-Sacker bifurcation (TR) and then disappears due to a supercritical Hopf bifurcation (HB). In panel B, the LA-SA, shown in the green curve, emerges due to a homoclinic bifurcation involving a saddle-node equilibrium at $\epsilon \approx 0.1175$ and then disappears due to a SNLC, when it collides with its unstable counterpart, in red, that is also born in a homoclinic bifurcation to a saddle-saddle equilibrium at $\epsilon \approx 0.07285$. The bifurcation diagram is identical for the SA-LA attractor, due to their symmetry.

to the coupling vector ϵg_i on unit i , depicted as the circles whose colors vary along the trajectory, from dark blue to light blue. Under this coupling, the trajectory crosses $W^s(x_s^{\text{unc}})$ in this projection, and is effectively reinjected into the excitability region. For clarity, the trajectory of the coupled 4D system, when projected into the $x_i - y_i$ plane, crosses the stable manifold $W^s(x_s^{\text{unc}})$ of the saddle of the uncoupled 2D system. Naturally, it does not cross any invariant manifolds of the coupled system.

As this attractor is symmetric, the behavior described for unit 1 occurs identically for unit 2. The reinjection into the excitability region thus happens for both units, causing them to repeatedly pull on each other and reinject each other into the previously transient region. In this sense, we say that *the coupling traps the units in the excitability*

region, preventing them from following their local dynamics's tendency toward the stable equilibrium.

Why does this crossing happen so close to $\mathbf{x}_s^{\text{unc}}$? As we have seen in Sec. ??, the LA-LA attractor emerges in a saddle-node bifurcation of limit cycles (SNLC), and is not directly related to $\mathbf{x}_s^{\text{unc}}$. However, the local dynamics has a magnitude $|\mathbf{f}_i|$ that is small in the vicinity of $\mathbf{x}_s^{\text{unc}}$. So in this region the relative effect of the coupling $\epsilon \mathbf{g}_i$ increases. Near $\mathbf{x}_s^{\text{unc}}$ the unit tends to move very slowly due to its local dynamics, but at the same time the coupling intensity is relatively strong. As a result, the coupling overcomes the local dynamics and manages to pull the unit rightwards. In summary, the slowness near $\mathbf{x}_s^{\text{unc}}$ helps the coupling $\epsilon \mathbf{g}_i$ to overcome the local dynamics.

The slowness near $\mathbf{x}_s^{\text{unc}}$ also allows us to understand the bulge that occurs right after the trajectory crosses $\mathbb{W}^s(\mathbf{x}_s^{\text{unc}})$, on the right-hand side of Fig. ??A2. The trajectory in this region is quite slow. In fact, unit i spends most of its time on it while unit j traverses the rest of the oscillation. As j moves around the oscillation, the distance between the units increases significantly, and therefore so does \mathbf{g}_i (note the longer blue arrow for unit 1 in the bulge). The combination of the slowness of \mathbf{f}_i and the high value of \mathbf{g}_i means that the coupling dominates the sum, significantly impacting the trajectory, pulling it towards unit j , creating the upwards movement of the bulge for unit i (and vice-versa for unit j , because of the symmetry).

For bigger values of ϵ , the coupling becomes stronger and the slowness near $\mathbf{x}_s^{\text{unc}}$ becomes less relevant. In Fig. ??B1, note how the coupling is larger (longer arrows) for $\epsilon = 0.15$. Consequently, the coupling manages to pull unit i , in this $x_1 - y_1$ projection, across $\mathbb{W}^s(\mathbf{x}_s^{\text{unc}})$ earlier along the manifold - see the magnification in Fig. ??B2. The stronger coupling also affects the shape of the attractor. This is most visible close to $\mathbf{x}_s^{\text{unc}}$, which is considerably shifted rightward and upward if compared to the smaller ϵ in Fig. ??A1-A2. This region has the slowest dynamics, and is thus the one most sensitive to the coupling. Furthermore, similarly to the argument leading to the bulge in Fig. ??A1-A2, while unit i is in this slow region, unit j eventually becomes diametrically opposite it, and the coupling amplitude grows significantly. This increase, combined with the slow dynamics, pulls the units upward and rightward, explaining the shift. This decreases the amplitude of the oscillation, consistent with the behavior seen for larger networks (Figs. ??B-H), in which the amplitude of the oscillation is inversely proportional to the number of neighbors a unit has.

So far we have considered what happens in the case that the x and y directions are coupled with the same intensity, i.e., when $\epsilon = \epsilon_1 = \epsilon_2$. However, this is not required for new attractors to emerge. In particular, the LA-LA attractor still emerges when only the x -component of the coupling is kept (i.e., when $\epsilon_1 = \epsilon$ and $\epsilon_2 = 0$). The reinjection occurs similarly to before, as shown in Figs. ??C1-C2, where an illustrative trajectory of the coupled system can again be seen to cross $\mathbb{W}^s(\mathbf{x}_s^{\text{unc}})$. In fact, the y -component of the coupling is not necessary to generate the LA-LA attractor, although it helps. Decreasing ϵ_2 from $\epsilon_2 = \epsilon$ to $\epsilon_2 = 0$ has the effect of increasing the critical value of ϵ_1 for the saddle-node bifurcation of limit cycles that creates the attractor, effectively postponing its emergence, but not inhibiting it. The example in Figs. ??C1-C2 occurs soon after the LA-LA attractor emerges. Note that the coupling is much bigger than it was for Figs. ??A1-A2. Conversely, decreasing ϵ_1 from $\epsilon_1 = \epsilon$ to $\epsilon_1 = 0$ can either destroy the LA-LA attractor through a SNLC bifurcation or cause it to lose stability. Therefore, the x -component is necessary to generate this attractor.

In Fig. ??D1 we return to the case $\epsilon_1 = \epsilon_2 = \epsilon$ and examine the asymmetric attractor

LA-SA. Its geometry differs from the previous cases, since now there is an asymmetry between the units. As in the previous cases, unit 1 oscillates in the excitability region with a large amplitude. Meanwhile, unit 2 (squares) is positioned, in the $x_2 - y_2$ projection, between the stable equilibrium (green cross) and the saddle point $\mathbf{x}_s^{\text{unc}}$ of the uncoupled dynamics (red cross). Both units can be seen in Figs. ??D1, represented respectively as circles and squares. Their colors denote different time points along the trajectory. In this configuration, unit 1 is pulled downwards and to the left by unit 2, as illustrated in Fig. ??D2, which shows $\epsilon \mathbf{g}_1$. This pull is capable of causing unit 1 to cross $\mathbb{W}^s(\mathbf{x}_s^{\text{unc}})$ and to be reinjected into the excitability region, as shown in Figs. ??D1-D2. Meanwhile, unit 2 is pulled rightwards and upwards by unit 1. This pull is counteracted by the attraction it feels towards the stable equilibrium, with the result being a small-amplitude oscillation. This competition is illustrated in Fig. ??D3, where two arrows are associated with unit 2 for a representative time point of the trajectory: the upward and rightward arrow is $\epsilon \mathbf{g}_2$, which pulls unit 2 towards unit 1; the downward and leftward arrow is \mathbf{f}_2 , which pulls unit 2 towards the stable equilibrium.

With this configuration of the units in the LA-SA attractor, the x -direction is actually counter-productive. To see this, we can focus on the region to the right of the saddle point - in Fig. ??D1, several instances of unit 1 can be seen accumulated in this region with light blue colors. This accumulation is a result of the slow dynamics of trajectories moving near the saddle point. In this region, unit 1 is pulled leftwards back towards $\mathbb{W}^s(\mathbf{x}_s^{\text{unc}})$. The x -direction is thus acting against the reinjection mechanism, and so may be impeding the emergence of the LA-SA attractor. We can verify this qualitative claim by decreasing ϵ_1 from $\epsilon_1 = \epsilon$ towards $\epsilon_1 = 0$. By doing this, we see that indeed the critical value of ϵ_2 that leads to the emergence of the attractor decreases. If $\epsilon_1 = 0$ the attractor can still emerge. Therefore, the LA-LA and LA-SA attractors exhibit different dependencies on the x - and y -components of the coupling, due to their distinct geometries. This distinction is crucial in various applications where coupling can model diverse phenomena. For example, in ecology, coupling in the x -direction might represent migration between prey species, while coupling in the y -direction could denote migration among predator species.

Another intriguing attractor is the torus that emerges from the LA-LA attractor (cf. Fig. ??F), in which the two units continue to oscillate with a large amplitude, but quasi-periodically. Its geometry resembles that of the LA-LA attractor, but the increased coupling strength causes the units to exert a stronger mutual influence. Consequently, the reinjection still occurs, but now one unit pulls on the other so forcefully that the trajectory no longer follows a closed curve. Indeed, as ϵ increases, the torus expands, becoming wider.

Therefore, the reinjection mechanism, which acts to trap units in the excitability region of their uncoupled dynamics, underlies the emerging attractors we observe. This is true for the two distinct geometries: LA-LA and LA-SA, which emerge from different bifurcations. The mechanism also occurs for different dynamics: periodic and quasi-periodic.

3.4 Discussions

In this chapter we have shown that diffusive coupling acting on excitable dynamics can create multistability of oscillations. The variety of coexisting attractors, which can be periodic, quasiperiodic, and even chaotic, emerge in a similar way: through the trapping

of units in the excitability region of their local dynamics. This local dynamics consists of three equilibria living in the units' state space: an unstable focus, a saddle point $\mathbf{x}_s^{\text{unc}}$ and a stable equilibrium, which is the only attractor in the uncoupled system. The stable manifold $\mathbb{W}^s(\mathbf{x}_s^{\text{unc}})$ of $\mathbf{x}_s^{\text{unc}}$ is extended in state space and has one branch that spirals out of the unstable focus. As a consequence, it separates the nearby state space into two regions: one that directly converges to the stable node and another that has to go on a long excursion around the stable manifold before converging to the node. On top of this, the units feel the attractive diffusive coupling, which pulls one unit toward the other. The dynamics of the coupled units is determined by the interaction of these two effects: the local dynamics attempting to pull the units towards the stable node and the diffusive coupling attempting to pull the units towards each other.

This competition is controlled by the coupling strength ϵ . As already described in the literature for similar systems, there are two extremes [?]. For sufficiently small ϵ , the local dynamics dominates, and the only attractor is the stable node. For sufficiently large ϵ the coupling dominates, and the units converge to each other. When they do so, the coupling becomes zero, and then they again follow their uncoupled dynamics and converge to the stable node only. It is in between these extremes that interesting dynamics can occur [?]. In this case, the coupling is strong enough to impact the trajectory of the uncoupled system, but not enough to completely overrule it. Because of the geometry of state space, the coupling can manage to pull the units away from the stable node and into the excitability region. The units find a stable configuration in which they are repeatedly reinjected into the excitability region, generating permanent oscillations. The type of these oscillations depends on the coupling strength, the number of interacting units, and the network's topology.

It has been known that diffusive coupling on units with a single stable equilibrium in a region of state space can create oscillations. These oscillations can be periodic, originating from a Hopf bifurcation of the equilibrium [?, ?] or chaotic oscillations [?] originating from a Shilnikov homoclinic bifurcation [?]. However, as we have shown, the scenario for an excitable system, with the additional interaction of two unstable equilibria, has important differences to the single equilibrium case. First, for $N = 2$ coupled units, we have shown that periodic attractors can coexist with other periodic attractors and with the stable equilibrium, leading to a multistable coupled system. Further, these periodic attractors are qualitatively different: in one attractor, both units oscillate with a large amplitude (LA-LA attractor); in the other attractor, one unit instead has a very small amplitude oscillation, almost stationary (LA-SA and SA-LA attractors). The $N = 2$ case also supports the emergence of a quasiperiodic oscillation, which coexists with the stable equilibrium. The bifurcations giving rise to the periodic attractors also differ: the periodic attractors emerge either through a saddle-node bifurcation of limit cycles (SNLC) bifurcation or through a homoclinic (HOM) bifurcation.

In the bigger network, with $N = 10$ units, we have shown that the multistability becomes even richer. In this case, all these types of dynamics can coexist. The sheer number of coexisting attractors is also large (we observed up to 84 attractors for only $N = 10$ units), with a dominance of periodic solutions. Since units can be either trapped in the excitability region, with large amplitude oscillations, or oscillate with low amplitude near $\mathbf{x}_s^{\text{unc}}$, adding more units leads to a higher number of possible combinations of which units are placed in which position. Not all of these combinations are necessarily invariant solutions; and the ones that are invariant are not necessarily stable. The invariance and stability are controlled by the topology of the network, and more research in the future

is needed to understand how exactly. It would be interesting to understand which topologies maximize the number of attractors, and which minimize them. This could provide further insights into other systems, for which a scaling of the number of attractors with the size of the network has been observed [?, ?, ?].

By studying the attractors from the point of view of the local dynamics competing with the coupling, we identified an impact that the topology has on the attractors of the coupled system. Units that receive more connections tend to have a stronger coupling term than units with fewer connections. A stronger coupling coupling term pulls the units more strongly towards the excitability region. This effect is stronger in the slower region of the oscillation, close to $\mathbf{x}_s^{\text{unc}}$, where the local dynamics is weaker. Thus, one could expect the oscillation of the units with more connections to be pushed away further from $\mathbf{x}_s^{\text{unc}}$, and thus have a smaller amplitude than units with fewer connections. This is indeed what we observe: units with more neighbors have smaller amplitudes.

On the attractors, the units are permanently reinjected into the excitability region by the coupling. In this sense, they are trapped in a transient region (transient for the uncoupled dynamics). Trapping in transient regions due to coupling appears to be a common mechanism for creating new attractors in networked systems. We have observed a similar behavior in an excitable model of an ecological predator-prey system based on the Truscott-Brindley model [?]. There, new equilibria are created by the coupling. On the equilibria, the coupling exactly balances out the local dynamics, and the units reach an equilibrium. Another example of trapping has been elucidated in units with chaotic saddles in their local dynamics [?, ?, ?]. Chaotic saddles are non-attracting invariant chaotic sets. Under some circumstances, when a sufficiently large number N of units are coupled diffusively, they can get trapped in this chaotic saddle and form a chaotic attractor [?, ?]. Another example has been recently elucidated in a system with a canard [?].

Interestingly, in the neuronal system we have studied, the trapping also works if the coupling is present in only one of the directions x or y . These directions have different effects in generating new attractors, due to the geometry of state space. If only the x -direction of the coupling is present, only the LA-LA attractor emerges, not the LA-SA or SA-LA. For coupling in the y -direction the reverse is true: LA-LA does not emerge, but LA-SA and SA-LA do. This coupling in y is not biophysically relevant for the neuronal system we study here, but is important in ecological systems. There, this may represent the difference between migration of predators or the migration of prey species. In particular for the x -direction, we also mention that multistability is still maintained in a bigger networks with $N = 10$ units. The coexisting oscillating attractors, with a mixture of some units oscillating at large amplitude and some at low amplitudes still occur, with more units in high-amplitude oscillations than in the case with the x and y -couplings. We believe our study could serve as inspiration for future studies in other systems, such as in ecological ones, to investigate these effects of the coupling in more detail. Furthermore, it also serves as simple yet powerful example of the more general phenomenon of multistability through trapping of units in transients.

Acknowledgment

K.L.R. was supported by the German Academic Exchange Service (DAAD). E.S.M and U.F. acknowledge the support by the Deutsche Forschungsgemeinschaft (DFG) via the project number 454054251 (FE 359/22-1) and by The São Paulo Research Foundation

(FAPESP) via the project number 2023/15040-0. The simulations were performed at the HPC Cluster ROSA, located at the Carl von Ossietzky Universität Oldenburg (Germany) and funded by the DFG through its Major Research Instrumentation Programme (INST 184/225-1 FUGG) and the Ministry of Science and Culture (MWK) of the state of Lower Saxony.

Supplemental material

Attractors for different local dynamics of the neurons

In the main text we study the behavior of the coupled neuronal units with fixed parameters. One important parameter we can vary is I . Taking it as a bifurcation parameter and increasing it, the manifolds of the saddle approach each other to form a homoclinic orbit at $I = I_{\text{HOM}} \approx 3.09$. At $I > I_{\text{HOM}}$, a stable limit cycle emerges from the homoclinic orbit, and now the unit is bistable. Increasing I further, the saddle and the node approach each other and a saddle-node bifurcation occurs at $I = I_{\text{SN}} \approx 4.8$, and the neuron goes back to being monostable, with only the stable limit cycle remaining.

To recall the attractors emerging at $I = 2.0$ and to provide a complementary view, we show in Fig. ?? a three-dimensional version of Fig. ???. One can notice the emergence of the LA-LA attractor, and its eventual replacement by a torus. Also one can see the emergence of the LA-SA attractors, which emerge touching the red circles, that denote saddle points of saddle-node type.

To understand how these attractors depend on the local dynamics of the units, particularly how they change when the units go through the homoclinic and saddle-node bifurcation, we have studied a two-parameter continuation curve of the bifurcations giving rise to both the LA-LA and the LA-SA attractors. This is shown in Fig. ??.

The SNLC bifurcation generating the LA-LA solution converges to $(\epsilon, I) = (0, I_{\text{HOM}})$. For $I > I_{\text{HOM}}$ the LA-LA seems to occur for any value $\epsilon > 0$ that we tested. Therefore it seems that the LA-LA SNLC curve becomes vertical for $I > I_{\text{HOM}}$ at $\epsilon = 0$. The SNLC bifurcation destroying the LA-SA attractor converges to $(\epsilon, I) = (0, I_{\text{SN}})$.

The attractors therefore exist for a wide range of parameters in the local dynamics of the units. Further, for $I > I_{\text{HOM}}$, another attractor emerges, in which both units synchronize completely in the limit cycle that is now stable in the local dynamics.

Simple local dynamics: polynomial model

In the neuronal system, new attractors are created by an interplay between the coupling and the uncoupled vector field. There, units are trapped in a large excitability region wherein they oscillate. Trapping can occur more broadly in other systems. To illustrate this, we study a much simpler system. The basic result is that new attractors also emerge from this interplay. In particular, similarly to before, stable equilibria or limit cycles can appear for a finite interval of positive coupling strengths.

We take the uncoupled system as $f(x) = -(x+2)(x+1)x(x-1)(x-2) + d = -x^5 + 5x^3 - 4x + d$ for $d = 2$, such that it has 3 equilibria. The coupled system is then

$$\dot{x}_1 = -x_1^5 + 5x_1^3 - 4x_1 + d + \epsilon(x_2 - x_1) \quad (3.8)$$

$$\dot{x}_2 = -x_2^5 + 5x_2^3 - 4x_2 + d + \epsilon(x_1 - x_2). \quad (3.9)$$

For $\epsilon = 0$ it therefore has 3^2 equilibria. By plotting the system's nullclines, it is easy to verify that an increase in ϵ causes them to move toward each other such that at $\epsilon \approx 0.2419$ a saddle-node (SN) bifurcation occurs that generates a new attractor. In fact, because of the permutation symmetry between the units, two SN bifurcations are happening, generating two new stable equilibria. These new intersections live until $\epsilon \approx 0.94$, when another SN bifurcation destroys them. These equilibria exist as the coupling term $\epsilon(x_2 - x_1)$ exactly balances out the local dynamics $f_1(x_1)$ of unit 1 (and equivalently for unit 2). In this sense, on the equilibria, the units are also trapped. These two new attractors therefore emerge (and disappear) due to the coupling. We summarize this behavior in a continuation curve performed using XPPAUT [?].

These equilibria become limit cycles if one introduces a rotation in the system. To do this, one can modify the uncoupled dynamics, defining x as a radial variable r in polar coordinates and introducing an angular variable θ :

$$\dot{r} = -r(r+2)(r+1)(r-1)(r-2) + d \quad (3.10)$$

$$= -r^5 + 5r^3 - 4r + d$$

$$\dot{\theta} = \omega. \quad (3.11)$$

This system can be viewed as the first system with a rotation. In this case, the equilibria we observed before become limit cycles, and they now emerge through a saddle-node bifurcation of limit cycles (SNLC) at the same parameter values as before. Also, similarly to the equilibria, the units on these emerging limit cycles are trapped by the coupling in a transient region of their uncoupled dynamics.

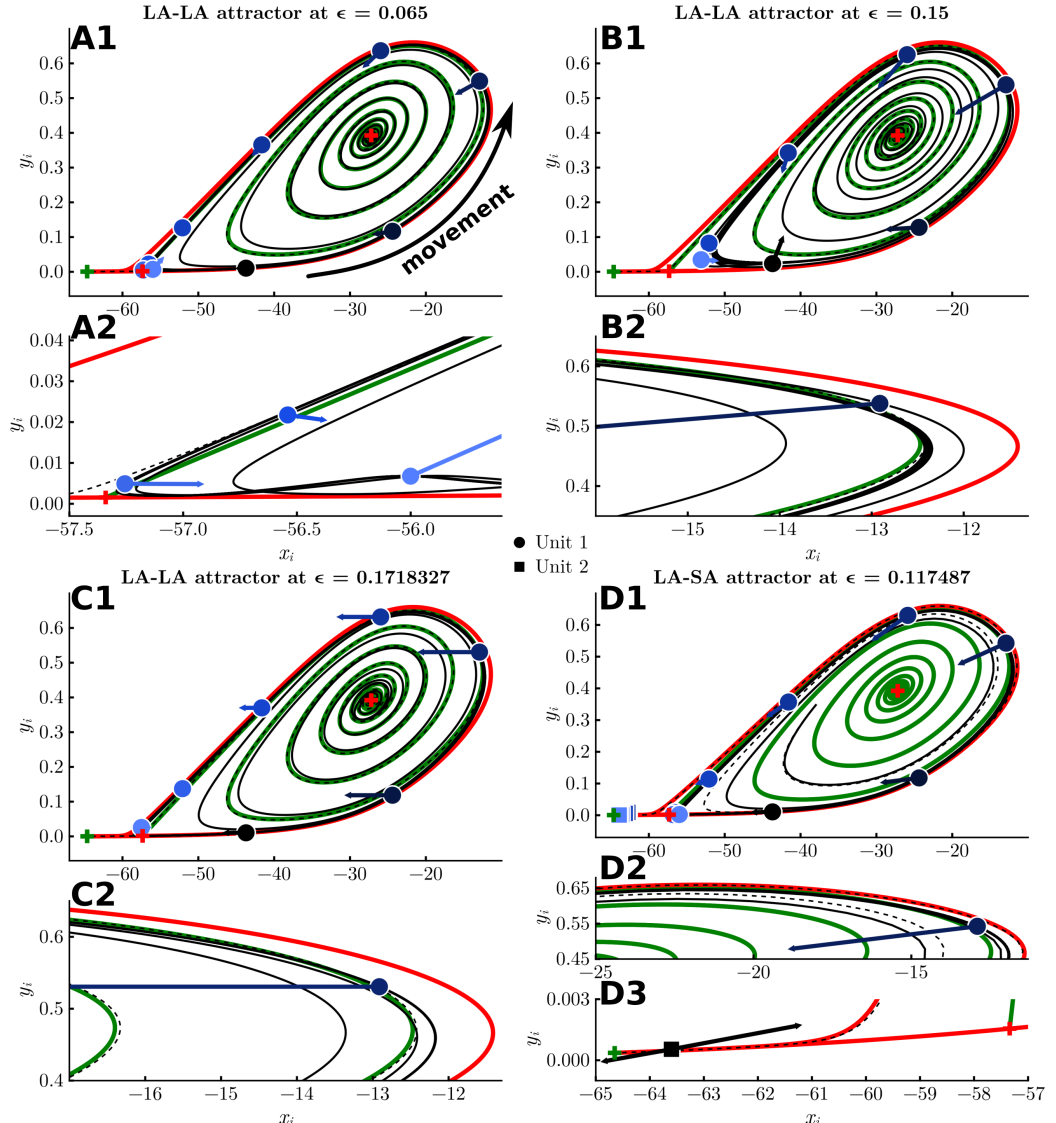


Figure 3.5: Illustration of the trapping phenomenon. Each panel shows a projection of the full 4D state space into the subspace $x_i - y_i$ of unit i . The three symmetric equilibria in the coupled system are shown: the stable equilibrium as a green cross, the unstable focus and the saddle point $\mathbf{x}_s^{\text{unc}}$ as red crosses. The stable $W^s(\mathbf{x}_s^{\text{unc}})$ and unstable $W^u(\mathbf{x}_s^{\text{unc}})$ manifolds of the saddle $\mathbf{x}_s^{\text{unc}}$ in the uncoupled system are also shown as green and red lines, respectively. The black solid lines represent an illustrative trajectory converging to one of the emerging attractors. A trajectory starting with the same initial condition but with $\epsilon = 0$ is shown in black dashed lines. The position and coupling vector ϵg_1 of unit 1 at specific time points are plotted respectively as circles and arrows. The unit's colors vary from black to light blue to indicate the passage of time. The emerging attractor in panels A1-A2 is the LA-LA attractor for $\epsilon = 0.065$. The magnification in panel A2 shows that the projection of the trajectory of the coupled system crosses $W^s(\mathbf{x}_s^{\text{unc}})$, corresponding to a reinjection into the excitability region. The attractor is the same in B1-B2 but at a stronger coupling $\epsilon_1 = 0.15$, showing that the reinjection occurs earlier along $W^s(\mathbf{x}_s^{\text{unc}})$ when ϵ increases. Panels C1-C2 show that this attractor still emerges if $\epsilon_2 = 0$, at the cost of requiring a larger value of ϵ_1 . Panels D1-D3 show the geometry of the LA-SA attractor, with the position of unit 2 (projected into $x_2 - y_2$) also shown as squares. In this case, unit 1 is also seen to cross $W^s(\mathbf{x}_s^{\text{unc}})$ and thus to be trapped in the excitability region. Panel D3 is added specifically to indicate the behavior of unit 2, with two arrows: the upward and rightward pointing arrow is the coupling ϵg_2 , and the leftward and downward arrow is the unit's uncoupled dynamics f_2 .

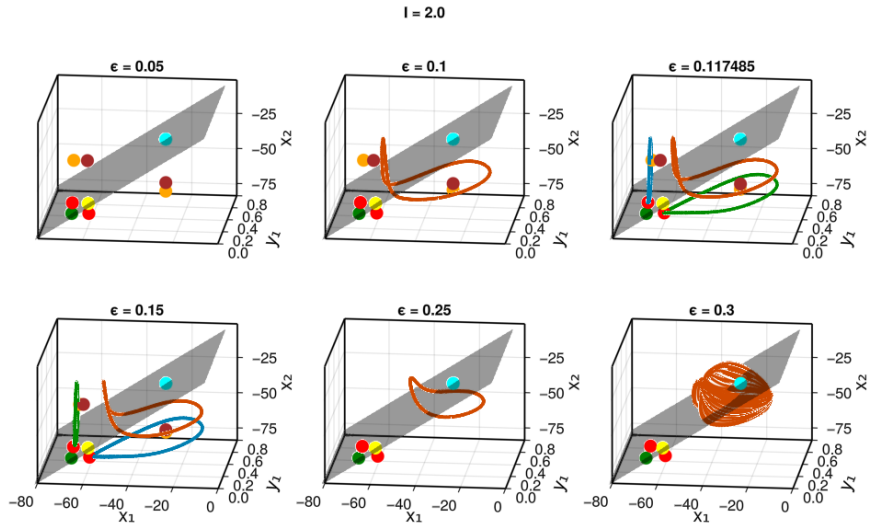


Figure 3.6: Attractors transformed or created by the diffusive coupling for $I = 2.0$. Each panel is a projection onto 3D space spanned by $x_1 - y_1 - x_2$. The gray plane denotes the plane with $x_1 = x_2$. The circles' colors denote types of equilibria. These equilibria are formed as combinations of the three equilibria in the single units, and are labeled according to this combination: green for stable node, yellow for saddle-saddle (two positive, two negative eigenvalues), cyan for focus-focus (two pairs of complex conjugate eigenvalues with positive real part), red for saddle-node (three positive, one negative eigenvalue), orange for node-focus (one pair of complex conjugate eigenvalues with positive real part, two negative eigenvalues) and brown for saddle-focus (one pair of complex conjugate eigenvalues with positive real part, one positive and one negative eigenvalues). One attractor emerges at $\epsilon \sim 0.065$ corresponding to two units oscillating with large amplitude. Two (symmetric) attractors emerge at $\epsilon \sim 0.117485$ corresponding to one unit oscillating with small amplitude around the saddle-node point and the other oscillating with large amplitude. The symmetric attractors die out at $\epsilon \approx 0.22$. A torus emerges at $\epsilon \sim 0.25$. More bifurcations keep happening until all new attractors die out, and only the stable equilibrium is left.

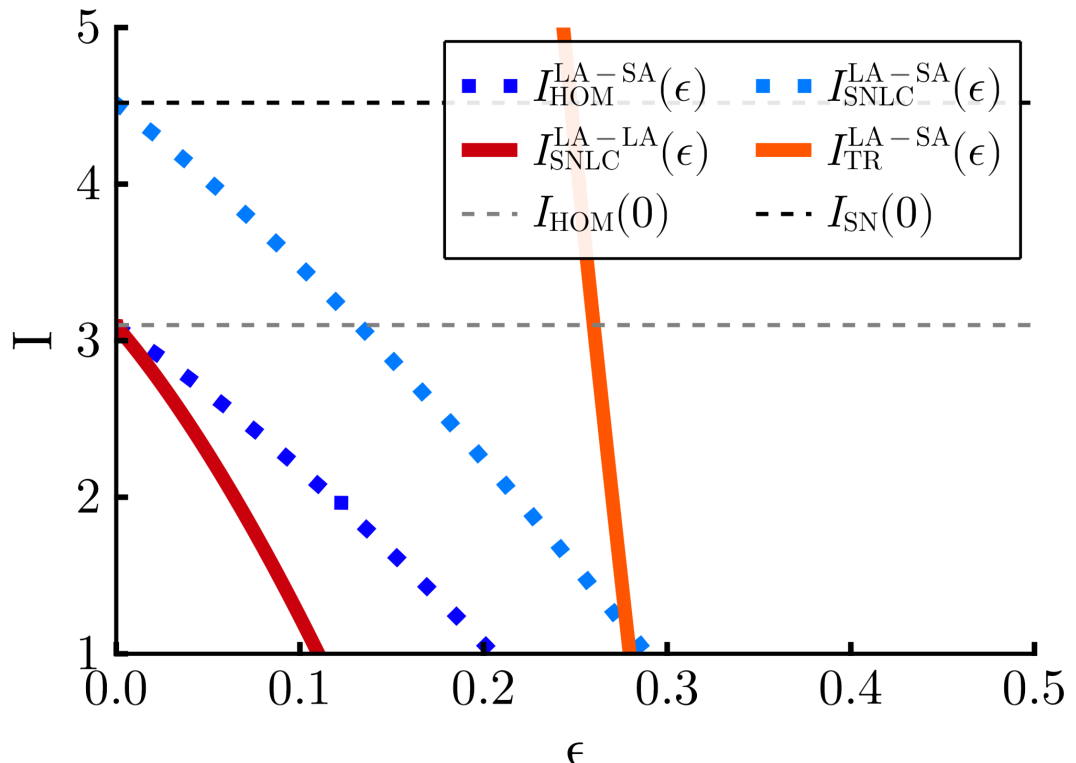


Figure 3.7: Two-parameter continuation curves across I and ϵ . The curves denote the $I(\epsilon)$ combinations that lead to each labelled bifurcation. The red and orange solid curves denote the bifurcations for LA-LA attractors, born through a SNLC bifurcation and de-stabilized through a torus (TR) bifurcation. The LA-LA is thus stable in between those curves. The blue and cyan dotted curves denote bifurcations occurring for the LA-SA attractor, born through a homoclinic (HOM) bifurcation and disappearing through a saddle-node bifurcation of limit cycles (SNLC). The LA-SA exists in between those curves. The homoclinic and saddle-node of equilibria (SN) bifurcations occurring in the uncoupled ($\epsilon = 0$) case are respectively shown in grey and black dashed lines. Continuations were done using XPPAUT [?]

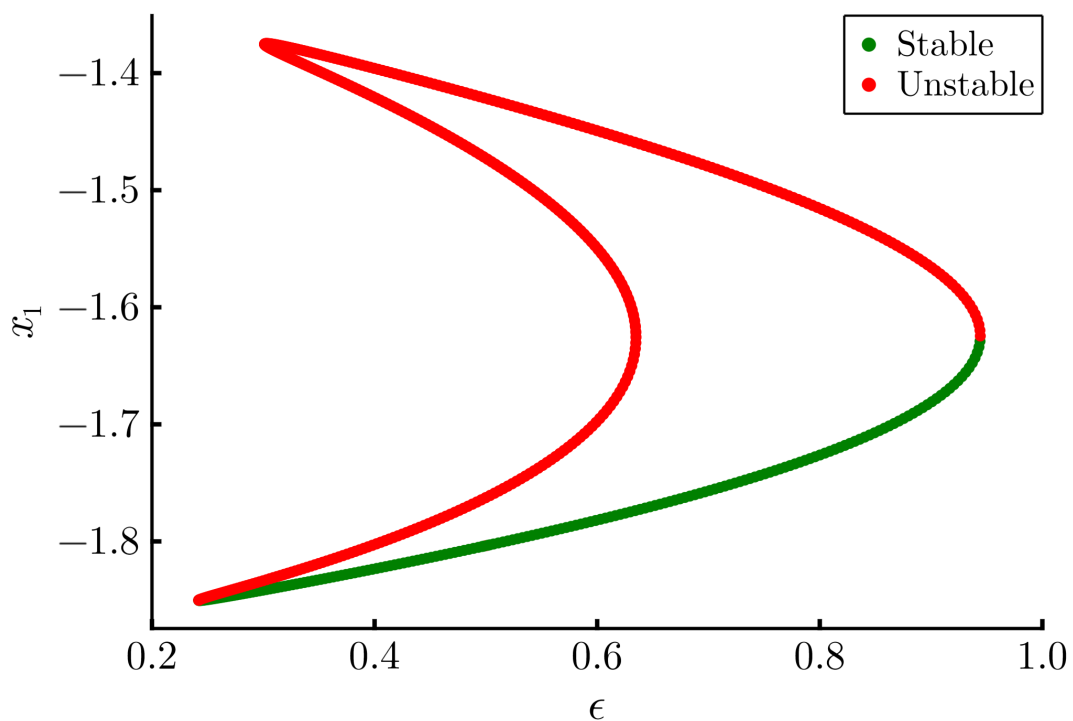


Figure 3.8: Continuation of stable equilibrium emerging due to diffusive coupling in the simple algebraic system. Similarly to the stable limit cycles we see in the neuronal system, the emerging attractor exists for an interval of coupling strengths, here approximately $[0.24, 0.94]$. It emerges and disappears in a saddle-node bifurcation.

Chapter 4

Conclusions

Science is typically reductionist [?]. We break a hard problem into smaller parts that are easier to understand separately. We have achieved tremendous success with this effort, but we have not solved everything; indeed, we have found out that putting everything back together can be quite complicated: the interactions between the parts can generate complex behavior that is not present in any one of the parts alone. The field of complex systems arose from the need to understand this *emergent phenomena* - to (re)construct the full system's behavior from knowledge of its parts. In the case of networked systems, studied in this thesis, the challenge can be phrased as the need to understand how the whole system's behavior arises from the coupling between the units. A major challenge still today is to develop tools that allows us to characterize and understand complicated emergent behavior.

One such complicated behavior in networks is the coexistence of multiple stable solutions to the same equations with the same parameters - *multistability*! How do these solutions come about, where they are situated and how they are separated in state space - these are all questions under active research [?, ?, ?].

Some of these stable solutions may correspond to synchronized regimes, which brings into light another important phenomenon: *synchronization*. Here again the field of complex systems has to contend with another problem: how individually distinct units can cooperate together and start to operate in unison, in a beautiful example of an emergent phenomenon. The study of synchronization - both frequency and phase synchronization - also has important practical motivations, for instance in the study of power grids. In power grids, and other complex networks, understanding the robustness of solutions, in particular of synchronized solutions has been an object of active research.

Combining these two research areas, Chapter ?? investigated the robustness of solutions in a complex network of Kuramoto oscillators, a paradigmatic model for studies on synchronization phenomena and complex networks in general. The idea was to investigate how the network behaves - how the solutions change - when we alter the parameter of a single unit in the network. We found that the *dynamical malleability* of the network depends on how strongly coupled the units are, and the topology of the connections. Roughly, we showed that for very weak coupling strength the individual tendencies of the oscillators win and most of them oscillate incoherently. For sufficiently strong coupling, most of the oscillators become phase locked - they oscillate at the same frequency. This is the same behavior as in all-to-all networks (see Sec.??). The spatial pattern of the phases, which we can measure via the degree of phase synchronization, was then determined by the topology. For several of the coexisting attractors, including the most phase synchronized attractor, the following tendency was observed: networks dominated by short-range connections tend to have attractors with short-range patterns (phase desynchronized), while networks dominated by long-range connections tend to have attractors with long-range patterns (phase synchronized). In parameter space, phase synchronization in these networks lives in the region of sufficiently high coupling strength and number of long-range connections. Changing the parameters toward this region therefore makes the system undergo a transition to phase synchronization. We showed that precisely during this transition their dynamical malleability increases con-

siderably. To the point that changing a single unit radically alters the pattern of phases in the network, potentially changing it from phase synchronized to phase desynchronized.

The mechanism for this dynamical malleability is two-fold. First, it is related to *increased sample-to-sample fluctuations* near a phase transition [?, ?]. This mechanism does not require multistability. In fact, suppose the systems have a single attractor, like the randomly connected networks. Each change to a parameter of a unit leads to a different dynamical system, which may have a different attractor. In particular, the transition to phase synchronization of this attractor may occur at different coupling strength values, earlier or later compared to the system before the change. If we enact this change but keep the coupling strength fixed, we switch to an attractor that has a smaller or larger value of phase synchronization - this is the fluctuation from one sample to another. If the systems have multiple attractors, this effect is still there, but there is the added possibility of switching to other attractors, which might be even more different. The *multistability* increases the possible fluctuations that may occur. This explains our observation that for Watts-Strogatz networks the malleability and multistability seem to go hand in hand. It also explains why these networks have a considerably larger malleability than the distance-dependent networks, which do not seem to be multistable.

An important concept in the area of complex systems is that of global stability, typically taken to mean the relative size of the basin of attraction of each attractor. In this view, attractors whose basins occupy larger regions of state space are more globally stable [?]. The rough idea is that trajectories on attractors with bigger basins of attraction are more likely to require bigger perturbations in order to be kicked across the basin boundary and into another attractor. This is not necessarily the case, however, since the situation depends on the geometry of the basin of attraction [?], but it highlights the importance of studying perturbations applied to the state of a system. In general, more attractors means they are sharing state space more and therefore the global stability is smaller, meaning the system is less robust (or less resilient, depending on terminology [?]). In this work we show that multistability affects the robustness of the system in another way: by affecting its malleability. So not only is it dangerous to kick the state of the system, it is also dangerous to change its parameters - even the parameter of one single unit!

Another important observation was the study of how malleability, and multistability, depend on the topology of the system. Topologies that put the systems in the vicinity of a transition to phase synchronization, which were in the small-world range, made it very malleable. An important question that is left for future work is why these specific topologies lead to a higher number of attractors - which properties do they possess that lead to the emergence of the attractors, compared to, say, the random topologies, which do not induce multistability? The distance-dependent networks also do not seem to be multistable, a factor that would also be interesting to investigate.

A related question is about the generality of these results. Malleability due to sample-to-sample fluctuations is very common, being extensibly described in statistical physics literature [?]. We also described it initially in a network of spiking neurons [?], and observed it in the Kuramoto model under different topologies of distributions of the natural frequency, and under other models, such as a simple model of excitable cells. We believe that the multistability results will also generalize somehow - supported by the available evidence from other works - but this is also object of future research. Understanding better the mechanisms generating the multistability will also help answer

this.

In a similar vein, we also investigated how multistability emerges when excitable neurons are coupled diffusively. Excitability in the individual units here occurs due to the presence of a saddle and an unstable equilibrium in state space, which force part of the trajectories to go around on a long excursion before eventually converging to the stable equilibrium. These region where trajectories go through is called the *excitability region*. We showed that the coupling can trap trajectories in this excitability region by repeatedly reinjecting them there. This mechanism underlies all the emergent attractors we observed, even though they arise due to different bifurcations: saddle-node of limit cycles and homoclinic. For two units, it can create three coexisting periodic attractors, and can also create a quasiperiodic attractor. For more units, it can create a larger number of attractors, including potentially a chaotic attractor. Based on the trapping mechanism and preliminary results, we conjecture that the topology of the networks plays a key role in dictating which attractors emerge, and how many. This could be very similar to Kuramoto networks, and a more in-depth comparison is definitely warranted. It would be very interesting in the future to explore how exactly the size and topology of the networks control the emerging attractors.

In this initial work we decided to focus mainly on the pure dynamics of the system, so we showed most of the results in the case where the coupling is applied to both the x and y directions of the system. In some models, such as ecological models - where the diffusive term would model a migration of species - this might be very sound. For the neuronal case, however, only the x -coupling is biophysically sound. Motivated by this fact, we also investigated how the attractors change when the coupling is applied to only one variable. Interestingly, the mechanism is still present, but the two main types of attractors we observed split up when the coupling is split. The exclusive x -coupling leads to the attractor with two units trapped in the excitability region (LA-LA); the exclusive y -coupling leads to the one with only one unit in the excitability region (LA-SA or SA-LA). We confirmed this with a bifurcation analysis and also qualitatively explained it based on the geometry of the attractors and the trapping mechanism. This is important in terms of potential applications. First, it means that adding a gap junction between two otherwise silent neurons could make them bistable, with the possibility of periodic or even quasiperiodic spiking. In fact, there is some evidence that this seems to occur in neurons coupled under gap junctions in the motor cortex of fruit flies [?]. It is also interesting in the ecological direction, if we consider that only some species in an ecological niche might be migrating between patches.

Furthermore, we focused for simplicity on the excitable case, where the trapping mechanism creating the attractors is more easily seen. But attractors still emerge similarly in a bistable regime, where the stable equilibrium coexists with a stable limit cycle. We can achieve this by changing the input current I of the model. A difference in this case is that the uncoupled neuron already has an oscillating attractor. Therefore, when they are diffusively coupled they can also synchronize together in this oscillating attractor. This system thus has the possibility of achieving full synchronization on a periodic attractor. In this case, one could reframe the study in terms of the stability, global and linear, of the synchronized state, and how the coupling might create new attractors and thus reduce the relative size of the basin of the synchronized attractor.

We initially arrived at this problem when trying to understand the synchronization behavior of a network of bursting neurons [?]. The degree of phase synchronization in that system changes nonmonotonically as a function of the coupling strength: increas-

ing the coupling initially increases the phase synchronization, then actually decreases it in a certain region, before increasing it again for very strong coupling. This is also reminiscent of a behavior observed in networks with chaotic saddles in Ref. [?]. We also studied a network of bursting neurons following another model, and found that a chaotic saddle was important there but also a slow region of system's limit cycle was related to the multistability that emerged. From the work on excitable neurons, we understand that slowness can help generate attractors, at least for the reinjection mechanism we observed. It would be interesting in the future to go back and finish the initial studies.

When working on a project, I believe it is not an uncommon feeling to find an interesting paper, try to replicate its results and not quite manage. Then, to look at the source code that the authors hopefully provided, and to be underwhelmed. While working on a paper, it is often the case that people might want spend as little time as possible implementing the algorithms they need, leading usually to confusing code, which might not be as efficient as it could, and not as well-tested - and thus, more susceptible to errors. One solution to this is to create a unified library that implements efficient code, tests and documents it. And to make it open-source, to share it with the whole community. Then, anyone can scrutinize the code, find improvements and test it further. Also, more importantly, everyone can use it. This saves implementation time, potentially run times due to improved code efficiency, and also re-implementation time for poor students aiming to replicate papers. This is the philosophy of the dynamical systems library [?], started by Dr. George Datseris, written in the Julia programming language. With this idea in mind, we also collaborated to implement algorithms related to finding attractors and their basins. In particular, I worked on the algorithm used in the two multistability works in this thesis. It is a brute-force algorithm that integrates trajectories, converts them into vectors of features, and selects attractors as unique groups of features [?, ?, ?]. Together with Prof. Alexander Wagemakers, we also implemented an algorithm that applies attractor-finding algorithms across a parameter range, in a continuation manner. The result of this work was the *Attractors.jl* package, also co-developed by more collaborators, and a publication describing this novel algorithm and improvements to previous literature [?].

So far on the study of dynamical systems we have mostly focused on attractors. The motivation for this is that attractors represent a system's long-term dynamics: after some *transient* time, trajectories converge to attractors. There is, however, a key assumption here: that the period of time during which we observe the system T_{obs} is longer than the convergence time T_{conv} to the attractor. It is a matter of time-scales: of the observation versus the relaxation to the attractor. Whether this can be guaranteed or not depends on the application. In power grids, for instance, one is generally interested in the long-term dynamics of the system. In the brain, however, changes may be occurring too fast, and there may not be enough time to wait for convergence to an attractor. The time-scales can also vary within the same system: as we saw in the excitable units, trajectories starting on one side of the state space converge rapidly to the attractor, whereas trajectories starting on the excitability region spend a relatively long time performing an excursion in space before reaching the attractor. This problem is made more complicated due to the fact that there are many mechanisms that can generate long - potentially arbitrarily long - transients. An example is chaotic saddles, wherein trajectories can stay indefinitely long [?]. Therefore, the behavior that is actually observed in some studies may be a transient. Moreover, some of these long-lived transients occur inside attractors. One example can be seen in ghost states

inside chaotic attractors - such as for the Logistic map or the Lorenz system - where the trajectories switch between clearly chaotic and seemingly periodic dynamics (cf. Chap. ??). Another example is the stable heteroclinic cycle: the cycle as a whole can be an attractor, but trajectories on it switch between the neighborhoods of saddle-points, describing sequences of metastable regimes. Yet another example is crawl-by motion, in which a limit cycle is in the proximity of a saddle-point. The region near the saddle-point may have very slow dynamics, and trajectories on the cycle take a long time to pass through (crawl-by) this region [?]. These examples illustrate the intricate relation between multistability - and attractors - and metastability.

Transients can play important roles. A specific example that illustrates the role of sequences of transient states is the Turing machine, the paradigmatic model for *computations* [?, ?]. It is a simple finite state machine with a head that stores a certain state and can read, write, and move along a tape. The tape is subdivided into cells containing symbols (e.g., 0's and 1's). The head represents a modern computer's central processing unit, while the tape represents the memory. Accordingly, the head follows a set of instructions that take the current state, currently read symbol on the tape and outputs the new state, the new symbol it writes on the tape, and the direction it moves. Computations are done by traversing a sequence of such state-symbol combinations. The machine may run forever - it is said to not halt -, in which case the computation is not completed. If the machine does halt, the computation is finished. From this point of view, therefore, the computation is only complete once the machine terminates the previous sequence of states. This sequence can therefore be seen as a type of transient behavior, which is crucial for the computation performed by the machine. This remark is not just an analogy - dynamical systems can be constructed that implement Turing machines [?].

More concretely, in the brain, transients have been shown to play important roles [?, ?]. There is a plethora of observations showing neural activity going through sequences of distinct states, which are all therefore transient [?, ?]. In several cases, these states are long-lived (i.e., metastable). Understanding the exact roles that *metastable regimes* play in neural circuits is crucial to understanding how they perform computations, a central question in neuroscience and also artificial intelligence [?, ?, ?]. Recent work, based on theoretical and experimental results, has shown that ghosts of saddle-node equilibria, which generate long transients, are a particularly important mechanism [?, ?, ?, ?]. It is expected, however, that other mechanisms are also present in circuits. For instance, a wide literature in neuroscience uses attractors to perform computations, and adds external perturbations to induce changes between regimes [?, ?, ?, ?]. It will be important in the future to contrast these two ideas to see the actual roles played by each of them.

To better understand the role of transients on computations in neural circuits, it is therefore important to have both an in-depth as well as a general understanding of metastable dynamics. Under this logic we developed a *general conceptual framework* for metastability, collecting and refining ideas from the neuroscience and dynamical systems literatures. As seen in Chap. ??, we proposed that the main concept behind metastability is that of long-lived transients, and showed many dynamical mechanisms capable of generating it. In the future, one can use this framework to actively compare the different mechanisms, with a view towards experiments - both biological as well as in silico, looking to understand how networks perform computations [?].

Besides the metastable regimes themselves, perhaps the actual *sequences* play an

important role. This is the case in the Turing machine, but there is also evidence in biological networks. An important example, already mentioned in the Introduction and in Chap. ??, showed in a series of works that sequences of metastable regimes are elicited when mice are fed tastants [?]. The sequence of regimes is unique to each tastant, suggesting they play an active role in encoding the stimuli [?]. Sequences of metastable regimes have been linked to computations in other experiments also [?, ?, ?]. In this case, a useful concept coming from dynamical systems theory is that of excitable networks by Ashwin and Postlethwaite [?, ?]. They developed methods that allow one to construct systems with prescribed connections between equilibria states. These connections may be spontaneously activated (as in connected ghosts) or via a perturbation (by perturbing across the basin boundary). This is an example of how the theory of dynamical systems is offering many tools and mechanisms that can be used to model and better understand how circuits are actually solving tasks and performing computations. This is an exciting area for future research.

Taking everything together, the field of complex systems is under intense research, with lots of us aiming to develop theory and tools to understand emergent dynamical phenomena like synchronization, the coexistence of multiple long-term solutions and the (transient) path to them. I believe that during my PhD we managed to provide some timely contributions in these directions, but there is still much to be done - with applications being very significant in biology, technology and even climate. I am very excited to help put all these pieces together.

Bibliography

- [1] Ulrike Feudel. Complex Dynamics In Multistable Systems. *International Journal of Bifurcation and Chaos*, 18(06):1607–1626, 2008.
- [2] Alexander N. Pisarchik and Alexander E. Hramov. Multistability in Physical and Living Systems, Characterization and Applications. *Springer Series in Synergetics*, 2022.
- [3] Alexander N. Pisarchik and Ulrike Feudel. Control of multistability. *Physics Reports*, 540(4):167–218, 2014.
- [4] Ronghui Zhu, Jesus M. del Rio-Salgado, Jordi Garcia-Ojalvo, and Michael B. Elowitz. Synthetic multistability in mammalian cells. *Science*, 375(6578):eabg9765, 2022.
- [5] Erzsébet Ravasz Regan and William C. Aird. Dynamical Systems Approach to Endothelial Heterogeneity. *Circulation Research*, 111(1):110–130, 2012.
- [6] Tahmineh Khazaei, Rory L. Williams, Said R. Bogatyrev, John C. Doyle, Christopher S. Henry, and Rustem F. Ismagilov. Metabolic multistability and hysteresis in a model aerobe-anaerobe microbiome community. *Science Advances*, 6(33):eaba0353, 2020.
- [7] Frank Hellmann, Paul Schultz, Patrycja Jaros, Roman Levchenko, Tomasz Kapitaniak, Jürgen Kurths, and Yuri Maistrenko. Network-induced multistability through lossy coupling and exotic solitary states. *Nature Communications*, 11(1):592, 2020.
- [8] Lukas Halekotte, Anna Vanselow, and Ulrike Feudel. Transient chaos enforces uncertainty in the British power grid. *Journal of Physics: Complexity*, 2(3):035015, 2021.
- [9] Hugh R. Wilson and Jack D. Cowan. Excitatory and Inhibitory Interactions in Localized Populations of Model Neurons. *Biophysical Journal*, 12(1):1–24, 1972.
- [10] Jennifer Foss, André Longtin, Boualem Mensour, and John Milton. Multistability and Delayed Recurrent Loops. *Physical Review Letters*, 76(4):708–711, 1996.
- [11] Mathieu Golos, Viktor Jirsa, and Emmanuel Daucé. Multistability in Large Scale Models of Brain Activity. *PLoS Comput Biol*, 11(12):1004644, 2015.
- [12] Andrew Flynn and Andreas Amann. Exploring the origins of switching dynamics in a multifunctional reservoir computer. *Frontiers in Network Physiology*, 4:1451812, 2024.
- [13] Alexander Robinson, Reinhard Calov, and Andrey Ganopolski. Multistability and critical thresholds of the Greenland ice sheet. *Nature Climate Change*, 2(6):429–432, 2012.

- [14] Ulrike Feudel, Celso Grebogi, Leon Poon, and James A. Yorke. Dynamical properties of a simple mechanical system with a large number of coexisting periodic attractors. *Chaos, Solitons & Fractals*, 9(1-2):171–180, 1998.
- [15] Miri Adler, Avi Mayo, Xu Zhou, Ruth A. Franklin, Matthew L. Meizlish, Ruslan Medzhitov, Stefan M. Kallenberger, and Uri Alon. Principles of Cell Circuits for Tissue Repair and Fibrosis. *iScience*, 23(2):100841, 2020.
- [16] Arkady Pikovsky, Michael Rosenblum, and Jürgen Kurths. *Synchronization: A Universal Concept in Nonlinear Science*, volume 70. Cambridge University Press, 2001.
- [17] Stefano Boccaletti, Alexander N. Pisarchik, Charo I. del Genio, and Andreas Amann. *Synchronization: From Coupled Systems to Complex Networks*. Cambridge University Press, 2018.
- [18] Alex Arenas, Albert Díaz-Guilera, Jurgen Kurths, Yamir Moreno, and Changsong Zhou. Synchronization in complex networks. *Physics Reports*, 469(3):93–153, 2008.
- [19] Steven H. Strogatz. From Kuramoto to Crawford: exploring the onset of synchronization in populations of coupled oscillators. *Physica D: Nonlinear Phenomena*, 143(1-4):1–20, 2000.
- [20] W Singer. Neuronal synchrony: a versatile code for the definition of relations? *Neuron*, 24(1):49–65, 111, 1999.
- [21] Pascal Fries. Rhythms for Cognition: Communication through Coherence. *Neuron*, 88(1):220–235, 2015.
- [22] Thilo Womelsdorf and Pascal Fries. The role of neuronal synchronization in selective attention. *Current Opinion in Neurobiology*, 17(2):154–160, 2007.
- [23] Silvan Hürkey, Nelson Niemeyer, Jan-Hendrik Schleimer, Stefanie Ryglewski, Susanne Schreiber, and Carsten Duch. Gap junctions desynchronize a neural circuit to stabilize insect flight. *Nature*, 618(7963):118–125, 2023.
- [24] Juan A. Acebrón, L. L. Bonilla, Conrad J. Pérez Vicente, Félix Ritort, and Renato Spigler. The Kuramoto model: A simple paradigm for synchronization phenomena. *Reviews of Modern Physics*, 77(1):137–185, 2005.
- [25] Francisco A. Rodrigues, Thomas K.D.M. Peron, Peng Ji, and Jürgen Kurths. The Kuramoto model in complex networks. *Physics Reports*, 610:1–98, 2016.
- [26] R. C. Budzinski, K. L. Rossi, B. R. R. Boaretto, T. L. Prado, and S. R. Lopes. Synchronization malleability in neural networks under a distance-dependent coupling. *Physical Review Research*, 2(4):043309, 2020.
- [27] Kalel L. Rossi, Roberto C. Budzinski, Bruno R. R. Boaretto, Lyle E. Muller, and Ulrike Feudel. Shifts in global network dynamics due to small changes at single nodes. *Physical Review Research*, 5(1):013220, 2023.
- [28] Hyunsuk Hong, Hugues Chaté, Hyunggyu Park, and Lei Han Tang. Entrainment transition in populations of random frequency oscillators. *Physical Review Letters*, 99(18):1–4, 2007.

- [29] Hyunsuk Hong, Hyunggyu Park, and Lei Han Tang. Finite-size scaling of synchronized oscillation on complex networks. *Physical Review E*, 76(6):1–7, 2007.
- [30] Franziska Peter and Arkady Pikovsky. Transition to collective oscillations in finite Kuramoto ensembles. *Physical Review E*, 97(3):032310, 2018.
- [31] Paulo F. C. Tilles, Fernando F. Ferreira, and Hilda A. Cerdeira. Multistable behavior above synchronization in a locally coupled Kuramoto model. *Physical Review E*, 83(6):066206, 2011.
- [32] Maximilian Gelbrecht, Jürgen Kurths, and Frank Hellmann. Monte Carlo basin bifurcation analysis. *New Journal of Physics*, 22(3):033032, 2020.
- [33] Max Potratzki, Timo Bröhl, Thorsten Rings, and Klaus Lehnertz. Synchronization dynamics of phase oscillators on power grid models. *Chaos: An Interdisciplinary Journal of Nonlinear Science*, 34(4):043131, 2024.
- [34] Daniel A. Wiley, Steven H. Strogatz, and Michelle Girvan. The size of the sync basin. *Chaos: An Interdisciplinary Journal of Nonlinear Science*, 16(1):015103, 2006.
- [35] Alex Townsend, Michael Stillman, and Steven H. Strogatz. Dense networks that do not synchronize and sparse ones that do. *Chaos: An Interdisciplinary Journal of Nonlinear Science*, 30(8):083142, 2020.
- [36] Yuanzhao Zhang and Steven H. Strogatz. Basins with Tentacles. *Physical Review Letters*, 127(19):194101, 2021.
- [37] K. L. Rossi, R. C. Budzinski, B. R. R. Boaretto, T. L. Prado, U. Feudel, and S. R. Lopes. Phase-locking intermittency induced by dynamical heterogeneity in networks of thermosensitive neurons. *Chaos: An Interdisciplinary Journal of Nonlinear Science*, 31(8):083121, 2021.
- [38] J L Hindmarsh and R M Rose. A model of neuronal bursting using three coupled first order differential equations. *Proceedings of the royal society of London B: biological sciences*, 221(1222):87–102, 1984.
- [39] Eugene M Izhikevich. *Dynamical systems in neuroscience*. MIT press, 2007.
- [40] Everton S. Medeiros, Rene O. Medrano-T, Iberê L. Caldas, and Ulrike Feudel. Boundaries of synchronization in oscillator networks. *Physical Review E*, 98(3):030201, 2018.
- [41] Everton S. Medeiros, Rene O. Medrano-T, Iberê L. Caldas, Tamás Tél, and Ulrike Feudel. State-dependent vulnerability of synchronization. *Physical Review E*, 100(5):052201, 2019. Publisher: American Physical Society.
- [42] S. Smale. A Mathematical Model of Two Cells Via Turing’s Equation. In *The Hopf Bifurcation and Its Applications*, pages 354–367. Springer New York, 1976.
- [43] George Datseris and Alexandre Wagemakers. Effortless estimation of basins of attraction. *Chaos: An Interdisciplinary Journal of Nonlinear Science*, 32(2):023104, 2022.

- [44] Helena E. Nusse, James A. Yorke, and Eric J. Kostelich. Dynamics: Numerical Explorations, Accompanying Computer Program Dynamics. *Applied Mathematical Sciences*, 1994.
- [45] Merten Stender and Norbert Hoffmann. bSTAB: an open-source software for computing the basin stability of multi-stable dynamical systems. *Nonlinear Dynamics*, pages 1–18, 2021.
- [46] George Datseris, Kaleb Luiz Rossi, and Alexandre Wagemakers. Framework for global stability analysis of dynamical systems. *Chaos: An Interdisciplinary Journal of Nonlinear Science*, 33(7):073151, 2023.
- [47] Roberto C Budzinski, Alexandra N Busch, Samuel Mestern, Erwan Martin, Luisa H B Liboni, Federico W Pasini, Ján Mináč, Todd Coleman, Wataru Inoue, and Lyle E Muller. An exact mathematical description of computation with transient spatiotemporal dynamics in a complex-valued neural network. *arXiv*, 2023.
- [48] Daniel Koch, Akhilesh Nandan, Gayathri Ramesan, and Aneta Koseska. Biological computations: Limitations of attractor-based formalisms and the need for transients. *Biochemical and Biophysical Research Communications*, 720:150069, 2024.
- [49] Akhilesh Nandan, Abhishek Das, Robert Lott, and Aneta Koseska. Cells use molecular working memory to navigate in changing chemoattractant fields. *eLife*, 11:e76825, 2022.
- [50] Emmanuelle Tognoli and J. A.Scott Kelso. The Metastable Brain. *Neuron*, 81(1):35–48, 2014.
- [51] B. A. W. Brinkman, H. Yan, A. Maffei, I. M. Park, A. Fontanini, J. Wang, and G. La Camera. Metastable dynamics of neural circuits and networks. *Applied Physics Reviews*, 9(1):011313, 2022.
- [52] Lauren M. Jones, Alfredo Fontanini, Brian F. Sadacca, Paul Miller, and Donald B. Katz. Natural stimuli evoke dynamic sequences of states in sensory cortical ensembles. *Proceedings of the National Academy of Sciences*, 104(47):18772–18777, 2007.
- [53] Giancarlo La Camera, Alfredo Fontanini, and Luca Mazzucato. Cortical computations via metastable activity. *Current Opinion in Neurobiology*, 58:37–45, 2019.
- [54] Peter beim Graben, Antonio Jimenez-Marin, Ibai Diez, Jesus M. Cortes, Mathieu Desroches, and Serafim Rodrigues. Metastable Resting State Brain Dynamics. *Frontiers in Computational Neuroscience*, 13:62, 2019.
- [55] Michael Dellnitz and Robert Preis. Symbolic and Numerical Scientific Computation, Second International Conference, SNSC 2001, Hagenberg, Austria, September 12–14, 2001. Revised Papers. *Lecture Notes in Computer Science*, pages 183–209, 2003.
- [56] Gary Froyland. Statistically optimal almost-invariant sets. *Physica D: Nonlinear Phenomena*, 200(3-4):205–219, 2005.

- [57] Strogatz. *Nonlinear Dynamics and Chaos*. Studies in nonlinearity. Westview, 2002.
- [58] Anant Kant Shukla, T R Ramamohan, and S Srinivas. A new analytical approach for limit cycles and quasi-periodic solutions of nonlinear oscillators: the example of the forced Van der Pol Duffing oscillator. *Physica Scripta*, 89(7):075202, 2014.
- [59] John H. Argyris, Gunter Faust, Maria Haase, and Rudolf Friedrich. *An Exploration of Dynamical Systems and Chaos*. Springer Berlin, Heidelberg, 2 edition, 2015.
- [60] John Milnor. On the concept of attractor. *Communications in Mathematical Physics*, 99(2):177–195, 1985.
- [61] Robert L.V. Taylor. Attractors: Nonstrange to Chaotic. *SIAM Undergraduate Research Online*, 4:72–80, 2011. Publisher: Society for Industrial & Applied Mathematics (SIAM).
- [62] Henk Broer and Floris Takens. *Dynamical Systems and Chaos*. Applied Mathematical Sciences. 2011.
- [63] Jorge V. José and Eugene J. Saletan. *Classical Dynamics: A Contemporary Approach*. Cambridge University Press, Cambridge, 1998.
- [64] Paul Glendinning. *Stability, Instability And Chaos: An Introduction To The Theory Of Nonlinear Differential Equations (cambridge Texts In Applied Mathematics)*. Cambridge Texts in Applied Mathematics. Cambridge University Press, Cambridge [England], 1 edition, 1994.
- [65] Yuri A. Kuznetsov. Elements of Applied Bifurcation Theory. *Applied Mathematical Sciences*, 2004.
- [66] D. Koch, A. Nandan, G. Ramesan, I. Tyukin, A. Gorban, and A. Koseska. Ghost Channels and Ghost Cycles Guiding Long Transients in Dynamical Systems. *Physical Review Letters*, 133(4):047202, 2024.
- [67] Björn Sandstede. Constructing dynamical systems having homoclinic bifurcation points of codimension two. *Journal of Dynamics and Differential Equations*, 9(2):269–288, 1997.
- [68] Ed Bullmore and Olaf Sporns. Complex brain networks: graph theoretical analysis of structural and functional systems. *Nature Reviews Neuroscience*, 10(3):186–198, 2009.
- [69] Pietro Landi, Henintsoa O. Minoarivelo, Åke Brännström, Cang Hui, and Ulf Dieckmann. Complexity and stability of ecological networks: a review of the theory. *Population Ecology*, 60(4):319–345, 2018.
- [70] D J Watts and S H Strogatz. Collective dynamics of 'small-world' networks. *Nature*, 393(6684):440–442, 1998.
- [71] Yoshiki Kuramoto. *Chemical Oscillations, Waves, and Turbulence*, volume 19 of *Springer Series in Synergetics*. Springer Berlin Heidelberg, Berlin, Heidelberg, 1984.

- [72] Richard Taylor. There is no non-zero stable fixed point for dense networks in the homogeneous Kuramoto model. *Journal of Physics A: Mathematical and Theoretical*, 45(5):055102, 2012.
- [73] Ulrike Feudel, Alexander N. Pisarchik, and Kenneth Showalter. Multistability and tipping: From mathematics and physics to climate and brain - Minireview and preface to the focus issue. *Chaos*, 28(3):33501, 2018.
- [74] Adilson E. Motter, Seth A. Myers, Marian Anghel, and Takashi Nishikawa. Spontaneous synchrony in power-grid networks. *Nature Physics*, 9(3):191–197, 2013.
- [75] Yu Meng, Ying-Cheng Lai, and Celso Grebogi. The fundamental benefits of multiplexity in ecological networks. *Journal of the Royal Society Interface*, 19(194):20220438, 2022.
- [76] Laura N. Driscoll, Krishna Shenoy, and David Sussillo. Flexible multitask computation in recurrent networks utilizes shared dynamical motifs. *Nature Neuroscience*, 27(7):1349–1363, 2024.
- [77] Shai Pilosof, Mason A. Porter, Mercedes Pascual, and Sonia Kéfi. The multilayer nature of ecological networks. *Nature Ecology & Evolution*, 1(4):0101, 2017.
- [78] Goran Söhl, Stephan Maxeiner, and Klaus Willecke. Expression and functions of neuronal gap junctions. *Nature Reviews Neuroscience*, 6(3):191–200, 2005.
- [79] Michael V.L Bennett and R.Suzanne Zukin. Electrical Coupling and Neuronal Synchronization in the Mammalian Brain. *Neuron*, 41(4):495–511, 2004.
- [80] Tomislav Stankovski, Tiago Pereira, Peter V. E. McClintock, and Aneta Stefanovska. Coupling functions: Universal insights into dynamical interaction mechanisms. *Reviews of Modern Physics*, 89(4):045001, 2017.
- [81] Alessandro Loppini, Matthias Braun, Simonetta Filippi, and Morten Gram Pedersen. Mathematical modeling of gap junction coupling and electrical activity in human -cells. *Physical Biology*, 12(6):066002, 2015.
- [82] Thomas B. Kepler, Eve Marder, and L. F. Abbott. The Effect of Electrical Coupling on the Frequency of Model Neuronal Oscillators. *Science*, 248(4951):83–85, 1990.
- [83] Bernd Blasius, Amit Huppert, and Lewi Stone. Complex dynamics and phase synchronization in spatially extended ecological systems. *Nature*, 399(6734):354–359, 1999.
- [84] Everton S. Medeiros, Ulrike Feudel, and Anna Zakharova. Asymmetry-induced order in multilayer networks. *Physical Review E*, 104(2):024302, 2021.
- [85] Guofu Liang, Hanbo Niu, and Yan Li. A multi-species approach for protected areas ecological network construction based on landscape connectivity. *Global Ecology and Conservation*, 46:e02569, 2023.
- [86] Alexander Sadykov and Keith D. Farnsworth. Model of two competing populations in two habitats with migration: Application to optimal marine protected area size. *Theoretical Population Biology*, 142:114–122, 2021.

- [87] Mahtab Mehrabbeik, Sajad Jafari, Riccardo Meucci, and Matjaž Perc. Synchronization and multistability in a network of diffusively coupled laser models. *Communications in Nonlinear Science and Numerical Simulation*, 125:107380, 2023.
- [88] Ekkehard Ullner, Alexei Zaikin, Evgenii I. Volkov, and Jordi García-Ojalvo. Multistability and Clustering in a Population of Synthetic Genetic Oscillators via Phase-Repulsive Cell-to-Cell Communication. *Physical Review Letters*, 99(14):148103, 2007.
- [89] Ekkehard Ullner, Aneta Koseska, Jürgen Kurths, Evgenii Volkov, Holger Kantz, and Jordi García-Ojalvo. Multistability of synthetic genetic networks with repulsive cell-to-cell communication. *Physical Review E*, 78(3):031904, 2008.
- [90] T. Yanagita, T. Ichinomiya, and Y. Oyama. Pair of excitable FitzHugh-Nagumo elements: Synchronization, multistability, and chaos. *Physical Review E*, 72(5):056218, 2005.
- [91] Aneta Koseska, Evgeny Volkov, and Jürgen Kurths. Oscillation quenching mechanisms: Amplitude vs. oscillation death. *Physics Reports*, 531(4):173–199, 2013.
- [92] Michael F Crowley and Irving R Epstein. Experimental and theoretical studies of a coupled chemical oscillator: phase death, multistability and in-phase and out-of-phase entrainment. *The Journal of Physical Chemistry*, 93(6):2496–2502, 1989.
- [93] Olaf Sporns, Siegfried Roth, and Friedrich Franz Seelig. Chaotic dynamics of two coupled biochemical oscillators. *Physica D: Nonlinear Phenomena*, 26(1-3):215–224, 1987.
- [94] D.G. Aronson, E.J. Doedel, and H.G. Othmer. An analytical and numerical study of the bifurcations in a system of linearly-coupled oscillators. *Physica D: Nonlinear Phenomena*, 25(1-3):20–104, 1987.
- [95] Arnab Mondal, Argha Mondal, Sanjeev Kumar Sharma, Ranjit Kumar Upadhyay, and Chris G. Antonopoulos. Spatiotemporal characteristics in systems of diffusively coupled excitable slow–fast FitzHugh–Rinzel dynamical neurons. *Chaos: An Interdisciplinary Journal of Nonlinear Science*, 31(10):103122, 2021.
- [96] Gerrit Ansmann, Klaus Lehnertz, and Ulrike Feudel. Self-induced switchings between multiple space-time patterns on complex networks of excitable units. *Physical Review X*, 6(1):011030, 2016.
- [97] Alexander Pogromsky, Torkel Glad, and Henk Numeijer. On diffusion driven oscillations in coupled dynamical systems. *International Journal of Bifurcation and Chaos*, 9(04):629–644, 1999.
- [98] L.M. Kocarev and P.A. Janjic. On Turing instability in two diffusely coupled systems. *IEEE Transactions on Circuits and Systems I: Fundamental Theory and Applications*, 42(10):779–784, 1995.
- [99] Eddie Nijholt, Tiago Pereira, Fernando C. Queiroz, and Dmitry Turaev. Chaotic Behavior in Diffusively Coupled Systems. *Communications in Mathematical Physics*, 401(3):2715–2756, 2023.

- [100] Everton Medeiros, Rene Medrano-T, Ibere Caldas, and Ulrike Feudel. The impact of chaotic saddles on the synchronization of complex networks of discrete-time units. *Journal of Physics: Complexity*, 2(3):035002, 2021.
- [101] Max Contreras, Everton S. Medeiros, Anna Zakharova, Philipp Hövel, and Igor Franović. Scale-free avalanches in arrays of FitzHugh–Nagumo oscillators. *Chaos: An Interdisciplinary Journal of Nonlinear Science*, 33(9):093106, 2023.
- [102] Everton S. Medeiros, Oleh Omel’chenko, and Ulrike Feudel. Transient chimera states emerging from dynamical trapping in chaotic saddles. *Chaos: An Interdisciplinary Journal of Nonlinear Science*, 33(9):093130, 2023.
- [103] C. Morris and H. Lecar. Voltage oscillations in the barnacle giant muscle fiber. *Biophysical Journal*, 35(1):193–213, 1981.
- [104] Jeff Bezanson, Alan Edelman, Stefan Karpinski, and Viral B Shah. Julia: A fresh approach to numerical computing. *SIAM Review*, 59(1):65–98, 2017.
- [105] Bard Ermentrout. *Simulating, Analyzing, and Animating Dynamical Systems*. Society for Industrial and Applied Mathematics, 2002.
- [106] Christopher Rackauckas and Qing Nie. DifferentialEquations.jl – A Performant and Feature-Rich Ecosystem for Solving Differential Equations in Julia. *Journal of Open Research Software*, 5(1):15, 2016.
- [107] George Datseris. DynamicalSystems.jl: A Julia software library for chaos and nonlinear dynamics. *Journal of Open Source Software*, 3(23):598, 2018. Publisher: The Open Journal.
- [108] George Datseris, Jonas Isensee, Sebastian Pech, and Tamás Gál. DrWatson: the perfect sidekick for your scientific inquiries. *Journal of Open Source Software*, 5(54):2673, 2020.
- [109] Simon Danisch and Julius Krumbiegel. Makie.jl: Flexible high-performance data visualization for Julia. *Journal of Open Source Software*, 6(65):3349, 2021.
- [110] Leonhard Schülen, Maria Mikhailenko, Everton S. Medeiros, and Anna Zakharova. Solitary states in complex networks: impact of topology. *The European Physical Journal Special Topics*, 231(22-23):4123–4130, 2022.
- [111] J. Tyson and S. Kauffman. Control of mitosis by a continuous biochemical oscillation: Synchronization; spatially inhomogeneous oscillations. *Journal of Mathematical Biology*, 1(4):289–310, 1975.
- [112] J. E. Truscott and J. Brindley. Ocean Plankton Populations As Excitable Media. *Bulletin of Mathematical Biology*, 56(5):981–998, 1994.
- [113] Steven Strogatz. *Sync: The Emerging Science of Spontaneous Order*. Hyperion Press, 2003.
- [114] Peter J. Menck, Jobst Heitzig, Norbert Marwan, and Jürgen Kurths. How basin stability complements the linear-stability paradigm. *Nature Physics*, 9(2):89–92, 2013.

- [115] Hana Krakovská, Christian Kuehn, and Iacopo P Longo. Resilience of dynamical systems. *European Journal of Applied Mathematics*, pages 1–46, 2023.
- [116] Didier Sornette. *Critical Phenomena in Natural Sciences, Chaos, Fractals, Self-organization and Disorder: Concepts and Tools*. Springer Series in Synergetics. 2006.
- [117] Ying-Cheng Lai and Tamás Tél. *Transient Chaos: Complex Dynamics on Finite-Time Scales*. Applied Mathematical Sciences. Springer New York, NY, 2009.
- [118] Alan Hastings, Karen C. Abbott, Kim Cuddington, Tessa Francis, Gabriel Gellner, Ying-Cheng Lai, Andrew Morozov, Sergei Petrovskii, Katherine Scranton, and Mary Lou Zeeman. Transient phenomena in ecology. *Science*, 361(6406), 2018.
- [119] A. M. Turing. On Computable Numbers, with an Application to the Entscheidungsproblem. *Proceedings of the London Mathematical Society*, s2-42(1):230–265, 1937.
- [120] George S. Boolos, John P. Burgess, and Richard C. Jeffrey. *Computability and Logic*. Cambridge University Press, 5 edition, 2007.
- [121] Claire M. Postlethwaite, Peter Ashwin, and Matthew Egbert. A Continuous Time Dynamical Turing Machine. *IEEE Transactions on Neural Networks and Learning Systems*, PP(99):1–13, 2024.
- [122] Peter Ashwin and Marc Timme. When instability makes sense. *Nature*, 436(7047):36–37, 2005.
- [123] Ofer Mazor and Gilles Laurent. Transient Dynamics versus Fixed Points in Odor Representations by Locust Antennal Lobe Projection Neurons. *Neuron*, 48(4):661–673, 2005.
- [124] Saurabh Vyas, Matthew D. Golub, David Sussillo, and Krishna V. Shenoy. Computation Through Neural Population Dynamics. *Annual Review of Neuroscience*, 43(1):249–275, 2020.
- [125] David Sussillo and Omri Barak. Opening the Black Box: Low-Dimensional Dynamics in High-Dimensional Recurrent Neural Networks. *Neural Computation*, 25(3):626–649, 2013.
- [126] Rodrigo Laje and Dean V Buonomano. Robust timing and motor patterns by taming chaos in recurrent neural networks. *Nature Neuroscience*, 16(7):925–933, 2013.
- [127] Peter Ashwin and Claire Postlethwaite. Excitable networks for finite state computation with continuous time recurrent neural networks. *Biological Cybernetics*, 115(5):519–538, 2021.
- [128] Peter Ashwin, Muhammed Fadera, and Claire Postlethwaite. Network attractors and nonlinear dynamics of neural computation. *Current Opinion in Neurobiology*, 84:102818, 2024.

Acknowledgments

Doing a PhD is not trivial (no citation needed here, I think). It is made possible not just from one's own hard work, but with help and support from many others.

To start, the PhD was possible due to financial support from the German Academic Exchange Foundation (DAAD, in german). I am very thankful for the opportunity to do all this work with their warm support. In this sense, I am also grateful to the University of Oldenburg for the structures provided that allowed me to work.

Moving from the material to the intellectual and personal support, I am extremely grateful to Prof. Ulrike Feudel, my supervisor for all of these years! We had a lot of fun, and I learned so much from her. On top of the specific knowledge of the area, I think maybe the most important skill she developed on me was the ability to refine a thought and rigorously develop an idea until you are confident about it. On top of all the actual science we made, I find it amazing how many conferences I had the opportunity to participate in, and how many people I met - a lot of this I owe to Ulrike's support. In a similar vein I also want to deeply thank my friend and collaborator, Prof. (yes, Prof.!) Everton Medeiros. Maybe without even noticing, he also taught me so much. He was a crucial aid in making this whole process a lot more fun and exciting - with, of course, better science. I will always remember this fondly - as will I remember his legendary goal from the corner of the pitch in Spiekeroog. Football's loss is academia's gain.

Moving more to the emotional (and personal still) support, I am above all thankful to my mom and my sister for just about everything. Moving abroad is not easy - for anyone involved - but their unwavering love, warmth, and understanding made it all happen! This extends to my whole family, in fact.

Friends are also a crucial ingredient to a nice life. And in this I also have had the luck to count on some amazing figures. I will only name some - their egos will have to be satisfied. In no particular order I want to thank from the bottom of my heart Jakob and Bianca Weik, Roberto Budzinski, Bruno Boaretto, Maira Theisen, Gabriel Gubert, Lucas Polyceno, Carlos Martins, Alexandre Camargo, Rafa Jakuboski, Joao Paludo, Marcos Sato, George Datseris, Bryony Hobden, Patryk Bielski, Luis Gustavo, and Deoclecio Valente - and many others I equally love but, come on, the list was already too big.

Finally, I mentioned I met a lot of amazing people doing science, some of whom I already mentioned. For all the discussions, support, and fun, I want to especially thank Klaus Lehnertz, Lyle Muller, Pete Ashwin, Aneta Koseska, Vyacheslav Kruglov, Ryan Deeley, and Jan Freund.

Eidesstattliche Erklärung

Hiermit versichere ich, dass ich diese Dissertation selbstständig verfasst habe und nur die hier angegebenen Hilfsmittel und Quellen benutzt habe. Zudem versichere ich, dass diese Dissertation weder in ihrer Gesamtheit noch in Teilen einer anderen Hochschule zur Begutachtung in einem Promotionsverfahren vorliegt oder vorgelegen hat. Bis auf die angegebenen Teilpublikationen, ist diese Arbeit noch nicht veröffentlicht worden. Die Leitlinien guter wissenschaftlicher Praxis an der Carl von Ossietzky Universität Oldenburg wurden befolgt. Für dieses Promotionsvorhaben wurden keine kommerziellen Vermittlungs- oder Beratungsdienste in Anspruch genommen.

Oldenburg, den 07.11.2024
Kalel Luiz Rossi